DEVELOPMENT OF NEW ANTIBODY BASED THERANOSTIC AGENTS TARGETING

THE RECEPTOR FOR ADVANCED GLYCATION END-PRODUCT (RAGE)

A Dissertation
Submitted to the Graduate Faculty
of the
North Dakota State University
of Agriculture and Applied Science

By

Faidat Jyoti

In Partial Fulfillment
for the Degree of
DOCTOR OF PHILOSOPHY

Major Department:
Pharmaceutical Sciences

August 2012

Fargo, North Dakota

North Dakota State University
Graduate School

Title
DEVELOPMENT OF NEW ANTIBODY BASED THERANOSTIC

AGENTS TARGETING THE RECEPTOR FOR ADVANCED

GLYCATION END-PRODUCT (RAGE)

By

FAIDAT JYOTI

The Supervisory Committee certifies that this *disquisition* complies with

North Dakota State University's regulations and meets the accepted standards

for the degree of

DOCTOR OF PHILOSOPHY

SUPERVISORY COMMITTEE:

ESTELLE LECLERC
Chair

JAGDISH SINGH

BENEDICT LAW

KATIE REINDL

Approved:

09/04/2012	JAGDISH SINGH
Date	Department Chair

ABSTRACT

The Receptor for Advanced Glycation End products (RAGE) interacts with several classes of structurally unrelated ligands. The activation of RAGE by its ligands results in the cellular activation of several kinases and transcription factors including mitogen activated protein kinases (MAPKs) and nuclear factor kappa-light-chain-enhancer of activated B cells (NF-κB) resulting in sustained inflammation, which is involved in pathologies such as diabetes, cancer, Alzheimer's disease, multiple sclerosis and other diseases associated with chronic inflammation. Current mouse models of human disease have shown that RAGE activity can be efficiently suppressed using either soluble RAGE (sRAGE) or anti-RAGE antibodies as inhibitors. Our goal was to generate new monoclonal antibodies against RAGE that can serve as diagnostic as wells as therapeutic tools in RAGE related pathologies.

The chapters in this dissertation are a complete documentation of the development of these anti-RAGE antibodies. Additionally, an introductory review of antibodies, which includes structure and function, types of antibodies and production and basic understanding of RAGE and its ligands, has been provided to facilitate the understanding of the chapters. The first chapter details the development and characterization of anti-RAGE antibodies produced from hybridoma. The next chapter explores the effects of the generated antibodies to mammalian cells in *in vitro* settings and the final chapter applies the generated antibodies *in vivo*.

During the course of this work, the antibodies developed showed binding to RAGE at nano-molar affinities which are comparable to the affinities of current antibodies used for therapeutic purposes, diagnostic and research purposes. We were also able to delineate that the possible mechanism of action of the antibodies is by preventing binding to RAGE. Lastly, we observed that one of the generated antibodies was able to reduce tumor growth *in vivo* in a melanoma xenograft mouse model.

ACKNOWLEDGMENT

I'd like to thank everyone involved in the completion of this project especially my committee

members; Dr. Estelle Leclerc, Dr. Jagadish Singh, Dr. Benedict Law and Dr. Katie Reindl.

TABLE OF CONTENTS

LIST OF TABLES

LIST OF FIGURES

LIST OF ABBREVIATIONS

ABAM............Antibiotic/Antimycotic

AD.................Alzheimer's disease

AGE ....Advanced glycation end-product

AP ....Alkaline phosphatase

APP ....Amyloid precursor protein

ATCC.............American type culture collection

Aβ ....Amyloid beta

AβA ....Amyloid beta aggregate

BACE1...........Beta-site amyloid precursor protein cleaving enzyme 1

BBB................Blood brain barrier

BCA ....Bicinchoninic acid

BSA................Bovine serum albumin

cAMP.............Cyclic adenosine monophosphate

CDR ....Complementarity determining region

CNS................Central nervous system

CO_2.................Carbon dioxide

CREB ....cAMP response element-binding

DCCT.............Diabetes control and complications trial

DCFH-DA......Dichlorofluorescein-diacetate

DMEM ....Dulbecco's Modified Eagle Medium

DNA...............Deoxyribonucleic acid

DOPA.............Dihydroxyphenylalanine

ECL ....Enhanced chemiluminescence

EDTA ....Ethylenediaminetetraacetic acid

ELISA ....Enzyme linked immunosorbent assay

ERK ....Extracellular signal-regulated kinases

esRAGE ....Endogenous secretory receptor for advanced glycation end-product

Fab ....Fragment antigen binding

FACS ....Fluorescence activated cell sorting

FBS ....Fetal bovine serum

Fc ....Fragment crystalline

FDA ....Food and Drug Administration

FITC ....Fluorescein isothiocyanate

GSK ....Glycogen synthase kinase

GTPases ....Guanosine triphosphatase

HCl ....Hydrochloride

HEK ....Human embryonic kidney

HEPES ....Hydroxyethyl piperazineethanesulfonic acid

HMGB1 ....High mobility group box 1

HRP ....Horseradish peroxidase

IACUC ....Institutional Animal Care and Use Committee

ICAM ....Intercellular adhesion molecule

IGF ....Insulin-like growth factor

IgA ....Immunoglobulin A

IgD ....Immunoglobulin D

IgD ....Immunoglobulin E

IgG ....Immunoglobulin G

IL...................Interleukin

IPTG..............Isopropyl β-D-1-thiogalactopyranoside

JNK ....c-Jun-NH$_2$-terminal kinase

k$_a$ ....Association rate

K$_D$..................Dissociation constant

k$_d$ ....Dissociation rate

KD.................Kilo Dalton

LB ....Luria broth

Mab ....Monolconal antibody

MAPK...........Mitogen activated protein kinase

MHC ....Major Histocompatibility complex

MIP ....Macrophage inflammatory protein

NaCl..............Sodium chloride

NADPH..........Nicotinamide adenine dinucleotide phosphate

NF-κB ....Nuclear factor kappa-light-chain-enhancer of activated B cells

NIH ....National Institute of Health

NIRF ....Near infra-red fluorescence

NO.................Nitric oxide

PBS ....Phosphate buffered saline

PDGF ....Platelet-derived growth factor

PEG...............Polyethylene glycol

PMSF ....Phenylmethylsulfonyl fluoride

p-NPP.............para-Nitrophenylphosphate

RAG ....Recombinant activating gene

RAGE.............Receptor for advanced glycation end-product

RNS................Reactive nitrogen species

ROS................Reactive oxygen species

RPM ....Revolutions per minute

RT ....Room temperature

SAPK ....Stress activated protein kinase

SCID ....Severe combined immunodeficiency

SDS-PAGE ....Sodium dodecyl sulfate polyacrylamide gel electrophoresis

SPR ....Surface plasmon resonance

sRAGE ....Soluble receptor for advanced glycation end-product

STAT..............Signal transducers and activators of transcription family

TBS ....Tris buffered saline

TBST..............Tris buffered saline/tween

TEV................Tobacco etch virus

TNFα..............Tumor necrosis factor-alpha

VCAM............Vascular cell adhesion protein

V_H.........................Variable domain of heavy chain

V_L.........................Variable domain of light chain

INTRODUCTION/GENERAL OVERVIEW

A Brief History of Antibodies

The discovery of antibodies cannot be attributed to a single individual because the knowledge of antibodies has continued to evolve over time throughout history. Even before the activity of an antibody was demonstrated towards its antigen of interest, western civilization has indirectly relied on antibodies through vaccination of antigenic substances for therapeutic purposes as far back as the 1700's [1]. Although Edward Jenner is highly regarded as the pioneer of immunization in the western world for demonstrating the vaccination of cow pox into healthy individuals, Lady Mary Wortley Montagu was the original crusader of the cause [1, 2]. Seventeenth and Eighteenth century Europe was plagued with a new epidemic, the small pox. It killed approximately half a million people per year [3] including Lady Montagu's brother.

In 1715, she was afflicted with a case of small pox but survived. Unfortunately, her revered beauty was severely marred because she lost her eyelashes and her face was riddled with pitted scars from the illness [4]. Two years later she accompanied her husband, a British ambassador to Turkey, where she observed the practices of the eastern people [4]. One of the practices she observed was the inoculation of the live small pox virus from a mild case of the disease into the veins of healthy individuals. She observed that the process prevented inoculated individuals from the deadly disease; therefore, she got her children inoculated [5].

Upon her return to England, she promoted the procedure but was heavily criticized by the medical community because it was unconventional [6, 7]. To prove that it was safe, she made several convicted murderers and orphans undergo the procedure. The procedure was documented by Charles Maitland, a surgeon [2, 4, 8, 9].   When the outcome proved to be safe, several upper class citizens including members of the royal family underwent the procedure and it spread amongst the scientific population over the next few years [4, 9]. Many notable discoveries took

place after the popularization of vaccination as a preventative intervention in disease but scientists were still not certain of the mechanism of action involved in vaccination.

Several decades later, diphtheria and tetanus became another leading cause of death especially amongst children [10]. In 1890, two physicians working in Robert Koch's lab, Emil von Behring and Kitasato Shibasaburo, published several papers which demonstrated that the serum obtained from the blood of an animal, infected with a non-lethal form of both bacteria, could serve as an antitoxin for both diseases [10]. The first mankind application of the serum was on a boy suffering from diphtheria in 1891 [10]. Although favorable results were obtained from the treatment, there was no means of measuring the exact amount of the antitoxin needed for treatment.

In the same year, Paul Ehrlich, another scientist under Koch's supervision published a paper titled "Experimental studies on immunity". In the conclusion of the article, he states that "if two substances give rise to two different antikörper, then they themselves must be different". The term antikörper is the German word for antibody. This was the first time anyone ever used the term [11]. A few years later he established a standardization method for measuring the content of the antitoxins for diphtheria and tetanus. This critical process allowed for the mass production of a standardized serum [10, 12]. Ehrlich also proposed that side chains present on the cells, which we now know as receptors, can bind to toxins in a lock-and-key interaction and it is this interaction that leads to the generation of antibodies [13]. Together, all these findings gave grounds to the application of serum therapy as a prophylaxis and a treatment for both diphtheria and tetanus.

Unfortunately, the use of the serum also resulted in a severe anaphylactic reaction [14]. Behring proposed that the antitoxin effect was present in a particular protein fraction in the

serum. He did further work on the serum by precipitating the protein fraction. This precipitated fraction reduced the side effects but did not completely eliminate them [14]. In the following years, a lot of work went into the isolation of antibodies from sera. In 1924, Lloyd B. Felton, a scientist at Harvard, was the first to announce the successful isolation of a white crystalline powder from the anti-sera of horses immunized with *S. pneumonia* [15]. He was able to demonstrate in mice that the powder was composed of similar therapeutic properties as compared to the anti-serum that generated it, without its usual side effects [15, 16]. Subsequently, Felton used the isolated white crystalline powder to treat human patients with pneumonia. It was observed that all the patients recovered from their infections without any of the side effects usually observed with the serum [16].

After the first isolation of antibody from serum, several notable hypotheses and discoveries happened including John Marrack's antigen-antibody binding theory. Marrack's work focused on the interpretation of the reaction between antigen and antibody, specifically immunoprecipitation [17]. In his experiments, using diphtheria toxin and its antitoxin, he noted that increasing amounts of antigen resulted in an increase in the proportion of antibody found in the complexes [17]. He described the interaction between antigens and antibodies similar to that between molecules in a crystal lattice. Marrack suggested that if the antibody, like the antigen, had more than one binding site, the antigen-antibody complexes would bind together in the form of a lattice [17, 18]. Many studies, in line with Marrack's work, were confirmed by Michael Heidelberger and Frank Kendall between 1920 and 1940 [19-22].

Another major contribution to the knowledge of antibodies took place in the 1940s, when Linus Pauling confirmed the lock-and-key theory which had been earlier proposed by Ehrlich in 1897. Pauling was able to show that the interactions between antibodies and antigens depended

more on their shape than their chemical composition [23]. In 1948, Astrid Fagraeus was able to use her histological and tissue culture studies to show that antibodies were produced by B cells [24]. Her findings were subsequently corroborated in the article titled "Studies on antibody production. I. A method for the histochemical demonstration of specific antibody and its application to a study of the hyperimmune rabbit" published by Coon and his colleagues in 1955 [25] .

The next major development resulted in a Nobel Prize in physiology and medicine in 1972 won by Gerald M. Edelman and Rodney R. Porter for their discoveries concerning the chemical structure of antibodies [26]. Rodney Porter was able to chemically split apart an antibody molecule. He was able to deduce that antibodies are made up of fragment antibody binding (Fab) and fragment crystalline (Fc) portions which gave them their Y-shaped structure. Around the same time, Edelman was also able to show that antibodies were composed of two types of polypeptide chains, referred to today as light and heavy chains [27]. He was also able to discern that the heavy and light chains were linked by disulfide bonds. Edelman went on to determine the complete amino acid sequence of the immunoglobulin which was a thirteen hundred amino acid sequence. This was considered a great feat as it was the longest amino acid sequence ever characterized at the time [26]. Their research work gave rise to many clinical applications of antibodies in the diagnostic field.

Several significant efforts in the understanding of antibodies took place in the interim of immunoglobulin characterization between the 60s and the 70s. These included the discovery of other antibody isotypes such as immunoglobulin A (IgA), which were identified by Thomas Tomasi [28, 29], the identification of IgD by David S. Rowe and John L. Fahey [29] and the discovery of IgE by Kimishige Ishizaka and Teruko Ishizakathe [30]. As the knowledge of

antibodies expanded, so did their application in research, diagnosis and therapy. Unfortunately these accomplishments were also accompanied by several characteristics of polyclonal antibodies such as their heterogeneous property, their lack of consistency from batch to batch during production, purity issues [31] and side effects like fevers, itching, hives, rashes, joint pain and swollen lymph nodes that were observed when used as therapeutic agents [14].

In 1975, Cesar Milstein and George Köhler were able to achieve what is perhaps regarded as the biggest landmark in the history of immunology, secondary to vaccination, *the generation of the first monoclonal antibody* [32]. Köhler and Milstein conducted independent studies on antibody production in a laboratory setting [33-35]. At the time, Milstein was able to successfully develop cancerous forms of antibody-producing cells that grew and multiplied forever. Unfortunately the antibodies produced from the cancerous cell line resulted in antibodies of unknown specificity [33]. Coincidentally, Kohler had successfully been able to generate normal antibody-producing cells to produce specific antibodies, but the antibody-producing cells were only able to survive for a few days in culture [35]. Together, they were able to fuse Kohler's normal antibody-producing cells with Milstein's tumor cells, which formed a hybrid that was both immortal and could create a specific antibody [34, 36, 37].

At the time, the introduction of monoclonal antibodies to the scientific community proved to be immensely useful but scientists discovered that they were still unable to fulfill their inherent potentials as therapeutic intervention because of certain limitations. A major problem observed with the use of monoclonal antibody produced in rodents was that the generated antibodies were of rodent type and not human antibody [38]. Scientist observed that the difference between the two types of antibody was sufficient enough to invoke an immune response after the administration of multiple doses [38]. These immune responses were similar to

that observed in serum sickness. Additionally, rodent antibodies were not as effective as human antibodies in the activation of the immune system. Using recombinant technology, scientists were able to overcome these obstacles, by combining the genetic material from the rodent source with the genetic material from a human being [38]. However, there were still some reported cases of immunogenicity depending on the percentage of non-human genetic material used in the recombination of the chimeric antibody. This gave rise to the creation of fully human monoclonal antibody with the help of phage display technology in 1990 by McCafferty and colleagues. They were able to generate variable antibody domains using filamentous phage which could then be produced using a suitable expression organism [39].

The quest for generation of full-sized monoclonal antibodies continued, and by the mid - 1990s transgenic mice were genetically engineered to generate full-sized human antibodies [40, 41]. The use of recombinant technology and transgenic mice in the generation of monoclonal antibodies for therapeutic purposes has become standard and has been exploited by many commercial organizations to produce monoclonal antibodies in the treatment of diseases such as macular degeneration, multiple sclerosis, cardiovascular diseases, inflammatory diseases, transplant rejection, viral infection and cancer [42].

Antibodies have consistently served as a major protector within living organisms from the harmful effect of microbes and/or toxins before mankind was aware of its vast potential. In the twenty first century, antibodies still continue to serve as one of the top selling bio-medical tools thanks to numerous important theories and discoveries that have expanded our current understanding of how antibodies work and how we can use them to our advantage. Together all these efforts have contributed irrefutably to our modern use of antibodies and continue to form the scientific basis of further antibody discoveries.

Structure and Function of Antibodies

Antibodies are glycoprotein molecules generated by B lymphocytes to mediate a humoral immune response in the defense against extracellular microbes [43]. An antibody molecule belongs to the immunoglobulin (Ig) super family of cell surface molecules and soluble proteins [43]. An antibody typically consists of four different components, which are two heavy chains (50 kDa each) and two light chains (23 kDa each) [44, 45]. Structurally an antibody is composed of one heavy chain that is bound to a light chain and connected to the other heavy chain through a disulfide bound giving it a Y-shape configuration (Figure 1.1).
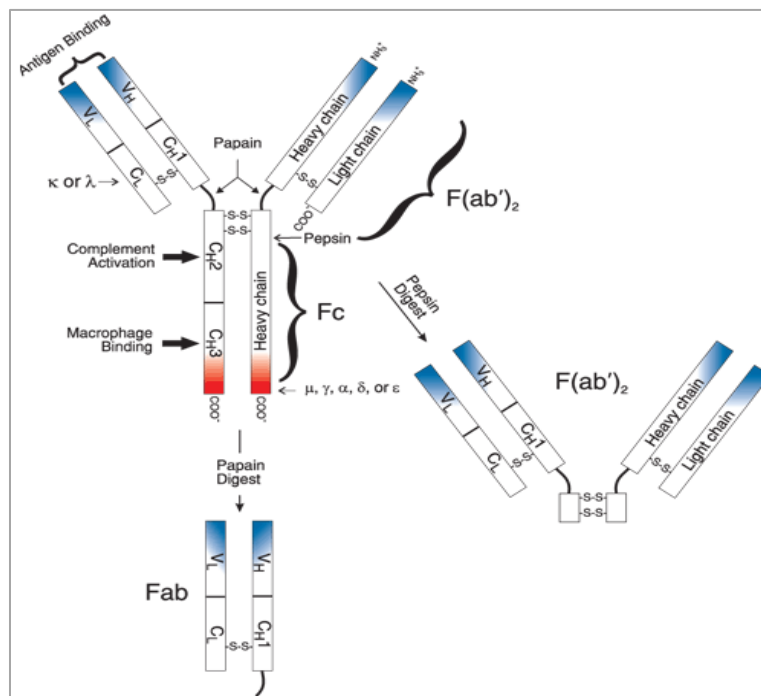
Figure 1.1: Schematic representation of an antibody molecule. Image obtained from invitrogen.com [46].

Antibodies are usually folded into several domains of three dimensional structures known as immunoglobulin domains. A heavy chain molecule typically has four or five domains which consist of one variable domain (V domain) and three to four constant domains (C domain). A light chain has one V domain and one C domain [43]. The variable domains on the heavy (V_H) and light chain (V_L) typically have three complementarity determining regions (CDR1, CDR2

7

and CDR3), which are also known as hyper-variable regions. Out of the three regions, CDR3 has the highest amount of variability which is responsible for the specificity of an antibody towards its antigen of interest [43].

In 1959, R. R. Porter was able to separate IgGs, obtained from rabbit, into three fragments using papain from plant [47]. He discovered that two of the fragments were identical and still retained their ability to bind antigens. These identical units are now known as Fab fragment. Fabs are usually composed of the light chain of an antibody attached to the V_H and first C_H domain of the heavy chain molecule. The third fragment was shown to be able to perform effector functions and could also be crystallized [47]. This part of an antibody is referred to as the Fc portion. Therefore each immunoglobulin molecule consists of two antigen binding sites and one effector site. An antibody molecule also has a hinge region located between the Fab and Fc regions. The hinge region provides flexibility for each antigen binding site to move simultaneously and to allow independent binding on an antigen [43]. The flexibility provided by the hinge region of an antibody also allows the antigenic binding site to conform to a shape that can accommodate nearly any antigen. Therefore, antibodies are capable of binding a series of structurally different macromolecules [43].

The light chain of an antibody can either be expressed as a κ or a λ chain. The difference between both types of light chain exists within the C domain but the chains do not differ in function [43]. Heavy chains can be expressed as five different types which are α, δ, ε, γ and μ. Each heavy chain can be expressed with any light chain which results into different classes of antibodies [43]. Human antibodies can be classified into five different classes based on the type of heavy chain expressed. The five classes of antibodies are IgA, IgD, IgE, IgG and IgM. These

classes of antibodies have different physical characteristics and therefore different physiological functions [48].

Mature B cells typically express membrane bound IgM and IgD. Stimulation of antigen specific clones of mature B lymphocytes by an antigen leads to expansion and differentiation of B cells into progenies that secrete the different classes of antibodies [43]. Figure 1.2 has a summary of different antibody classes, their corresponding heavy chain, physical characteristics and physiological functions. IgE, IgD and IgG are monomeric in nature and therefore have two binding sites [43]. IgA is a dimer and has four binding sites while IgM is expressed as a pentameric molecule and has ten binding sites. An increase in number of binding sites can increase the total strength of binding which is known as avidity [48]. It is important to note that increase in avidity is only possible when the epitopes to be recognized by the antibodies with multiple binding sites are identical and in close vicinity [48]. Antibodies recognize the portion of an antigen known as epitope or determinant. These epitopes can be recognized by an antibody based on the sequence of amino acids which could be a linear or "conformational" sequence [43]. The interactions between an antibody and its antigenic epitope are usually non-covalent, reversible interaction which consists of mainly electrostatic bonds in nature, although hydrogen bonds can also occur [48]. Typically, the interaction between an antigen and an antibody is measured in molar concentration as dissociation constant (K_D). The K_D or affinity measures the concentration of antigen necessary to bind to half the available antibodies present in a solution. Therefore a lower molar concentration translates to a higher affinity and a higher molar concentration means that the antibody has a low affinity for the antigen [43]. Antibodies affinities found in the immune system typically range from 10^{-6} to 10^{-11}M [43].

Antibody isotypes of mammals
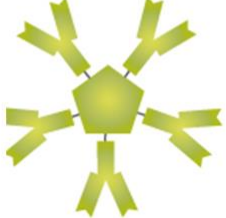
Name	Types	Description
IgA	2	Found in mucosal areas, such as the gut, respiratory tract and urogenital tract, and prevents colonization by pathogens. Also found in saliva, tears, and breast milk.
IgD	1	Functions mainly as an antigen receptor on B cells that have not been exposed to antigens. It has been shown to activate basophils and mast cells to produce antimicrobial factors.
IgE	1	Binds to allergens and triggers histamine release from mast cells and basophils, and is involved in allergy. Also protects against parasitic worms.
IgG	4	In its four forms, provides the majority of antibody-based immunity against invading pathogens. The only antibody capable of crossing the placenta to give passive immunity to fetus.
IgM	1	Expressed on the surface of B cells and in a secreted form with very high avidity. Eliminates pathogens in the early stages of B cell mediated (humoral) immunity before there is sufficient IgG.

Heavy Chain Type

α

δ

ε

γ

μ

Antibody Complexes

Monomer
IgD, IgE, IgG

Dimer
IgA

Pentamer
IgM

Figure 1.2: Summary of the characteristics of the different antibody classes (Iso-types). IgA has two different subtypes known as IgA1and IgA2a. IgG also has four different types IgG1, IgG2, IgG3 and IgG4. Image obtained from bioatlas.com and modified [49, 50].

Typically, an antibody with a higher affinity has a more stable bond to its antigen of interest which allows for an efficient induction of the immune system but antibodies in the system with lower affinity also have crucial roles in the defense against pathogenic substances [48]. In 1968, Theis and Siskind detected persistence levels of low affinity antibodies within the immune system. They theorized that these low affinity antibodies may serve as a front line defense against foreign substances because they could bind to one site on the antigen, activate the complement system, dissociate quickly because of their low affinity and then subsequently

10

bind to a second site on the antigen, which could result in the amplification of the complement system [51].

Antibodies are capable of eliminating antigenic substances within an organism in a number of ways. Antibodies can offer protection by serving as neutralizing antibodies; they can bind to foreign substances and block the interaction between the receptor and toxins or viruses [43]. Furthermore, the interaction between cell surface receptors and the Fc portion of an antibody can enhance communication between the various cell types of the immune system to trigger several biological functions [43]. These include inflammation, B cell activation and enhanced engulfment of antibody-antigen complex by macrophages [43]. Although antibodies are not capable of direct destruction of antigenic substances, they can serve as markers on foreign molecules and tag them for destruction by phagocytic cells such as neutrophils and macrophages [43]. Additionally antibodies such as IgG and IgM can activate the complement system to phagocytose foreign substances and promote bacterial lysis [43]. Apart from activation of the complement system, interaction with a cell surface receptor to neutralize antigens, and activation of an effector cell, antibodies have also been involved in prenatal transfer to protect fetuses and regulate certain catabolic pathways [52-54].

The structural similarity and tremendous diversity between antibody molecules offer advantages to the humoral immune system as the major pathways for defense against microbes because B cells can produce antibodies in response to a variety of molecules regardless of their structural composition, size or type [43, 55].

Methods of Antibody Production

Antibodies have become an invaluable tool in the field of research, diagnosis, and therapeutics. Their ability to specifically bind target molecules, accessibility and adaptability to

several diagnostic and therapeutic applications has made them indispensable tools in the

biomedical field. This section discusses the different techniques used in the production of

antibodies and the types of antibodies that can be generated.

Polyclonal Antibodies versus Monoclonal Antibodies; Factors to Consider

Polyclonal antibodies are the original products obtained from the serum of immunized

animal. As indicated by its name, it is a mixture of thousands of different antibodies binding to

several epitopes on an antigen [31]. Polyclonal antibodies typically have a large range of affinity

for different epitopes on the antigenic molecule. In contrast, monoclonal antibodies are generated

from a single type of immunoglobulin binding to a single epitope on the antigen used for

immunization [31]. Therefore they are more selective as compared to polyclonal antibodies.

There are several factors to consider in the generation of polyclonal versus monoclonal

antibodies. The first should be based on the level of sensitivity toward the antigen of interest.

The heterogeneous nature of polyclonal antibodies may reduce its ability to recognize minute

amounts of antigenic material present on cells [56]. The second consideration is the supply of

antibodies. The sera of immunized animals can contain large quantities of antibodies but the

mixture of antibody generated can vary from one immunization to the next. Theoretically,

hybridoma clones used in the generation of monoclonal antibodies are supposed to continuously

produce antibodies indefinitely [56]. Unfortunately, this is not practically feasible because

hybridoma clones typically end up over-grown with non-producing strains which eventually

require cloning the antibody genes into a new expressing system that is time consuming and

costly. The next factor to consider is ethical concerns surrounding the use of animals as there are

many strict regulations in the use of animals. Initial immunization is required for both

monoclonal and polyclonal antibodies although some recombinant procedures have greatly

reduced or totally eliminated the need for animals [56]. The fourth factor to consider is time. Typically, the generation of either a polyclonal or monoclonal antibody is time consuming without the guarantee of success. The fifth factor to consider is cost of production technique. Regardless of monoclonal or polyclonal antibody generation, the type of production method used and the antibody yield can vary greatly especially with the development of bioreactor for mammalian and bacterial cells [56]. Finally, patents can limit the use of certain techniques as there are many legal issues to consider.

Regardless of the source of antibody, the final products are typically extremely useful because they can easily be transformed to suit many biotechnological applications for research, diagnostic and therapeutic needs, they are stable and can be stored in solution, frozen or lyophilized [56].

Generation of Polyclonal Antibodies

Polyclonal antibodies have continued to be an invaluable tool even with the introduction of monoclonal antibodies by Kohler and Milstein in 1975[33]. Polyclonal antibodies are important research tools used in virtually all areas in science to identify and quantify macromolecules and decipher the interaction between two molecules [31]. The heterogeneity of polyclonal antibodies makes their application non-specific; however, affinity purification of polyclonal antibodies using short peptide antigens that represent a specific epitope has resulted in the generation of mono-specific polyclonal affinity [56].

Polyclonal antibodies can be produced in virtually any animal that has an immune system. So far they have been raised in rabbits, rats, mice, hamsters, guinea pigs, goats, sheeps, cattle, horses, emus and chickens [56-58]. Choosing a host is typically dependent on the quantity of material needed for intended use. Therefore, the larger the quantity of antibody needed, the

13

larger the animal used in the immunization and vice versa [56]. Secondary to quantity needed, the type of immunogen used in the generation of antibodies is also a determinant factor. Certain antigenic substances can produce different immunogenicity. Large molecules >6 kDa will typically result in an immunogenic response. Smaller molecules can also give an immunogenic response but they typically have to be tagged onto carrier molecules such as keyhole limpet hemocyanin (KLC), bovine serum albumin (BSA), or ovalbumin. Conjugation of smaller-sized molecules to these proteins increase the size of the immunogen and presents to T-cells the necessary epitope to provide successful immune response [56].

The origin of antigen might also hinder proper immune response. Certain antigenic substances might not produce an immune response because of recognition by the immune system as self-antigen. Successful immune response can be achieved by using the immune system of a phylogenetically divergent species in relation to the source of antigenic substance. For example, the immune system of a chicken can be used with an antigenic substance obtained from mammals [56]. Unfortunately, it is impossible to predict the immunogenic response of an antigenic substance prior to immunization of the host. A researcher has to typically rely on previously published experimental data available to estimate the extent of immunogenicity [56].

The immunization procedure starts with primary injection of antigenic substance with complete adjuvant. An adjuvant is normally used to non-specifically stimulate the immune system, recruit antigen presenting cells, and preserve the half-life of the antigen. Some common adjuvants that are used are Freud's adjuvant, precipitated aluminum hydroxide, hunter's titer max, ribi adjuvant system, and GERBU adjuvant system [56]. After primary immunization, a rest period follows to allow the primary immune response and the memory cells to form. Typically, the immune response of the animal is determined by test bleeding the immunized

animals and performing serological tests. After the rest period, one or more booster injections of antigen is followed with incomplete adjuvant and serum is collected 10-14 days after last booster injection [56]. The route of injection can also depend on the amount of antigen and formulation. Certain routes are sometimes chosen to improve delivery of antigen to antigen presenting cells in specific sites in the animal. For example, immunization can take place orally to produce gut-associated antibody or nasal immunization to stimulate secretory IgA. For bigger animals like rabbits and goats, the subcutaneous route is usually preferred. Small rodents like mice and rats are usually injected with antigen via the intraperitoneal route. Other routes of delivery have also been used but usually present some disadvantages. For instance, intramuscular and intradermal administration usually slows down exposure of immunogen to the immune system while intravenous administration allows for fast metabolism of antigenic substance [56].

The most important consideration in the use of animals for the production of antibodies is perhaps the expertise of handlers. Proper care needs to be provided when handling animals which typically require experience and patience from trained individuals to ensure proper treatment of animals [56].

Generation of Monoclonal Antibodies

In many ways the production of monoclonal antibodies starts in a similar fashion as that of polyclonal antibodies. Like polyclonal antibodies, the generation of monoclonal antibodies starts with immunization of the animals to generate the proper immune response. Activation of the immune response typically results in the production of a pool of antibodies by many different B cells [31]. This pool of antibodies is composed of monoclonal antibodies and can be subjected to affinity purification to obtain mono-specific antibodies (Figure 1.3).

The discovery of hydridoma technology in 1975 allowed for the continuous production of the same antibody from a single B-cell clone. During this process, the animal is immunized in the same fashion that was described when generating polyclonal antibodies. Subsequently after the final boost with antigen, the spleen of the animal is isolated under standard protocols and B lymphocytes are isolated. Isolated lymphocytes are fused with myeloma cells that do not secrete immunoglobulin and are lacking the enzyme hypoxanthine guanine phosphoribosyl transferase (HGPRT) [56, 59, 60]. The most popular fusion agent used is polyethylene glycol (PEG). The chemical combination of both cells results in the combination of DNA of both cells. After the hybridization process, a mixture of unfused myeloma cells, unfused spleen cells and hybrid cells will remain in the culture. It is important to select for only hydrid cells during the process [56, 60]. Typically the unfused spleen cells will eventually die but the unfused myeloma cells, if left in the culture, will eventually outgrow the hybrid cells. Spleen cells possess the enzyme (HGPRT) which is usually lacking in myeloma cells. Therefore the culture medium is supplemented with hypoxanthine, amphoterin and thymidine (HAT) [56]. Amphoterin leads to cell death by blocking the pathway of nucleic acid synthesis. The addition of hypoxanthine and thymidine allows the growth of cells possessing the enzyme, HGPRT, which uses a different salvage pathway for the synthesis of nucleic acid. Therefore culturing the fusion products in media containing HAT will eventually lead to cell death for unfused myeloma cells while fused cells will survive [59, 61].

During the next phase, hybridoma cells producing monoclonal antibodies with desired specificity are screened. The typical screening test used is an ELISA procedure [56]. After screening for positive cells, the cells are subjected to cloning to ensure that each hybrid is monoclonal in nature. The most popular method used in cloning is limited dilution in either a

liquid or semi-solid phase such as agar to eventually achieve one cell per well [56]. After obtaining monoclonal clones, cells are cultured and subsequently frozen and stored for preservation. To produce monoclonal antibodies, individual clones are cultured using growth medium, appropriate growth temperature and humidity, in the appropriate cell culture compartments. Successful growth has been achieved using batch tissue culture flask, semi-permeable membrane based-systems, and bioreactor. During cell growth, the monoclonal antibodies are secreted by hybridoma cells into the supernatant which is then harvested and purified [59, 60].

In vivo production of ascites containing very large quantities of antibodies have been used for the generation of monoclonal antibodies in certain situations when hybridoma cells do not adapt well *in vitro* conditions. Antibody generation using ascites obtained from animals provides large quantities in a short amount of time which makes it relatively more economical than *in vitro* methods [62, 63]. However, the use of animals for this purpose is tightly regulated; therefore, researchers must provide evidence that the *in vitro* method used has failed to produce sufficient antibodies before approval can be granted for *in vivo* production. Another disadvantage to using *in vivo* production of antibodies in animals is possible contamination of monoclonal antibodies with other non-specific mouse antibodies. Antibodies obtained from the ascites fluid may also be contaminated with viruses and bacteria from the mouse [62, 63].

Scientists have also taken advantage of modern technology and have discovered other ways to produce monoclonal antibodies. These include phage display and the use of transgenic mice. Phage display using recombinant technology has allowed for the construction of smaller antibody fragments like Fab or single chain variable fragment (scFv) in *E.coli* [65]. Typically the

DNA encoding for the heavy and light chain regions are amplified from the cDNA obtained from the mRNA of the spleen of mice immunized with the immunogenic substance. The DNA is the inserted into a phagemid genome which displays the proteins on its phage coat [66]. The immunogenic substance is introduced to the displayed protein on the phage coat and allowed to bind Phages that bind to the immunogenic material with desired affinity are selected by a screening process [67].
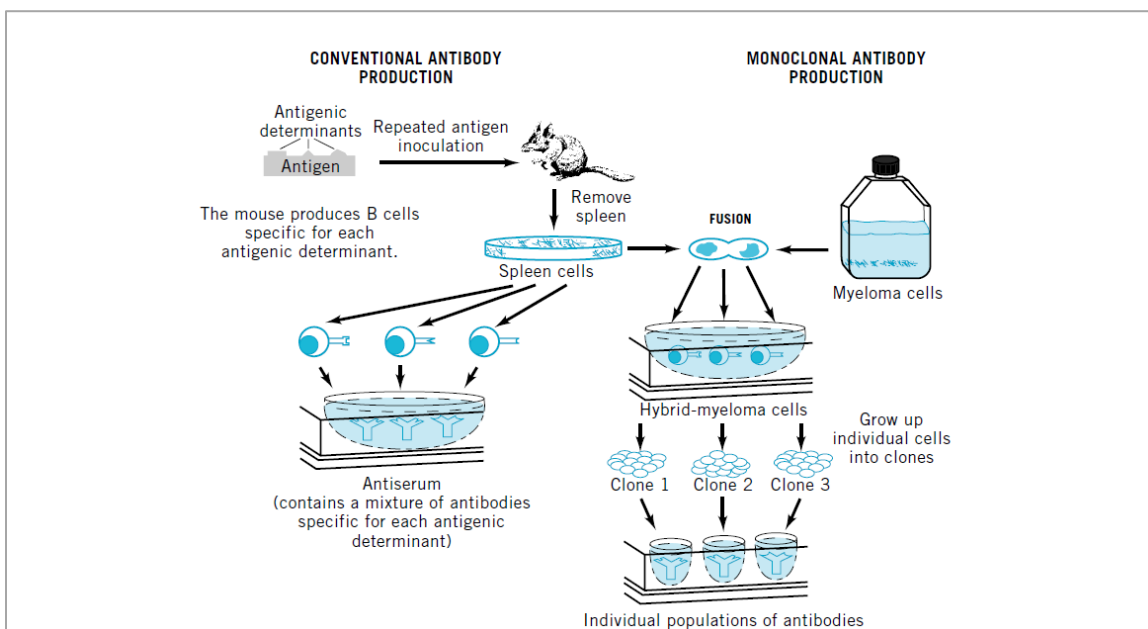
Figure 1.3: Schematic representation of production of polyclonal and monoclonal antibodies. Image obtained from www.wiley.com/legacy/products/subject/life/elgert/CH04.pdf [64].

Apart from the obvious advantage of not using animals in the production of antibodies, the use of phage display to generate monoclonal antibodies of smaller fragments include certain desired pharmacokinetic properties and, reduced immunogenicity. Smaller antibody fragments can also be used in the generation of immunotoxins and gene therapy vectors [56]. However this method also has certain limitations which include time consumption and lack of efficiency as only a relatively small amount of antibodies with desired specificity are typically generated against immunogenic compound. Additionally, the amplification of heavy and light chain genes,

cloning of genes into vector, the number of transformed cells and the difficult expression of antibody fragments in bacteria can compound existing problems in the proper yield of antibody .

Each method used in the generation of antibodies has several advantages and disadvantages. Although all the methods are well established, researchers have continued to fine-tune the process to be less time-consuming, cost effective and accessible so that optimal yield can be attained with the use of each system.

Current Therapeutic Antibodies

For many decades, antibodies have been used for several biotechnological purposes in research, but their greatest potential as the magic bullet lies in the field of therapeutics. In 1986, The Food and Drug Administration (FDA) approved the first monoclonal antibody called muromomab [68]. Muromomab is a murine antibody approved for steroid-resistant solid organ transplant recipient [68]. Since then, there has been 28 more FDA approved therapeutic antibodies (Table 1.1) [69]. These antibodies have been approved for use in treatment of diseases such as cardiovascular disorders, cancers, asthma, arthritis, psoriasis, Crohn's disease, autoimmune disorders and transplant rejection [69].

The use of monoclonal antibodies in particular has garnered tremendous excitement and attention because of the continuous increase in available antigenic targets, the ability to specifically target these antigens and the advances in molecular engineering that has led to the optimization of producing a variety of monoclonal antibodies [69]. These advances have resulted in the generation of chimeric, humanized and fully human antibodies that have significantly lower immunogenicity [70]. Additionally, technological advances such as generation of antibody libraries with mutations within the variable regions by error-prone PCR, *E. coli* mutator strains,

and site-specific mutagenesis, chain-shuffling, randomization of complementarity determining regions have also resulted in the increase in affinity between antibodies and antigens [71, 72].

In certain scenarios, monoclonal antibodies have been used to deliver cytotoxic agents to specific targets [73]. Apart from delivery of therapeutic agent, antibodies have also been used as hyper-immune antibody preparations [74]. These preparations are typically obtained from donors with an elevated titer of a specific antibody obtained as a result of either natural infection or vaccination. These antibodies are typically used for prophylactic purposes [74].

From an economic stand point, monoclonal antibodies form the largest group of biologics under development [75]. In 2007, the eight biggest selling biological therapeutic agents were all antibodies [75]. The increase in development, use and sales of monoclonal antibodies for therapeutics purposes is in part due to the major advances in technology, safety and efficacy established since the introduction of the very first therapeutic monoclonal antibody [75].

Table 1.1: Current FDA approved therapeutic monoclonal antibodies. The table shows a list of all monoclonal antibodies approved as of Feburaary 13, 2013. Other monoclonal antibodies approved but not on the list include Pfizer's Mylotarg (gemtuzumab ozogamicin) which was approved by the FDA in 2000 for acute myelogenous leukemia, but in 2010 Pfizer discontinued its commercial availability in the US and voluntarily withdrew the NDA and Genentech's and Merck's Raptiva (efalizumab) which was approved by the FDA in 2003 for psoriasis, but in 2009 it was voluntarily withdrawn from the market. The contents of this table are a modified version obtained from a [69] published article by Dimitrov and Marks, 2009 [69].

Trade Name	Generic Name	Target	Type	Year of approval	Therapeutic indications
Orthoclone OKT3®	Muromonab-DC3	CD3	murine	1986	Transplantation rejection
ReoPro®	abciximab	GPIIb/IIIa	chimeric	1994	High risk angioplasty
Rituxan®	rituximab	CD20	chimeric	1997	Non-Hodgkin's lymphoma Chronic lymphocytic leukemia Rheumatoid arthritis
Zenapax®	daclizumab	CD25	humanized	1997	Transplantation rejection
Herceptin®	trastuzumab	HER-2	humanized	1998	Breast cancer Metastatic gastric or gastro-esophageal junction adenocarcinoma
Remicade®	infliximab	TNFα	chimeric	1998	Crohn's disease Ulcerative colitis Rheumatoid arthritis Ankylosing spondylitis Psoriatic arthritis Plaque psoriasis
Simulect®	basiliximab	CD25	chimeric	1998	Transplantation rejection
Synagis®	palivizumab	RSV F protein	humanized	1998	Respiratory syncytial virus
Campath®	alemtuzumab	CD52	humanized	2001	B-cell chronic lymphocytic leukemia
Humira®	adalimumab	TNFα	human	2002	Rheumatoid arthritis Juvenile idiopathic arthritis Psoriatic arthritis Ankylosing spondylitis Crohn's disease Plaque psoriasis

Table 1.1: Current FDA approved therapeutic monoclonal antibodies (continued).

Trade Name	Generic Name	Target	Type	Year of approval	Therapeutic indications
Zevalin®	ibritumomab tiuxetan	CD20		2002	Non-Hodgkin's lymphoma
Bexxar®	Tositumomab and iodine 131 tositumomab	CD20	murine	2003	Non-Hodgkin's lymphoma
Xolair®	omalizumab	IgE	humanized	2003	Asthma
Avastin®	bevacizumab	VEGF	humanized	2003	Metastatic colorectal cancer Non-small cell lung cancer Metastatic breast cancer Glioblastoma multiforme Metastatic renal cell carcinoma
Erbitux®	cetuximab	EGFR	chimeric	2004	Head and neck cancer Colorectal cancer
Tysabri®	natalizumab	VLA-4	humanized	2004	Multiple sclerosis (relapsing) Crohn's disease
Lucentis®	ranibizumab	VEGF-A	humanized antibody fragment	2006	Neovascular (wet) age-related macular degeneration Macular edema following retinal vein occlusion
Vectibix®	panitumumab	EGFR	human	2006	Metastatic colorectal carcinoma
Soliris®	eculizumab	Complement C5	humanized	2007	Paroxysmal nocturnal hemoglobinuria
Cimzia®	certolizumab pegol	TNFa	humanized antibody fragment	2008	Crohn's disease Rheumatoid arthritis
Arzerra®	ofatumumab	CD20	human	2009	Chronic lymphocytic leukemia
Ilaris®	canakinumab	IL-1ß	human	2009	Cryopyrin-associated periodic syndromes, including familial cold autoinflammatory syndrome and Muckle-Wells syndrome

Table 1.1: Current FDA approved therapeutic monoclonal antibodies (continued).

Trade Name	Generic Name	Target	Type	Year of approval	Therapeutic indications
Simponi®	golimumab	TNF*a*	human	2009	Rheumatoid arthritis Psoriatic arthritis Ankylosing spondylitis
Stelara®	ustekinumab	IL-12 IL-23	human	2009	Plaque psoriasis
Actemra®	tocilizumab	IL-6	humanized	2010	Rheumatoid arthritis
Prolia® Xgeva®	denosumab	RANKL	human	2010	Postmenopausal osteoporosis Prevention of SREs in patients with bone metastases from solid tumours
Benlysta®	belimumab	BLyS	human	2011	Systemic lupus erythematosus (SLE)
Vervoy®	ipilimumab	CTLA-4	human	2011	Melanoma
Adcetris®	brentuximab	CD30 (conjugate of Mab and MMAE)	Chimeric ADC (antibody drug conjugate)	2011	Hodgkin lymphoma (HL), systemic anaplastic large cell lymphoma (ALCL)

Receptor for Advanced Glycation End-Product (RAGE)

RAGE is involved in various diseases such as diabetes, cancer, Alzheimer's disease, multiple sclerosis, and other abnormal pathological conditions associated with chronic inflammation [77]. RAGE is a cell surface trans-membrane protein encoded by chromosome 6 at the major histocompatibility locus (MHC) class II/III junction [78]. It is classified as a member of the immunoglobulin superfamily because its extracellular region has an immunoglobulin-like fold which consists of a variable type domain commonly known as the V domain, and two constant type domains known as C1 and C2 domain [77] (Figure 1.3). The V domain which serves as the predominant ligand binding site possesses two N-glycosylation sites which have been shown to assist in proper ligand-receptor interaction [79]. In addition to the extracellular

domain, RAGE also consists of a trans-membrane domain and a cytoplasmic tail necessary for

intracellular signal transduction [77].

RAGE can also be expressed as soluble RAGE (Figure 1.4). This form of the receptor

can either be generated by proteolytic cleavage of the membrane bound receptor [80] or by

alternative splicing of the mRNA which results in the production of various isoforms of the

receptor secreted from cells [81]. These are also referred to as endogenous secretory RAGE

(esRAGE). Currently, five human variants of soluble RAGE have been found in different tissues

[81, 82]. Recent studies have described the potential for sRAGE to be used as biomarker for

RAGE related pathologies because it is secreted into the extracellular milieu [83-86].
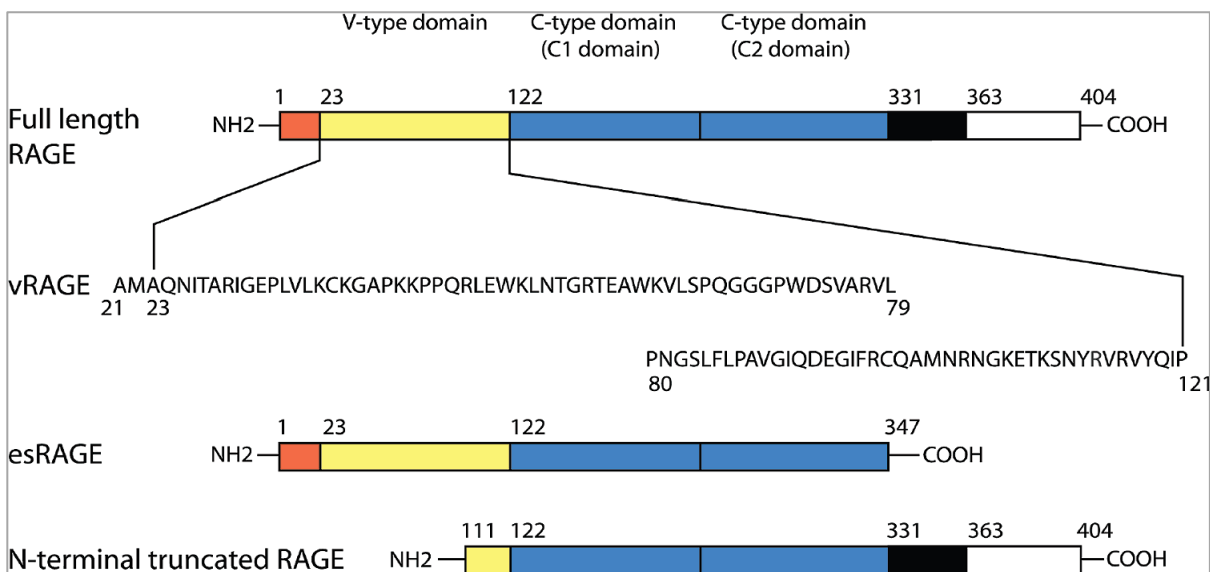
Figure 1.4: Representation of various isoforms of RAGE. Full-length RAGE, esRAGE (sRAGE), and N-terminally truncated RAGE are shown from top to bottom respectively. The signal sequence, variable domain, constant domain, transmembrane-spanning region, and cytoplasmic domain are represented by boxes colored red, yellow, blue, black, and white, respectively [76].

Unfortunately, the use of sRAGE as a biomarker is surrounded by several controversies

because most studies that have compared the levels of sRAGE in a disease state versus

homeostasis did not report total sRAGE [85]. Additionally, levels of sRAGE can vary based on

administration of certain medication. Administration of angiotensin II type 1 receptor blocker (telmisartan) showed a decrease in the levels of sRAGE in patients with hypertension [87] while administration of an angiotensin-converting enzyme inhibitor (perindopril) increased sRAGE levels [88]. Additionally, administration of a statin (atorvastatin) in hypercholesterolemic subjects [89] and rosiglitazone, used in the treatment of type 2 diabetes, resulted in an increase in sRAGE levels [90]. As a result of these confounding factors, the use of sRAGE to evaluate disease progression and monitor effectiveness of therapeutic aid needs to be carefully evaluated.

Depending on the type of cell and environment, engagement of RAGE by it ligand typically results in the activation of multiple downstream signaling events such as p38 mitogen-activated protein (MAP) kinase pathways, stress-activated protein kinase/c-Jun-NH2-terminal kinase (SAPK/JNK), extracellular signal-regulated kinase 1/2 (ERK1/2) [91], and the Wnt signaling pathway [92]. Activation of some of these pathways has been shown to result in the activation of signal transducers and activators of transcription family (STAT3) and transcription factors such as nuclear factor (NF-κB) and cAMP response element-binding (CREB) protein [93]. Many of these pathways have been implicated in the progression of inflammation [77].

Although the full mechanism of activation of downstream signaling in RAGE/ligand interaction is still not clearly understood, because of the structural diversity in ligands, researchers have found RAGE to be present in many cells of the immune system. These inflammatory responses have been observed subsequently after interaction with its ligands [94]. Additionally, RAGE has an NF-κB binding site in its promoter which makes RAGE a direct target gene of NF-κB signaling and has been implicated in the generation of RAGE ligands such as AGE and S100B [95]. Thus, accumulation of RAGE ligand in an area results in the up-

regulation of the receptor itself. The continuous expression of receptor and generation of ligands enables a cycle of sustained inflammation that is deleterious for cells.

RAGE has been shown to be highly expressed during embryonic development but down-regulated in normal healthy adults. The exception is the lung where RAGE is expressed at high levels throughout life [96]. A survey of the distribution of RAGE in tissue by Brett and colleagues in 1993 using monoclonal and polyclonal antibodies toward the receptor, showed that RAGE is also present in pheochromocytes, mononuclear cells, mesangial cells, vascular smooth muscle cells and endothelial cells [97]. They also observed significant amounts of the receptor in the skeletal muscles, lung, heart, liver, uterus, and brain [97]. The presence of the receptor in multiple types of tissue could explain why RAGE has been implicated in the progression of several pathologies such as Alzheimer's, cardiovascular disorders, cancers, and many chronic inflammatory diseases.

RAGE was initially found to bind to adducts modified by non-enzymatic glycosylation occurring on proteins and lipids. These are known as advanced glycation end-products (AGE), hence the name of the receptor. The presence of immunoglobulin domains in the receptor led to the hypothesis that it might bind to other ligands apart from AGEs, as other members of the immunoglobulin superfamily exhibit this characteristic [98]. Subsequent studies discovered the expression of the receptor in conditions not associated with the presence of AGE. These studies implicated RAGE as a receptor modulating various pathophysiological dysfunctions upon interaction with several ligands of structural diversity [99-101]. The ability of RAGE to recognize a varied selection of ligands has led to the hypothesis that it is a pattern-recognition receptor, which suggests that its interaction with the various ligands depends upon recognition of three dimensional structures rather than peptide sequences. Another hypothesis regarding RAGE

and its many ligands has been linked to the large number of positively charged residues present on the surface of the receptor. Researchers have hypothesized that these positive charges form electrostatic interactions with macromolecules possessing an equal amount of negative charges [102]. Currently RAGE is known to recognize a wide range of endogenous ligands, such as amphoterin also known as high mobility group box 1 [91], oxidized low density lipoproteins, macrophage 1 antigen (Mac-1) [103], amyloid aggregates and fibrils [104], and S100 proteins [105]. The next section discusses the different ligands that have been shown to interact with RAGE.

Ligands Associated with RAGE

Advanced Glycation End-Product (AGE)

AGEs have been implicated in chronic hyperglycemia and long-term diabetic complications long before RAGE was discovered [106-109]. AGE products are complex and heterogeneous in nature. Formation of AGEs is initiated by the association of a sugar molecule, particularly a reducing sugar like fructose or glucose, with the free amino groups of proteins, lipids, and nucleic acids. A series of subsequent reactions like dehydrations, oxidation-reduction reactions, and other arrangements, in a number of weeks or months, leads to the irreversible formation of AGEs [110]. This process is known as a maillard reaction. Typically, the formation of AGE products is catalyzed by transition metals but can also be inhibited by certain reducing compounds like ascorbate [111].

The excessive accumulation of AGEs has been shown to alter many physiologic functions like enzyme activity, binding of regulatory molecules, cross-linking of proteins, macromolecular recognition, and endocytosis [112-115]. Studies have shown that the interaction between AGEs and RAGE on the endothelium perturbs endothelial homeostasis by causing

27

abnormalities in the expression of pro-coagulant tissue factors, and by increasing cell adhesion molecules expression, vascular permeability, and transport of macromolecules across the monolayer [116-119]. This inability of endothelial cells to regulate the passage of small molecules and in some cases larger molecules is an early indicator of diabetic complications. Additionally, the interaction between AGEs and RAGE generates oxidative stress in various types of cells and subsequently induces macrophage and platelet activation, thrombosis, and vascular inflammation which are key players in the development and progression of vascular complications in diabetes [120].

According to the Diabetes Control and Complications Trial (DCCT), intensive control of blood glucose levels can only assist in slowing down progressive complications such as retinopathy, diabetic nerve disease, and diabetic kidney disease [121]. Unfortunately, the proposed therapy includes multiple visits to health care professionals thereby doubling the cost of managing the disease. Additionally, these intensive interventions increase the risk in hypoglycemia which could further complicate patients' health [121]. Consequently, the need for novel therapeutic agents to prevent diabetic vascular complications is paramount.

Apart from diabetic complications, AGE products have also been implicated in end stage renal disease [122], rheumatoid arthritis [123] and Alzheimer's [124]. Histological analyses have also shown accumulation of AGE products in the renal cortex, coronary atheroma, mesagium, cardiac muscles, liver and lung [120, 125]. AGE products can also accumulate within the body through exogenous sources such as food subjected to heat and many tobacco products [126, 127].

Many efforts have been made towards therapeutic interventions to target AGE products. These include the reduction of cross-link formation of AGE [120], enhanced cellular degradation of AGEs and subsequent uptake for clearance to prevent accumulation [128], quenching

28

hydroxyl radicals with the use of antioxidants such as aminoguanidine [129], vitamin C [130] and nicarnitine [131]. However, the heterogeneous nature of AGE products poses a substantial problem because the complex reaction involved in the formation of these products has not yet been completely elucidated. Additionally, the use of aminoguanidine in a phase three clinical trial showed the development of pernicious anemia, development of anti-nuclear antibodies, and crescentic glomerulonephritis [132]. Another area that has recently been explored is the use of antibodies that can target the receptor for AGE. Neutralizing antibodies will inhibit the interaction between AGE and RAGE and thus prevent AGE dependent intracellular signaling [133]. The use of a neutralizing antibody against the receptor that interacts with AGE could serve as a good candidate for therapeutic interventions in RAGE/AGE related pathologies.

S100 Proteins

Many scientific studies have shown compelling evidence associating the S100 family of proteins with various pathologies including cancers, cardiomyopathy, neurodegeneration, and inflammation [101, 134-136]. The S100 proteins are named as such because the first member of the family that was discovered is 100% soluble in ammonium sulfate at neutral pH [137]. So far, there are 21 members in the S100 family [138]. S100 proteins are typically small molecular weight calcium binding proteins that are expressed only in vertebrates. The calcium binding domains are connected by a hinge region [139] and are critical for conformational changes that result in the exposure of binding sites on the protein. Certain members of the family also bind to other metals such as copper and zinc [140]. S100 proteins can also form monomers, heterodimers and oligomers [105].

S100 proteins are involved in a variety of normal physiological functions such as cell cycle progression and regulation, cell differentiation, signal transduction, protein

29

phosphorylation, cell motility regulation, calcium homeostasis, cell growth and migration, cytoskeletal interactions, and membrane trafficking [138]. Clustering of many S100 genes has been found in the chromosome (1q21) region, which is susceptible to rearrangements, linking S100 proteins to cancer [141]. For the most part, S100 proteins share a close amino acid sequence which allows several members of the family to bind to the same proteins but exhibit different cellular activities [138, 142, 143]. Therefore, depending on the type of cancer, some members in the family are tumor suppressors while some act as tumor promoters [143].

In clinical settings, S100 proteins have been used to monitor diseases like chronic inflammation, neurodegeneration, cardiomyopathies, atherosclerosis, and cancers [144]. A significant difference in expression levels of S100A8, S100A9 and S100A12 was observed in healthy patients as compared to patients with inflammatory diseases such as rheumatoid arthritis, peritonitis, and bowel diseases [143]. In 1998, Rabee and colleagues were able to show high a concentration of S100B protein in patients after a traumatic brain injury [145]. Subsequently, many researchers discovered an increase in S100B and S100A6 concentrations in neurological pathologies such as Alzheimer's disease, Down syndrome and schizophrenia [134, 138, 142, 146]. Researchers have discovered that many of these S100 driven processes are mediated by the interaction with RAGE [101, 147, 148]. Interaction between RAGE and S100 proteins can differentially modulate cellular activities which can either result to cellular apoptosis or increased cellular proliferation, depending on the type and concentration of the S100 protein, via downstream signaling pathways [149]. Inhibition of activation of signaling pathways, by blocking the binding site of S100 proteins on its extracellular receptor, will reduce deleterious cellular activities associated with S100 protein/RAGE interactions.

Beta Amyloid Peptides

Although Alzheimer's disease (AD) is not completely understood, the molecular events involved in Alzheimer's disease include the cleavage of the amyloid precursor proteins (APP) by the secretase enzymes. The extracellular domain of APP, which is normally expressed in many tissue types but is more prevalent in the brain [150], is cleaved by β-secretase (β-site amyloid precursor protein cleaving enzyme, BACE1) producing an APP C-terminal fragment (APPs β). APPs β is further cleaved within the trans-membrane domain by γ-secretase, resulting in the release of β-amyloid (Aβ) peptides [151-154]. The continuous accumulation of Aβ in the brain is a central pathological event in Alzheimer's disease.

Aβ can bind to RAGE present on neurons, astrocytes, microglia and cells of the blood-brain barrier like endothelial and smooth muscle cells resulting in increased expression of the receptor as well as increased transport of Aβ across the blood brain barrier in a RAGE-dependent manner. Additionally, the central nervous system (CNS) employs microglia cells in its defense against infectious entities. The deposition of extracellular Aβ in the brain results in the recruitment of activated microglia which serves as mediator for neuro-inflammation. Microglia can secrete several pro-inflammatory cytokines such as interleukin (IL)-1β, M-CSF, macrophage inflammatory protein (MIP)-1α, IL-6, and nitric oxide (NO) [155, 156]. Also, the interaction between Aβ and RAGE on microglia has been shown to result in the eventual induction of NF-κB, as a result of generation of oxidative stress [100, 157-159].

A combination of these events leads to the progressive decline of brain cells associated with AD. There are several existing drug therapies available for the treatment of AD; unfortunately, the blood brain barrier (BBB) efficiently and effectively controls the passage of substance to and from the brain. Current therapies available in the treatment of AD facilitate the

transport of drugs across the BBB by employing the use of transporters, pumps or receptors

present on the brain endothelium. However, these strategies have shown limited success in

delivering the drugs into the brain [160]. The use of anti-RAGE antibody has been shown to

block the binding sites on RAGE on the surface of endothelial cells [161], preventing the access

of Aβ to RAGE which would decrease the amount of total Aβ uptake in the brain and generation

of inflammatory cytokines such as TNFα [100].

Antibodies generated against RAGE could be proteolytically processed to Fab Fragments

which could pass through the leaky BBB that is characteristic of AD. These antibody fragments

could also be used to monitor levels of RAGE relating to different stages in AD. Early diagnosis

would allow for administration of therapeutic measures during the early onset of AD. The

administration of therapeutic measures received during earlier stages of the disease could

eliminate extensive cognitive impairments and deterioration of brain cells which is crucial in the

prevention of advanced stages of the disease.

High Mobility Group Box 1 (HMGB1)/Amphoterin

Amphoterin is a small protein consisting of 215 amino acids and was named High

Mobility Group Box 1 (HMGB1) because of its ability to migrate quickly during electrophoresis

[162]. HMGB1 contains an unusual amount of positively charged amino acid and therefore

migrates slightly further than expected from its actual molecular weight of approximately 25 kDa

[163]. It consists of two DNA binding domains referred to as HMGB box A and B and a

negatively charged amino acid tail that regulates intercellular interactions [164]. HMGB1 is

expressed abundantly in mammals, typically in the nucleus. Expression of HMGB1 has also been

observed in the cytoplasm, the external side of the plasma membrane, and the extracellular

milieu [165, 166].

HMGB1 was initially thought to bind to the surface of neuroblastoma cells and brain neurons to initiate neurite extension and was named heparin binding p30 protein (amphoterin) [167, 168]. A few years later, another protein extracted from the thymus of a calf named HMG1 had an identical sequence as amphoterin [169, 170]. Intracellularly, HMGB1 binds to DNA to induce a bend in its structure which facilitates communication between DNA and regulatory proteins such as tumor suppressor (p53), NF-κB, recombination activating gene 1/2 (RAG 1/2), homeobox containing proteins, and steroid hormone receptor [171]. Therefore it has been linked to the regulation of transcription, replication, and DNA repair [172] . It has also been linked to regulation of pro-inflammatory activities [173], oligomerization of amyloid β peptide [174], and cell differentiation [175].

RAGE was first connected to HMGB1 when the search for ligands binding to the receptor was conducted using tissue extract [99]. The research conducted by the authors led to the discovery that HMGB1 binds to RAGE with nano-molar affinity. Interestingly, the C-terminal motif of HMGB1 that interacts with the receptor shares similar sequence homology with the N-terminal motif of S100 protein that binds to RAGE [176]. In neuroblastoma cells, studies have shown that HMGB1/RAGE interaction induced cytosolic signaling involved in cell motility regulation and neurite extension [99, 177]. Downstream signaling induced by HMGB1/RAGE interaction involves classic RAGE-mediated activation of NF-κB, which is dependent on activation of MAPK pathway [91, 178, 179]. These signaling induced by HMGB1/RAGE interaction have been associated with intestinal barrier dysfunction [180], cancer progression [91, 181], and atherosclerosis [182]. Blocking the interaction between HMGB1 and RAGE with antibodies specific for the receptor will suppress downstream signaling and attenuate the progression of HMGB1/RAGE associated pathologies.

Hypothesis and Project Goal

Although the role of RAGE in a large number of diseases has been demonstrated, there is currently no monoclonal antibody targeting RAGE in clinical trials. Blocking the interaction between RAGE and its ligands using either the soluble form of the receptor (sRAGE) or anti-RAGE polyclonal antibodies has been shown to reduce RAGE mediated cellular damages in animal models. However, the use of sRAGE as a therapeutic agent to act as a decoy for the membrane bound receptor will not only act as an antagonist to RAGE but to other receptors that require interaction with those ligands to carry out normal physiological functions. Additionally, polyclonal antibodies recognize multiple epitopes which results in increased non-specificity and undesired cross reactivity.

Hence, we generated new monoclonal antibodies against ligand specific domains of RAGE that will inhibit RAGE activation by its ligands. We hypothesize that using the generated antibodies in the blockade of the ligand-RAGE interaction and eventual inactivation of downstream pathways may serve as a novel therapeutic strategy for the treatment of RAGE dependent pathologies. These antibodies could also be used as research and diagnostic tools . In order to achieve this goal, the generated panel of monoclonal antibodies was characterized *in vitro* on recombinant RAGE domains and on mammalian cells. Subsequently, the generated monoclonal antibodies were used in cell-based assays to determine their potential mechanisms of action and finally in an animal model to observe their potential diagnostic and therapeutic properties.

CHAPTER 1: DEVELOPMENT AND CHARACTERIZATION OF NEW MONOCLONAL ANTIBODIES AGAINST THE RECEPTOR FOR ADVANCED GLYCATION END-PRODUCT (RAGE)

Introduction

In the last decade, RAGE has been identified as a central signal transducing receptor responsible for mediating long-lasting downstream activation in various cell types and animal models [183-186]. Several publications have shown that RAGE-ligand interaction leads to activation of a variety of intracellular signaling pathways involving the generation of ROS, subsequent activation of NF-κB, and phosphorylation of several kinases [77]. These intracellular events can result in the expression of genes regulating cytokine production and growth factors such as interferon-γ, TNF-α, IL-1, IGF-1 and PDGF [77, 187]. Additionally, these events can also result in the accumulation of adhesion molecules (ICAM-1, VCAM-1) and migration of macrophages that leads to sustained inflammation and subsequent disruption of several biological processes [119].

Blocking the interaction between RAGE and its ligands can diminish the pathological effect mediated via RAGE and prevent deleterious effects. In 1996, Wautier and colleagues were able to successfully use sRAGE to reduce hyperpearmeability in diabetic rats [118]. It was discovered that sRAGE can compete with membrane bound RAGE for ligands without activating downstream signaling pathways involved in a typical full-length receptor-ligand interaction because sRAGE is lacking the cytoplasmic tail necessary for signal transduction [118]. Subsequently, many efforts to block the interaction between RAGE and its ligands have predominantly revolved around the use of sRAGE. Researchers were able to use sRAGE to suppress the acceleration of advanced atherosclerosis in diabetic mice, restore wound healing in

diabetic mice, suppress tumor growth and metastases, and reduce several inflammatory responses involved in RAGE related pathologies [91, 118, 184, 188-194]. However, the use of sRAGE as a therapeutic agent to act as a decoy for the membrane bound receptor will not only act as an antagonist to RAGE but to other receptors that require interaction with those ligands to carry out normal physiological functions.

Researchers have also been able to demonstrate the use of anti-RAGE polyclonal antibodies to block the interaction between RAGE and its ligands [104, 149]. Unfortunately, polyclonal antibodies recognize multiple epitopes which results in increased non-specificity and undesired cross reactivity therefore renders them undesirable candidate for therapeutic purposes. Blockade of RAGE has also been achieved with the use of monoclonal antibodies to reduce RAGE mediated cellular damages [195, 196]. Researchers have been able to show the neutralizing effects of anti-RAGE monoclonal antibodies in the suppression of adverse effects on the kidneys of diabetic animal models [195, 197] and the reduction of atherosclerosis on uremic mouse models [196]. Although the effectiveness of anti-RAGE antibodies has been demonstrated in a number of diseases, there is currently no monoclonal antibody targeting RAGE in clinical trials. Hence, we propose to generate new monoclonal antibodies against ligand specific domains of RAGE that will inhibit RAGE activation by its ligands. Blockade of the ligand-RAGE interaction and eventual inactivation of downstream pathways may be novel therapeutic strategies for the treatment of RAGE-dependent pathologies. These antibodies could be used as new research, diagnostic and therapeutic candidates.

Materials and Methods

Expression and Purification of sRAGE and the RAGE Domains

DNA of human V and VC1C2 domains were amplified from pHGST-2T RAGE using a specific set of primers associated with the restriction sites, Xho1 and Nde 1, on pET-15b (Novagen). The amplified RAGE domains were subsequently ligated into pET-15b which has a T7/lac promoter and a gene for ampicillin resistance. The final construct contained a 6 x histidine tag at the N-terminal and the human V and VC1C2 domains at the C-terminal. pET-15b carrying human V and VC1C2 domains were transformed into T7 express competent *E.coli* cells (New England Biolabs) and plated on LB/ampicillin selective agar plates. Colonies present on selective agar plates were cultured in LB/ampicillin media until an optical density (OD) = 1. Cells were then induced with isopropyl β-D-1-thiogalactopyranoside (IPTG). After induction, cells were grown overnight at 22°C. Following overnight incubation in a shaker, the bacterial cell pellet was collected by centrifugation and lysed by sonication to release recombinant V and VC1C2 domain into the supernatant. The collected supernatant was filtered and passed onto a nickel chromatography column for purification. The purified fraction was eluted in a high concentration of imidazole and subsequently dialyzed twice in PBS pH 7.4. The dialyzed fraction was concentrated, aliquoted, and stored at -80ºC. SDS-PAGE indicated >98% purity of the final V and VC1C2 domain. Expression of V, C1, and C2 domain were purified as described by Dr. Leclerc [180]. The sRAGE was expressed in *Pichia pastoris* and purified as described previously [198].

Expression and Purification of Recombinant Human S100B (Provided by Varsha Meghnani,
Department of Pharmaceutical Sciences, NDSU)

Recombinant S100B was expressed in *E. coli* and purified as previously described [199]. The purity of the protein was evaluated by SDS-PAGE. After dialysis against phosphate-buffered saline (PBS), bacterial endotoxin was removed from the purified S100B by treatment with high capacity endotoxin removal resin (Pierce). The absence of endotoxin contamination was assayed Pierce LAL Chromogenic Endotoxin Quantitation Kit (Pierce).

Expression and Purification of Recombinant Human S100A6 (Provided by Dr. Vetter,
Department of Pharmaceutical Sciences, NDSU)

Human S100A6 gene was cloned into the pEX-N-GST vector from Origene. The resulting fusion construct contains an N-terminal His6-tag, followed by GST, a tobacco etch virus (TEV) protease cleavage site and human S100A6 at the C-terminal end. The protein was expressed in BL21 (DE3) cells in LB medium at 37ºC for 6 h. The protein was expressed well and was found to be in the soluble fraction. S100A6 purification was done in three steps. First, the GST-fusion was purified from the clarified cell lysate by GST-affinity chromatography using a GST-trap column (GE Healthcare). Next, the fusion protein was cleaved using TEV protease overnight. S100A6 was isolated after complete cleavage by hydrophobic interaction chromatography using a phenyl-sepharose column (GE Healthcare). S100A6 was eluted using 2 mM EDTA, concentrated, aliquoted, and stored frozen at -80ºC. SDS-PAGE indicated >98% purity of the final S100A6 protein.

Recombinant Human S100A8/A9

S100A8/A9 was a generous gift from Professor T. Vogl, University of Münster, Germany.

Preparation of Amyloid Beta Aggregates (AβA)

AβA were prepared by dissolving the lyophilized peptide, $AβA_{1-40}$ (CalBiochem), at 1mM in PBS. The dissolved protein was incubated for 2h at room temperature (RT).

Generation of Monoclonal Antibodies (Mab) in Hybridomas

Mice were immunized with sRAGE, which was produced in the yeast *Pischia pastoris* as previously described [198, 200]. The Hybridoma Core Facility of the University of Florida at Gainesville performed the immunization of the animals according to standard protocols. Briefly, female Balb/CByj mice between 6-8 weeks were immunized with sRAGE. Subsequently, the mice received additional immunization and were test bled. The serum of the immunized mice was tested for the presence of antibodies against sRAGE using standard ELISA. Additional immunization and serum testing was continued until the serum reached a high titer. The immunized mouse showing the best titer was boosted with sRAGE four days prior to the extraction of the lymphocytes. The mouse was sacrificed according to standard procedures and its spleen was extracted. The lymphocytes in the spleen were isolated and fused with mouse myeloma cells using 50% polyethylene glycol (PEG) 1500 as fusion agent. The fused cells were grown in media selective for B-cells myeloma hybrids. The supernatants of hundreds of hydridomas were characterized by ELISA against sRAGE produced from yeast. The hybridoma supernatants that gave the strongest positive signals in ELISA against sRAGE were further tested against the isolated recombinant RAGE domains expressed in *E.coli*: V, C1, C2, C1C2 and VC1C2. The 10 strongest hybridomas were then cloned into single colonies by limited dilution. The recombinant domains of RAGE and sRAGE were expressed in *E.coli* and yeast respectively and purified as previously described [198, 200].

Production and Purification of Monoclonal Antibodies (IgGs)

In a small scale production, hybridoma cells were cultured in batches of 75 cm^2 cells culture flasks, in DMEM containing 10% ultra-low IgG FBS (Invitrogen), 50 μg/ml gentamicin (Gibco) in the presence of antibiotic-antimycotic solution (ABAM) (Gibco). To obtain larger amounts of antibodies, approximately 1.5 x 10^6 viable cells / ml from a pre-culture was collected and re-suspended in 15 ml fresh medium (DMEM, 15% ultra-low IgG FBS, 50μg/ml gentamicin in the presence of ABAM solution.) The re-suspended cells were cultured in a CELLine CL 1000 flask (Integra). Supernatants from both production methods were collected every week and IgGs were purified from the supernatant of cultured hybridoma cells using a single step affinity chromatography method. Briefly, Protein G Sepharose 4 beads (GE Healthcare) were packed in a low pressure gravity chromatography column (Bio-rad) using PBS pH 7.4 as a binding buffer. Supernatants of cultured hybridoma cells were passed through the column and washed with PBS. An elution buffer containing 20 mM glycine at pH 2.2 was used to elute the IgGs. The eluted fractions were immediately neutralized with 1M Tris HCl pH 8.0 (10% volume of fraction). The percentage purity of the purified IgGs was determined by SDS-PAGE that were stained with commassie blue.

Enzyme Linked Immunosorbent Assay

High binding microtiter ELISA plates (Santa cruz) were coated with 50 μl of recombinant RAGE domains (V, C1, C2 & VC1C2) at a concentration of 50 μg/ml and with sRAGE at 100 μg/ml. Following adherence of recombinant RAGE domains and sRAGE overnight at 4°C, the coated wells were blocked with 3% BSA/TBS for 2 hours. Titrated concentrations of IgGs were added to the wells, in the presence of 1.5% BSA/PBS. After incubation at room temperature for 1 h, the wells were washed eight times with 0.05% TBS-T. An alkaline phosphatase (AP)

conjugated anti-mouse IgG secondary antibody (Jackson ImmunoResearch) was added in the presence of 1% BSA/PBS (diluted 1:3000). After 1 hour incubation at RT and a final wash with 0.05% TBS-T, the plates were developed with an AP substrate, *para*-nitrophenylphosphate (pNPP) (Gold biotechnology), the optical density was measured at 405 nm with a Biotek ELx-800 universal plate reader.

Surface Plasmon Resonance

The experiment was run on a Reichert SR7500DC instrument. The surface plasmon resonance experiments were run as previously described with some slight modifications [149]. Briefly, carboxy-methyl dextran-coated sensor chips were activated with 1-ethyl-3-(3-dimethylaminopropyl) carbodiimide/*N*-hydroxysuccinimide. The RAGE domains and sRAGE at a concentration of 50 µg/ml in 20 mM sodium acetate at pH 5 were injected over the sensor chip. After immobilization of the proteins, the surface of the sensor chip was blocked with ethanolamine prior to measurements. A series of increasing concentrations of IgGs was injected over the flow cells in PBS. Between each cycle of binding, the surface was regenerated by 1-min contact with 20 mM glycine at pH 2.2 containing 10% glycerol. The sensorgrams were analyzed by global analysis using the Scrubber 2.0, Biologic software.

Cell Culture Treatment

HEK-293/RAGE cells (Gift from Professor Heizmann, Children's Hospital, Zürich Switzerland) were grown in OPTI-MEM I, reduced medium supplemented with 4% fetal bovine serum (FBS), 1 mg/ml G418 solution (Gibco), 100 IU/ml penicillin, and 100 µg/ml streptomycin (Gibco). The cells were maintained at 37°C in a humidified incubator containing 95% air and 5% CO_2.

Fluorescence Activated Cell Sorting

HEK-293/RAGE cells were cultivated to approximately 60% confluence and detached using 5 mM EDTA/PBS. The detached cells were washed with 1% FBS/PBS and seeded in 96 well plates. The IgGs at titrated concentrations in the presence of 1% FBS/PBS were added to the wells. After incubation at 4°C for 30 minutes, the wells were washed with 1% FBS/PBS, and FITC conjugated anti-mouse IgG secondary antibody (Jackson ImmunoResearch) in 1% FBS/PBS was added for 20 mins at 4°C. After a final wash with 1% FBS/PBS, the fluorescence of the bound antibody was measured by an Accuri C6 flow cytometer (Core Biology, Department of Chemistry and Biochemistry, NDSU).

Immunofluorescence

HEK-293/RAGE cells were cultured on collagen coated slide until a confluence of approximately 60% was obtained. Cells were subsequently fixed with 4% paraformaldehyde in PBS. Fixed cells were then blocked with 1% BSA in PBS for 30 minutes and incubated with 100 nM IgGs diluted in 1% BSA/PBS for an hour at room temperature. Following incubation, cells were washed with PBS and incubated with FITC conjugated anti-mouse IgG secondary antibody (Jackson ImmunoResearch) in 1%BSA/PBS (diluted 1:1000) for 1 hour at room temperature. Cell nuclei were stained with Hoechst dye (Invitrogen) which stains DNA with bright fluorescent blue. After a final wash with PBS, the fluorescence of the antibody bound to RAGE on the cell surface was revealed using an Olympus fluorescence microscope.

Competition Assay

RAGE ligands specific for their extracellular domains were selected to compete against the generated antibodies. First, 50 μl of RAGE domain at a concentration of 50 μg/ml was coated on high binding ELISA plates and incubated overnight at 4°C. The coated wells were

blocked with 3% BSA/PBS. The IgGs were added at a fixed concentration (100 nM) in the

presence of increasing concentrations (0 to 50 μM) of RAGE ligands (S100A6, S100A8/A9,

S100B or AβA). The antibody/ligand mixtures were incubated at room temperature for 30 mins

before the complexes were added to the wells and incubated for an hour at room temperature.

Following incubation, the wells were washed with TBS/Tween and incubated with AP

conjugated anti-mouse IgG secondary antibody (Jackson ImmunoResearch) in 1% BSA/PBS

(1:3000) for 30 mins. After a final wash, the bound antibodies were detected with pNPP and the

plates were read at 405nm with a Biotek ELx-800 universal plate reader.

Statistical Analysis

Unless specified, data shown are presented as means ± standard deviation (SD). The

binding curves on the ELISA and FACs were fitted with a 1:1 binding site model.

Results

Purified Recombinant RAGE Domains

We utilized the *E.coli*'s system for the expression of recombinant RAGE domains,

S100A6 and S100B. We chose *E.coli* because it is the most wildly used host for the production

of recombinant proteins. The percentage purity of purified RAGE domains was determined by

SDS-PAGE. Staining with commassie blue confirmed that the eluted V and VC1C2 domains

were of > 95% pure and that they migrated at approximately 15 kDa (actual size is 14406.7) and

approximately 37 kDa (actual size is 35050.9), respectively, in reducing conditions (Figure 2.1).
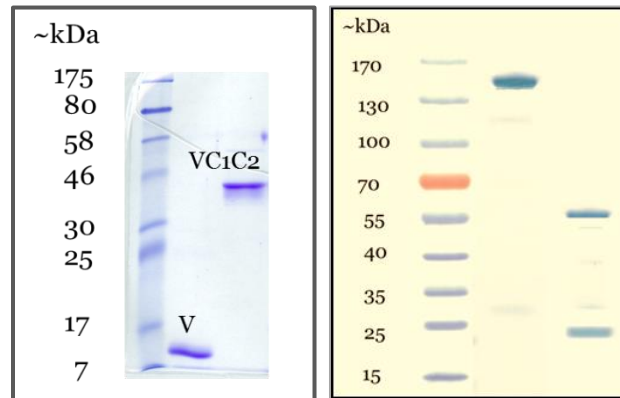
Figure 2.1: Purified fraction of V and VC1C2 recombinant RAGE domain. From left: purified V and VC1C2 recombinant RAGE domains under reducing conditions. Right: a representative image of the purified IgGs (From left to right, lane 1; ladder, lane 2; non-reduced form of IgG at ~150kDa and lane 3; reduced form of IgG at ~50 kDa and at ~25 kDa).

Panel of Generated Monoclonal Antibodies

Using the mouse immune system and hybridoma technology, we have successfully developed a series of monoclonal antibodies (IgGs) that specifically bind to the various domains on RAGE (Table 2.1). The antigen of interest, sRAGE, used in the immunization of the mice was generated in the yeast *Pischia pastoris*. We have chosen the yeast system to express sRAGE, because expression of sRAGE in yeast results in glycosylation of the protein. Glycosylation of protein has been known to assist in protein-protein interaction [79, 201]. We selected 10 out of 32 hybridoma supernatants that gave the strongest positive signals in ELISA against sRAGE. These 10 selected clones were further cloned by limited dilution and the resulting monoclonal hybridoma clones were further characterized for specificity against the isolated recombinant RAGE domains (V, C1, C2, C1C2 and VC1C2) expressed in *E.coli*. Out of the 10 clones selected, 5 clones (2A11, 3D1, 4D3, 5H5 and 2H9) showed specificity towards the V domain of RAGE, 3 clones (2A12, 2B6 and 6B8) showed specificity towards the C2 domain and 1 clone (2D3) showed specificity to the C1 domain. The clone 6B12 did not react against a single domain but was reactive against VC1C2, suggesting binding to a conformational epitope. The percentage purity of the purified IgGs was determined by sodium dodecyl sulfate polyacrylamide

44

gel electrophoresis (SDS-PAGE). Staining with commassie blue confirmed that the eluted

proteins were of > 95% purity and that they migrated at approximately 150 kD in non-reducing

conditions (Figure 2.1). The heavy chains and light chains migrated at approximately 50 kD and

25 kD respectively in reducing conditions (Figure 2.1).

Table 2.1: Reactivity of hybridoma supernatants against purified RAGE domains (V, C1, C2, C1C2 and VC1C2) by ELISA. + indicates a positive signal; - indicates a signal of the same level as the background.

	2A11	2A12	2B6	6B8	6B12	2D3	3D1	4D3	5H5	2H9
V	+	-	-	-	-	-	+	+	+	+
C1	-	-	-	-	-	+	-	-	-	-
C2	-	+	+	+	-	-	-	-	-	-
C1C2	-	+	+	+	-	+	-	-	-	-
VC1C2	+	+	+	+	+	+	+	+	+	+

Binding Affinity on Recombinant RAGE Domains and sRAGE

The interaction between the purified IgGs and the recombinant domains of RAGE was

evaluated by ELISA. In certain cases, glycosylation can alter the interaction between an antibody

and its target [202]. Therefore, our aim was to evaluate the effects of glycosylation between the

generated antibodies and RAGE. The glycosylation properties occurring on sRAGE might

interfere with proper adherence to the wells on the ELISA plate; therefore, the concentration

used to coat the ELISA plates was doubled compared to that of the non-glycosylated domains of

sRAGE. We examined the titration curves obtained from the binding of the generated antibodies

with recombinant VC1C2 domain and sRAGE. As expected, all generated antibodies bound to

sRAGE and VCIC2 with nanomolar affinity (Table 2.2). We also observed that the titration

curves obtained from all generated antibodies display similar binding pattern with VCIC2 and

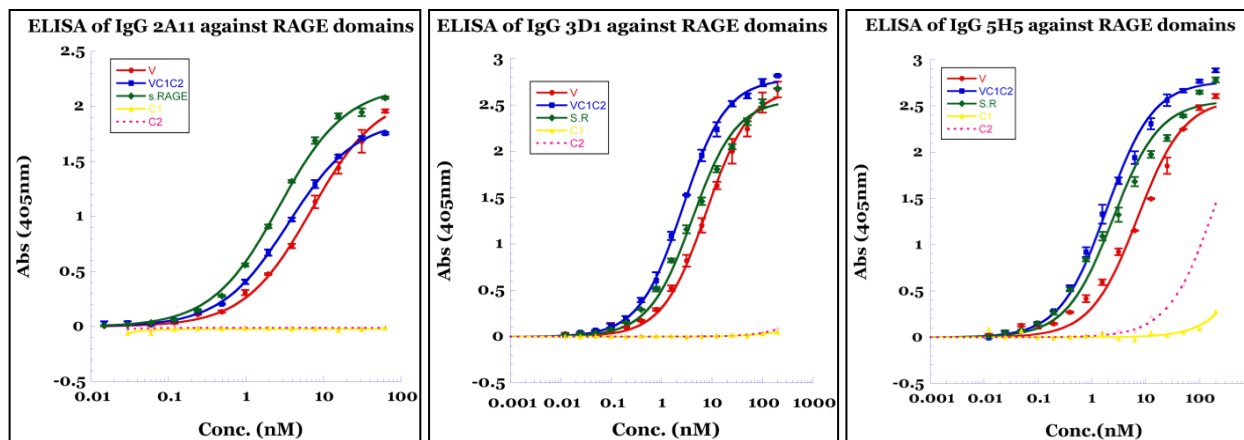sRAGE except for 6B12 (Figure 2.2 & 2.3).

Figure 2.2: Binding of IgG 2A11, 3D1 and 5H5 to V, VC1C2, sRAGE, C1 and C2 as determined by ELISA. From left to right, binding of IgG 2A11, 3D1 and 5H5 to V, VC1C2, sRAGE, C1 and C2 as determined by ELISA. Binding affinities were as follows: For IgG 2A11, K_D (V domain): 7.01 +/- 0.37 nM, K_D (VC1C2): 3.6 +/- 0.09 nM; K_D (sRAGE): 2.7 +/-0.14 nM. For IgG 3D1, K_D (V domain): 7.6+/- 0.43 nM, K_D (VC1C2): 2.6 +/- 0.09 nM; K_D (sRAGE): 4.1 +/-0.4 nM. For IgG 5H5, K_D (V domain): 7.1 +/- 0.9 nM, K_D (VC1C2): 1.9 +/- 0.14 nM; K_D (sRAGE): 2.5 +/- 0.4 nM. All experiments were performed in triplicates. The standard deviation is indicated by the error bar on each point on the curve.
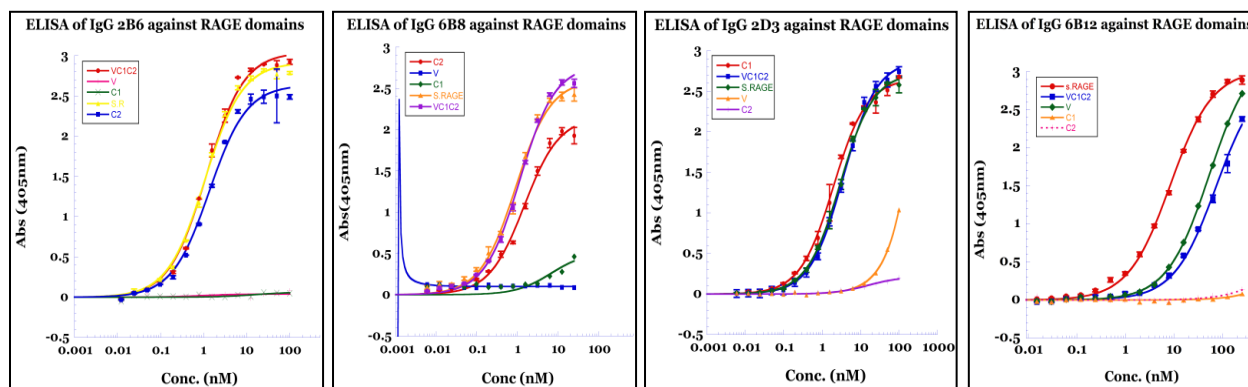

Figure 2.3: Binding of IgG 2B6, 6B8, 2D3 and 5H5 to V, VC1C2, sRAGE, C1 and C2 as determined by ELISA. From left to right, binding of IgG 2B6, 6B8, 2D3 and 5H5 to V, VC1C2, sRAGE, C1 and C2 as determined by ELISA. Binding affinities were as follows: For IgG 2B6, K_D (C2 domain): 1.36 +/- 0.09nM, K_D (VC1C2): 1.16 +/- 0.08nM; K_D (sRAGE): 1.07 +/- 0.06nM. For IgG 6B8, K_D (C2 domain): 1.46+/- 0.13nM, K_D (VC1C2): 1.1 +/- 0.07nM; K_D (sRAGE): 0.9 +/-0.08nM. For IgG 2D3, K_D (C1 domain): 1.97 +/- 0.09nM, K_D (VC1C2): 3.5 +/- 0.15nM; K_D (sRAGE): 2.95 +/-0.11nM. For IgG 6B12, K_D (VC1C2) > 72.6 +/- 5.55nM; K_D (sRAGE): 8.3 +/-0.3nM. All experiments were performed in triplicates. The standard deviation is indicated by the error bar on each point on the curve.

46

We observed that 6B12 bound with a stronger affinity (K_D = 8.3 +/- 10.3 nM) to sRAGE than to VCIC2 (K_D > 72.6 +/- 5.55 nM). This suggests that the interaction of 6B12 to the receptor is glycosylation dependent while the interaction of the other antibodies to the receptor (2A11, 5H5, 3D1, 2B6, 6B8 and 2D3) is glycosylation independent. The titration curves obtained from the ELISA also confirmed the specificity of 2A11, 5H5 and 3D1 to the V domain (Figure 2.2), the specificity of 2B6 and 6B8 to the C2 domain (Figure 2.3) and that of 2D3 to the C1 domain (Figure 2.3).

Table 2.2: K_D Values of the generated antibodies for their specific domains by ELISA. (-) represents non-specific binding to RAGE domain. Hybridoma clone 2H9, 2A12 and 4D3 (not included in table) did not generate antibodies; no values were obtained for binding affinity. The standard deviation is indicated. All values are expressed as nanomolars (nM).

Clones Domain	2A11	3D1	5H5	2B6	6B8	2D3	6B12
V	7.01 +/- 0.37	7.6 +/- 0.43	7.1 +/- 0.9	-	-	-	-
C1	-	-	-	-	-	1.97 +/- 0.09	-
C2	-	-	-	1.36 +/- 0.09	1.46 +/- 0.13	-	-
VC1C2	3.6 +/- 0.09	2.6 +/- 0.09	1.9 +/- 0.14	1.16 +/- 0.08	1.1 +/- 0.07	3.5 +/- 0.15	>72.6 +/- 5.55
sRAGE	2.7 +/- 0.14	4.1 +/- 0.4	2.5 +/- 0.4	1.07 +/- 0.06	0.9 +/- 0.08	2.95 +/- 0.11	8.3 +/- 0.30

Binding Affinity as Determined by Surface Plasmon Resonance (SPR)

We used SPR to further investigate the binding affinity of the generated antibodies to recombinant RAGE domains. SPR can be used to study biomolecular interactions in real time by providing high-quality kinetic data that can be calculated from association ('on rate', k_a) and dissociation rates ('off rate', k_d) provided by the SPR signal (response unit) [203]. Table 2.3 summarizes the affinity parameters obtained from the interaction between RAGE domains and all the generated antibodies. Analysis of the sensorgrams obtained from each antibody with its

specific domain after fitting with a 1:1 binding site model (Figure 2.4, 2.5 and 2.6), revealed

binding constants at a nano-molar affinity except for 6B12 and 2D3 (Table 2.3) which revealed a

binding constant at a sub-micromolar affinity to VC1C2 and C1, respectively. The sensogram of

6B12 (Figure 2.6) could not be fitted with a 1:1 binding model.
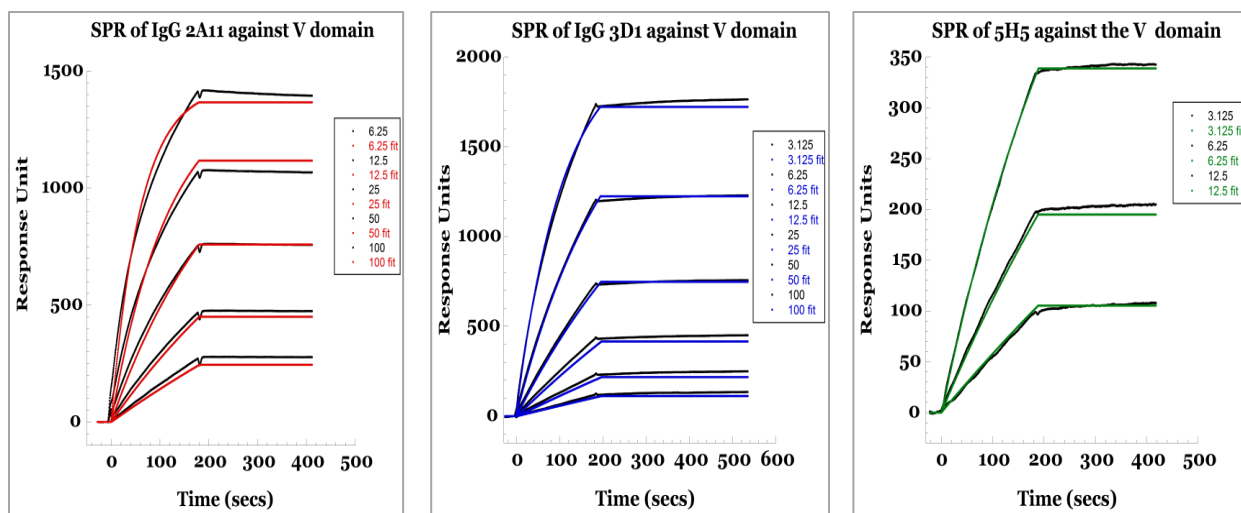

Figure 2.4: Sensogram showing binding of IgG 2A11, IgG 3D1 and IgG 5H5 to the recombinant V domain. From left to right; Sensogram showing binding of IgG 2A11, IgG 3D1 and IgG 5H5 to the recombinant V domain. For IgG 2A11 and IgG 3D1 concentrations used in the titration ranged from 6.25 to 100nM. Concentration ranging from 3.125 to 12.5nM was used for IgG 5H5. The red, blue and green sensograms represent the fits.
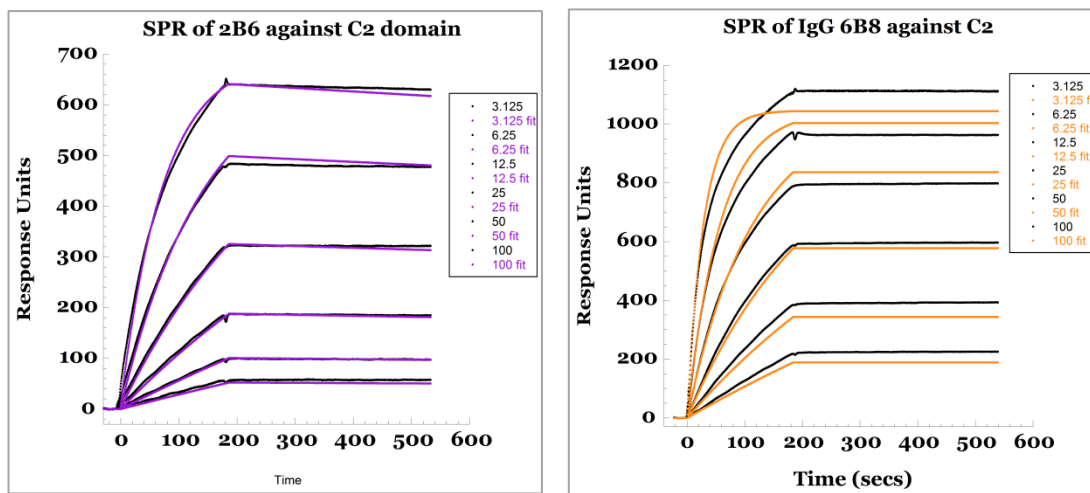

Figure 2.5: Sensogram showing binding of IgG 2B6 and IgG 6B8 to the recombinant C2 domain. From left to right; Sensogram showing binding of IgG 2B6 and IgG 6B8 to the recombinant C2 domain. Concentrations ranging from 6.25 and 100nM were used in the experiments. The purple and orange sensograms represent the fits.
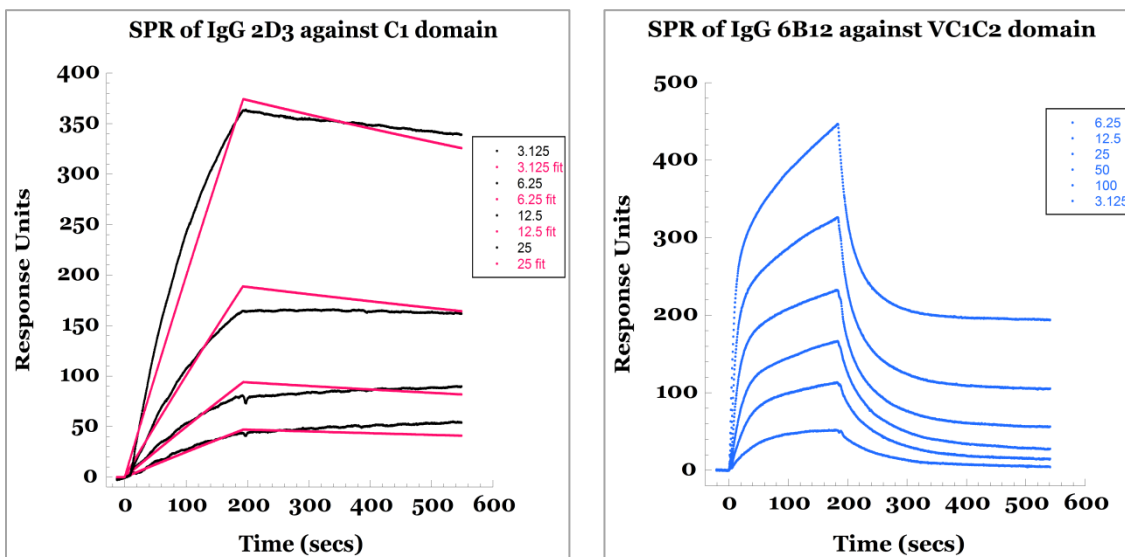
Figure 2.6: Sensogram showing binding of IgG 2D3 against C1 domain and IgG 6B12 to the recombinant VC1C2 domain. From left to right; Sensogram showing binding of IgG 2D3 against C1 domain and IgG 6B12 to the recombinant VC1C2 domain. Concentration ranging from 6.25 and 25nM was used in the experiments. The pink sensograms represents the fit for IgG 2D3.

Table 2.3: K_a, K_d and K_D Values of the generated antibodies for their specific domains by SPR. Hybridoma clone 2H9, 2A12 and 4D3 (not included in table) did not generate antibodies, no values were obtained for binding affinity

IgG	Domain	SPR Ka ($M^{-1} s^{-1}$)	SPR Kd s^{-1}	SPR K_D (M)
2A11	V	1.59×10^5	6.05×10^{-5}	3.8×10^{-10}
3D1	V	8.45×10^4	1×10^{-6}	1.18×10^{-11}
5H5	V	1.45×10^5	1.72×10^{-4}	1.18×10^{-9}
6B12	VC1C2	8.3×10^5	$8.7 \ 10^{-3}$	1.05×10^{-8}
6B8	C2	5.24×10^5	1×10^{-6}	1.9×10^{-12}
2B6	C2	1.74×10^5	5.9×10^{-5}	3.4×10^{-10}
2D3	C1	8×10^3	3.9×10^{-4}	4.88×10^{-8}

Binding Affinity on Mammalian Cells (HEK-293/RAGE)

To provide insights into the binding affinity of the generated antibodies on the surface of mammalian cells, FACS was used. This technique allows us to monitor the interaction between our antibodies and RAGE expressed on cell surface. As compared to ELISA, where adsorption of RAGE domain to the ELISA plate can result in distortion of binding sites available for binding, the principle of FACS allows us to measure the fluorescence intensity obtained from the interaction between our generated antibodies and RAGE on the surface of cells in suspension.

49

Additionally, the fluorescence intensity obtained from viable cells and non-viable cells can be sorted. We examined the binding affinity of the generated antibodies, at titrated concentrations, on RAGE expressed on HEK-293 cells. We observed that all the generated antibodies bound to RAGE on the cell surface at a nano-molar affinity except for 6B12 which binds at a sub-micromolar affinity (Figure 2.7 and 2.8). The lower affinity of 6B12 to cell surface RAGE suggests that 6B12 would not constitute a good antibody in experiment involving cells.
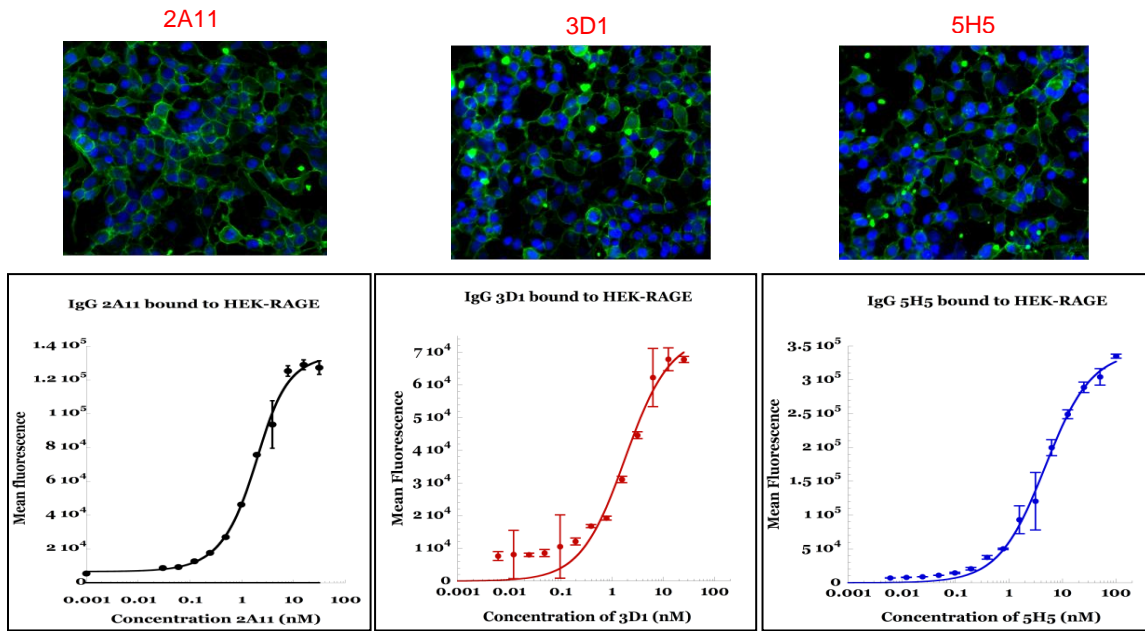

Figure 2.7: Binding of IgG 2A11, 3D1 and 5H5 to HEK-RAGE as determined by flow cytometry and corresponding immunochemistry image is shown above the binding curve for each antibody. From left to right, binding of IgG 2A11, 3D1 and 5H5 to HEK-RAGE as determined by flow cytometry. Binding affinities were as follows: For IgG 2A11, K_D: 1.8 +/- 0.66 nM. For IgG 3D1, K_D: 1.2+/- 0.44 nM. For IgG 5H5, K_D: 4.7 +/- 0.34nM. All experiments were performed in triplicates. The standard deviation is indicted by the error bars on each point on the curve. The corresponding immunochemistry image is shown above the binding curve for each antibody

Immunochemistry Analysis

With the aid of immunochemistry, we were able to visualize the IgGs bound to RAGE on cell surface with a FITC conjugated secondary antibody (green fluorescence). All the IgGs except for 6B12 show distinct binding to RAGE on cell surface (Figure 2.8). The

immunochemistry image of 6B12 shows non-specific binding of IgG 6B12 to RAGE on the surface of cells.
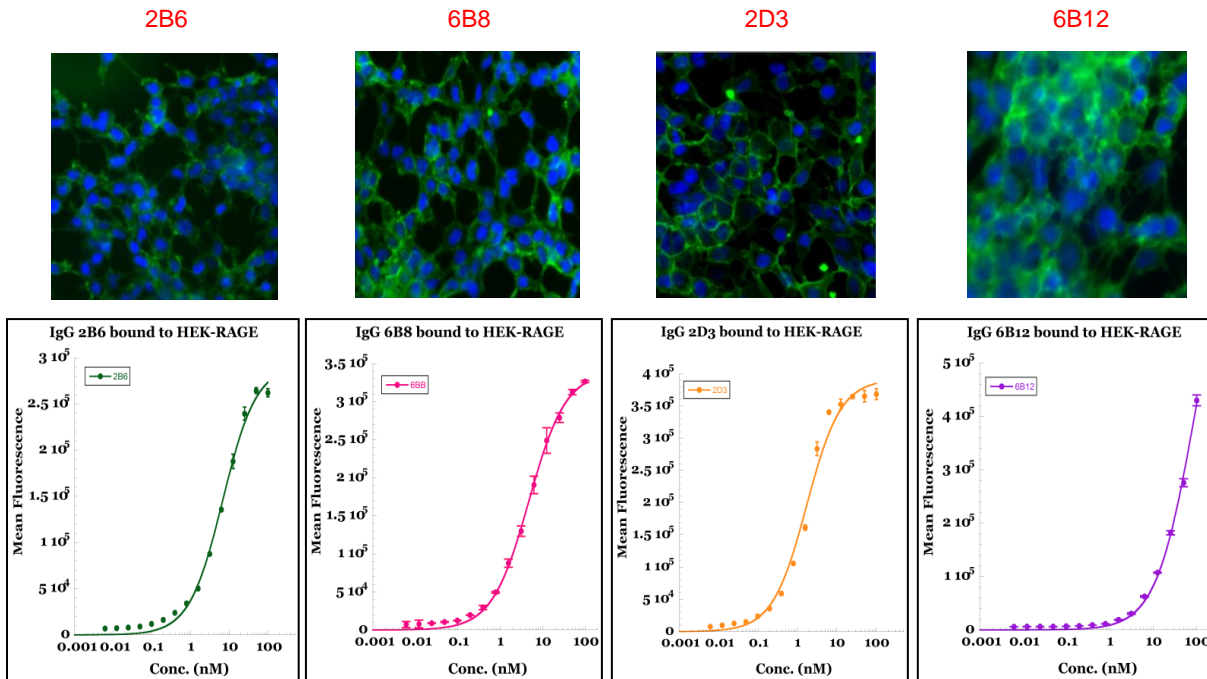

Figure 2.8: Binding of IgG 2B6, 6B8, 2D3 and 6B12 to HEK-RAGE as determined by flow cytometry and corresponding immunochemistry image is shown above the binding curve for each antibody. From left to right, binding of IgG 2B6, 6B8, 2D3 and 6B12 to HEK-RAGE as determined by flow cytometry. Binding affinities were as follows: For IgG 2A11, K_D: 1.8 +/- 0.66 nM. For IgG 3D1, K_D: 1.2+/- 0.44 nM. For IgG 5H5, K_D: 4.7 +/- 0.34nM. All experiments were performed in triplicates. The standard deviation is indicted by the error bars on each point on the curve. The corresponding immunochemistry image is shown above the binding curve for each antibody.

Competition for Binding Sites on RAGE Domains

We have designed the competition experiments to examine the ability of the generated antibodies to compete for RAGE ligand binding sites on recombinant RAGE domains. RAGE ligands specific for their extracellular domains were selected to compete against the generated antibodies. For the generated antibodies that bind specifically to the V domain (2A11, 3D11 and 5H5), S100B was used as a competitive ligand, because it has previously been shown to bind to the V domain of RAGE [149]. At a constant antibody concentration of 50 nM, lower concentrations of S100B do not compete with IgG 2A11, 3D1, and 5H5. We showed that S100B

51

was able to compete with IgG 2A11, 3D1, and 5H5 for binding to RAGE (Figure 2.9, 2.10 and

2.11). S100A6 has been shown to bind to the C2 domain [149]; therefore we used it as a

competitive ligand against the generated antibodies that bind to the C2 domain (2B6 & 6B8).

However, we did not observe any competition between S100A6 and IgG 2B6 and 6B8 (Figure

2.10). AβA was used as a competitive ligand against 2D3 because Sturchler and colleagues were

able to use an antibody against the C1 to block activation of downstream signaling [104].

Similarly, we did not observe any binding competition between IgG 2D3 and AβA (Figure 2.11).
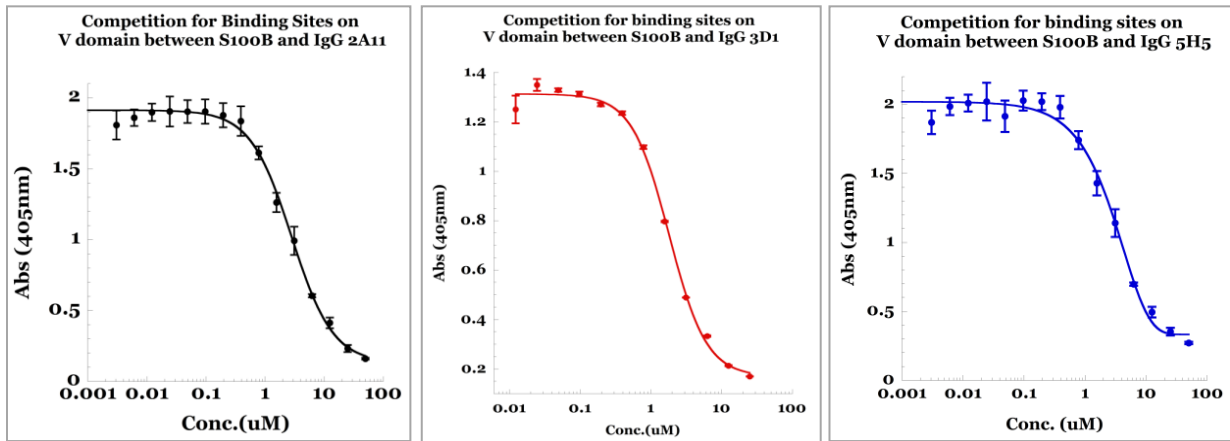
Figure 2.9: Competition between S100B/IgG 2A11, S100B/IgG 3D1 and S100B/ IgG 5H5. From left to right; Competition between S100B/IgG 2A11, S100B/IgG 3D1 and S100B/ IgG 5H5. The experiment was performed in triplicate. The standard deviation is indicted by the error bars on each point on the curve.

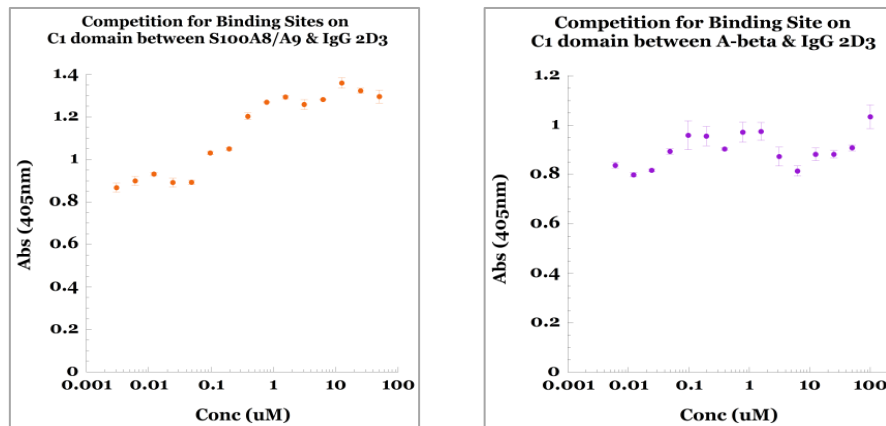Figure 2.10: Competition between S100A6/IgG 2B6 and S100A6/ IgG 6B8. From left to right; Competition between S100A6/IgG 2B6 and S100A6/ IgG 6B8. The experiment was performed in triplicate. The standard deviation is indicated by the error bar present on each concentration point.
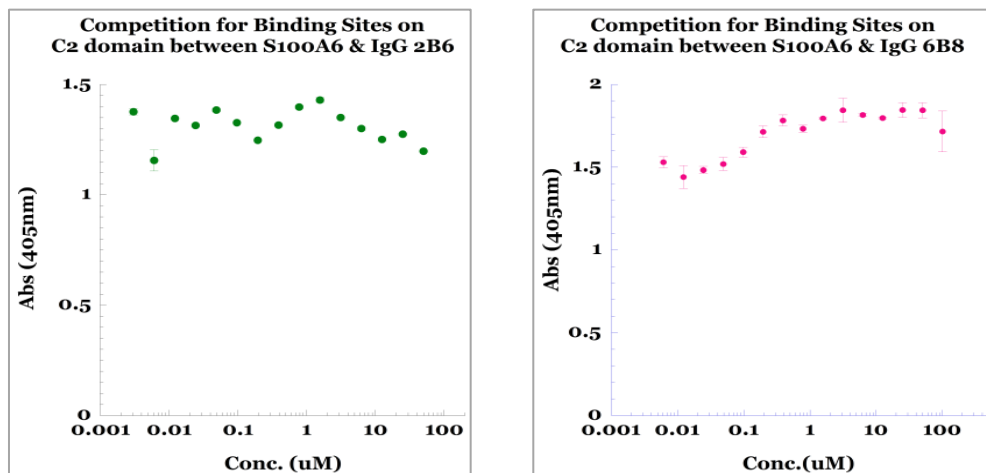
Figure 2.11: Competition between S100A8/A9/IgG 2D3 and AβA/IgG2D3. From left to right; Competition between S100A8/A9/IgG 2D3 and AβA/IgG2D3. The experiment was performed in triplicate. The standard deviation is indicated by the error bar present on each concentration point.

Discussion

Engagement of RAGE by its ligands results in the activation of various signaling pathways involved in a large number of pathologies such as diabetes, cancer, and Alzheimer's disease [77]. RAGE signaling is complex due to the large heterogeneity of its ligands. Blocking the interaction between RAGE and its ligand has been shown to reduce deleterious effects involved in RAGE related pathologies [91, 149, 193, 204].

In the present study, our goal was to generate new monoclonal antibodies that bind specifically to individual RAGE domains and sRAGE. These antibodies were generated with the intention to block the interaction between RAGE and its various ligands. With the help of hydridoma technology, we have used the immune system of the mice to generate hybridoma clones. The supernatants obtained from hybridoma clones were screened for specificity against sRAGE and recombinant RAGE domains. Out of several hundred clones, 10 clones were selected based on the highest positive signals in ELISA (Table 2.1). Upon further characterization of antibody isotypes, we discovered that nine out of the ten selected clones were

IgGs. The tenth clone, 4D3, was discovered to be an IgM.   We decided to set aside the characterization of 4D3 because of the physical characteristics of IgMs. IgMs are multivalent proteins with 10 antigen binding sites. This means that the total avidity is much greater than that of an IgG, which has two antigen binding sites. It is important to note that increase in avidity is only possible when the epitopes to be recognized by the antibodies with multiple binding sites are identical and in close vicinity. Therefore, depending on the orientation of the epitopes on the antigen, only about half of the binding sites on an IgM may eventually bind to an antigen.

To produce the remaining nine antibodies, we used two approaches. In one approach, the hybridoma cells were cultured in batches of $75cm^2$ cells culture flasks, using Dulbecco's modified eagle medium (DMEM), 10% ultra-low IgG FBS, 50 µg/ml gentamicin in the presence of ABAM solution. Using FBS with extremely low concentration of immunoglobulin prevented the purified anti-RAGE IgG fractions from having a substantial fraction of non-specific immunoglobulin contaminants. However, culturing hybridoma in small flasks is only suitable for small scale antibody production because it requires using several hundred flasks at once and large incubation space.

A second approach involves the use of special culture vessels partitioned by a semi-permeable barrier with low molecular weight cut off, the CELLine 1000. This method allows for the separation of the hybridoma cells and antibody produced in a small chamber to be isolated by the filter, with a cut off of $10K_D$, from a larger compartment that contains the culture media. The barrier allows for small molecules like nutrients and cell waste products to diffuse across the partition while the hybridoma cells and produced antibodies are retained in a smaller volume. This method allows for cells to grow to a very high density in the cell compartment allowing high concentrations of antibody to be retained. The supernatant is then harvested periodically

from the cell compartment and replaced with fresh media. The disadvantage of using this method

is the need to use very large volume of media at once. Therefore, in the event of an infection, the

entire system would suffer from contamination that cannot be isolated as compared to using

separate smaller batches.

We were able to use the former approach to successfully produce significant amounts of

antibody to perform the initial characterization of the IgGs *in vitro* except for clones 2A12 and

2H9. We have characterized the generated antibodies *in vitro* using ELISA, SPR, FACS,

immunofluorescence, and by competition assay. The results obtained from the assays show that

all antibodies except 6B12 bind to their domains of specificity at a nano-molar affinity (Table

2.3). Binding measurements with antibody 6B12 showed significantly low binding affinity for

VC1C2 although 6B12 supernatant showed strong "binding signal" (Figure 2.2). Therefore 6B12

was selected to be specific for VC1C2 domain during the screening process of supernatant

clones. It is possible that the supernatant used for screening had relatively higher amount of

antibody as compared to the other clones. The increase in antibody concentration in the

supernatant could have compensated for the weaker binding affinity observed during the

screening process of 6B12 to VC1C2. For all antibodies, SPR measurements showed similar

binding affinity values as compared to ELISA (Table 2.4).

Table 2.4: Summary of KD values of generated antibodies for their specific domains by ELISA and SPR and binding to RAGE on cell surface obtained by FACs.

IgG	Domain	ELISA K_D (nM)	SPR K_D (nM)	FACs K_D (nM)
2A11	V	7.01 +/- 0.37	0.38	0.94+/-0.36
3D1	V	7.6 +/- 0.43	0.0118	1.79+/-0.43
5H5	V	7.1 +/- 0.9	1.18	4.71+/-0.33
6B12	VC1C2	72.6 +/-5.55	10.5	> 85
6B8	C2	1.46 +/- 0.13	0.0019	4.75+/-0.24
2B6	C2	1.36 +/- 0.09	0.34	6.79+/-0.55
2D3	C2	1.97 +/- 0.09	48.8	1.70+/-0.19

The slight difference in K_D between the ELISA and SPR experiments could be attributed to the orientation of the domains when anchored to the sensor chip. Covalent coupling of RAGE domains to the sensor chip requires an amine functional group. In the event that a lysine residue is required in the epitope of RAGE domain to carry out proper ligand-antigen interaction, the antibody epitope could be altered, depending on the number of lysine residues present on the RAGE domain. The sensograms obtained from the binding of the generated antibodies to specific RAGE domains showed fast association and very slow dissociation except for 6B12 which exhibits fast association but also fast dissociation (Figure 2.4 – 2.6).

Immunofluorescence images (Figure 2.7 – 2.8) and FACs analysis revealed that the generated antibodies bound to RAGE expressed on the cell surface at a nano-molar range except for 6B12 which exhibits non-specific binding to cell surface RAGE (Figure 2.7 – 2.8). Since RAGE ligands bind to the V, C1 and C2 domains, we chose S100B, AβA and S100A6 respectively as competitive ligands against the generated antibodies because their binding affinities to the individual domains were recently described by Leclerc and colleagues [104, 149]. Competition for binding sites on the V domain of RAGE shows that S100B competed against 2A11, 3D1, and 5H5 for binding to the V domain. The data suggests that S100B, 2A11, 3D1 and 5H5 all bind to the V domain of the receptor. S100A6 did not displace bound 2B6 and 6B8 on the C2 domain. The data suggests that S100A6, 2B6 and 6B8 do not share the same binding site on the C2 domain. Similarly, AβA did not displace 2D3 on the C1 domain which suggests that 2D3 does not share similar epitope with 2D3 on the C1 domain of the receptor.

Conclusion

In conclusion, we have successfully developed and characterized a panel of monoclonal antibodies which are specific to RAGE domains and have nano-molar binding affinity towards

the receptor on cell surface. IgG 2A11, 3D1 and 5H5 were able to compete with an endogenous ligand of RAGE (S100B) for binding to the receptor. Based on these results we can conclude that IgG 2A11, 3D1, 5H5, 2B6, and 6B8 can potentially serve as good therapeutic candidates because of their nano-molar binding affinity (K_D). In the next chapters we will investigate the inhibitory activity of the generated antibodies in mammalian cells and in tumors *in vivo* by identification of suppressed RAGE/ligand dependent signaling pathway(s) and monitoring tumor size in mice model.

CHAPTER 2: TARGETING RAGE WITH MONOCLONAL ANTIBODIES IN
MAMMALIAN CELLS

Introduction

The search for cell surface receptors responsible for the mediation of cellular interaction

of the advanced glycation end-products (AGE) led to the identification of a 35 kDa polypeptide

present on endothelial cells [101]. This receptor was named the receptor for advanced glycation

product (RAGE). It was eventually discovered that RAGE has the ability to bind to a variety of

structurally unrelated ligands [100, 101, 205]. Binding of these ligands to RAGE leads to

activation of several pro-inflammatory signaling molecules including CDC42/Rac,

phosphoinositol-3 kinase, JAK/STAT, p38, SAPK/JNK and, ERK1/2(p44/p42) MAP kinases
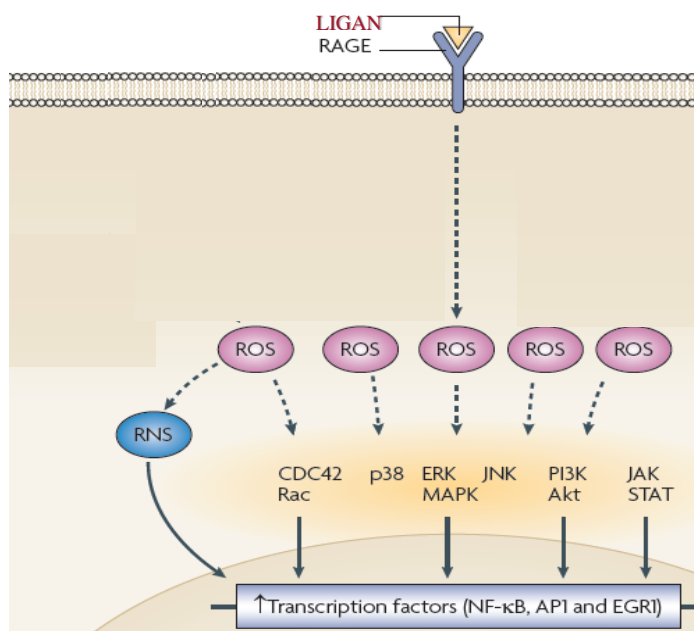
(Figure 3.1) [206].

Figure 3.1: Schematic of RAGE signaling. Interaction between RAGE ligands and RAGE results in the generation of reactive oxygen species (ROS) and reactive nitrogen species (RNS) which ultimately leads to the activation of several pro-inflammatory signaling molecules such as CDC42, p38, ERK/MAPK, JNK, PI3K/Akt and JAK/STAT. Image modified from Calcutt et al, 2009 [206].

A key factor that promotes downstream activation of these processes is the generation of reactive oxygen species (ROS). ROS have been known to exert their effects in many patho-physiological conditions by acting as intracellular signaling cascade modulators [206]. This signaling can lead to alterations in transcription factors and the resultant protein expression linked to various RAGE-related pathologies [207, 208]. Generation of reactive oxygen species can also lead to the subsequent activation of NF-κB, various adhesion molecules and the eventual recruitment of macrophages, neutrophils and production of various cytokines [209-214]. The translocation of activated pro-inflammatory transcription factor, NF-κB, into the nucleus leads to increased expression of RAGE. Additionally, generation of ROS such as hydrogen peroxide and superoxide can potentially react with NO normally secreted in endothelial cells to form peroxynitrite, a reactive nitrogen species (RNS), which is associated with the formation of RAGE ligands [215]. Therefore at sites where there is an accumulation of RAGE ligands, there is usually an up-regulation of RAGE [215].

Several publications have also linked the production of oxidative stress to the activation of RAGE-mediated NADPH oxidase, a superoxide producing enzyme, which is a major source of ROS [161, 216, 217]. NADPH oxidase is a membrane-bound enzyme consisting of two membrane-bound elements (gp91-phox and p22-phox), three cytosolic components (p67-phox, p47-phox, and p40-phox), and a low-molecular-weight G protein. Activation of NADPH oxidase is associated with the migration of the cytosolic components to the cell membrane and assembling with its membrane subunits [218, 219]. Recent publications have shown evidence that interrogating RAGE with anti-RAGE antibody could potentially attenuate intracellular pathways involved in RAGE related pathologies. We have successfully characterized a panel of anti-RAGE antibodies *in vitro* (Chapter 1). These antibodies show specific binding to the

receptor on the surface of mammalian cells (HEK-293/RAGE) at a nano-molar affinity. In the current study, we have investigated the inhibitory activity of one of our generated antibody (IgG 2A11) in cell-based assays. IgG 2A11 was used to prevent generation of reactive oxygen species and subsequent activation of NADPH oxidase complex.

We also used IgG 2A11 to identify suppressed RAGE/ligand dependent signaling pathway(s) and altered protein expression such as changes in Akt and activation of NF-κB and eventual cellular proliferation. The current study suggests that blocking the interaction between RAGE and its ligands using the generated anti-RAGE antibody can suppress downstream signaling pathways that have been shown to result into complications in diabetic patients, amyloidosis, chronic inflammatory response, tumor progression, angiopathy, and neurite extension [77].

Materials and Methods

Preparation of AGE Product (Provided by Venkata Indurthi, Department of Pharmaceutical Sciences, NDSU)

Bovine serum albumin (BSA) (Amresco, BSA Biotechnology Grade) was dissolved in a buffer containing 50 mM potassium phosphate at pH 8.0. Subsequently, 200 mM ribose was added to the protein. The ribose-BSA mixture was then incubated at 37°C for 21 days. After the incubation, the unreacted ribose was removed by dialysis against 300 volumes of a 50 mM phosphate buffer, pH 7.4. The final concentration of the protein was determined by the BCA assay. The samples were aliquoted and stored at -80°C.

Preparation of S100B

Please, refer to Chapter 1

WM115-RAGE and WM115-MOCK Cell Cultures (Provided by Varsha Meghnani, Department of Pharmaceutical Sciences, NDSU)

The human melanoma cell line, WM-115, was purchased from ATCC (Manassas, VA) and grown in Opti-MEM (Invitrogen, Carlsbad, CA) supplemented with 4% FBS (Invitrogen) in the presence of penicillin and streptomycin (JRScientific, Woodland, CA) at 37°C temperature and in the presence of 5% CO_2. The cells, at 70% confluence, were transfected with pcDNA3 (Invitrogen) that had been engineered to expressed full-length RAGE. The plasmid pcDNA3-RAGE was a generous gift from Prof. C.W. Heizmann (Children's Hospital, University of Zurich, Switzerland). The transfection was performed with SatisFection (Stratagene, Santa Clara, CA) according to the manufacturer's protocols. Prior transfection, the pcDNA3-RAGE plasmid was digested with the unique restriction site MfeI (NEB, Ipswich, MA) to improve the integration of the plasmid into the chromosomal DNA. The empty pcDNA3 vector was used as negative control for the transfection (WM115-MOCK). The transfected cells were selected in the presence of 1mg/ml G418 (WM115-RAGE) or 0.5 mg/ml G418 (WM115-MOCK).

Fluorescence Activated Cell Sorting

WM115-MOCK and WM115-RAGE cells cultivated to 70% confluence were detached using 5mM EDTA/PBS. The detached cells were washed with 1%FBS/PBS and seeded in 96 well plates. IgG 2A11 at titrated concentrations (0 nM to 200 nM) was added to wells in the presence of 1% FBS/PBS. After incubation at 4°C for 30 mins, the wells were washed with 1% FBS/PBS, and FITC conjugated anti-mouse IgG secondary antibody (Jackson ImmunoResearch) in 1% FBS/PBS was added for 20 mins at 4°C. After a final wash with 1% FBS/PBS, the fluorescence of the bound antibody was measured by an Accuri flow C6 cytometer.

Immunofluorescence

WM115-MOCK and WM115-RAGE cells were cultured on collagen coated slide until a confluence of approximately 60% was obtained. Cells were subsequently fixed with 4% paraformaldehyde in PBS. Fixed cells were then blocked with 1% BSA in PBS for 30 minutes and incubated with 100 nM IgG 2A11 diluted in 1% BSA/PBS for an hour at room temperature. Following incubation, cells were washed with PBS and incubated with FITC conjugated anti-mouse IgG secondary antibody (Jackson ImmunoResearch) in 1% BSA/PBS (diluted 1:1000) for 1 hour at room temperature. Cells were counterstained using Hoechst dye (Invitrogen). After a final wash with PBS, the fluorescence of the antibody bound to RAGE on the cell surface was revealed using an Olympus fluorescence microscope.

ROS Formation

WM115-MOCK and WM115-RAGE cells maintained in serum-free media for 24 hours were cultured in 96 well plates. Following 24 hours of serum starvation, cells were treated with 2 μM of S100B or 3 μM of AGE product. As a positive control, acrolein (Sigma-Aldrich) at a concentration of 10 μM was added as a treatment group. Negative control cells were treated with a similar volume of PBS. IgG 2A11 at 25 μg/ml was simultaneously added to the groups treated with S100B and the AGE product. The cells were also treated with IgG 2A11 alone to observe whether antibody alone had any effect on the cells. After treatment, the cells were incubated at 5% CO_2 at 37°C for 24 hrs. The cells were incubated with 10 μM cell permeable fluorescent dye 2′, 7′-dichlorofluorescein diacetate and washed with PBS, and fluorescence was measured with a microplate reader (excitation, 485 nm; emission, 520 nm).

Estimation of NADPH Oxidase Activity

The presence of NADPH-oxidase subunit, $p47^{Phox}$, in the cell membrane was investigated by Western blot. WM115-MOCK and WM115-RAGE cells maintained in serum free media for 24 hours were cultured in 6 well plates. Following 24 hours of serum starvation, the cells were treated with 2 µM of S100B or 3 µM of AGE product. For the control, the cells were treated with a similar volume of PBS. IgG 2A11 at 25 µg/ml was simultaneously added to the groups treated with S100B and AGEs. The cells were also treated with IgG 2A11 alone to observe whether the antibody alone had any effect on the cells. After treatment, the cytosolic and membrane fractions were prepared using Mem-PER Eukaryotic Membrane Protein Extraction kit (Pierce). 50 µg of membrane protein was loaded on a 12% SDS gel, followed by a transfer to a nitrocellulose membrane. The membrane was blocked with 3% BSA in TBS overnight at $4^{o}C$. The primary antibodies for $p47^{Phox}$ (Cell Signaling Technologies) and Na^{+}/K^{+}-ATPase (Cell Signaling Technologies) were added at a dilution of 1:2,000 in the presence of 1%BSA/TBS-T and incubated overnight at $4°C$. The blot was then washed three times in TBS-T and incubated for 1 hour with HRP conjugated secondary antibody (Jackson ImmunoResearch) at a 1:10,000 dilution in the presence of 1%BSA/TBS-T. The membrane was washed three times in TBS-T at 15 min intervals and developed with ECL Western blotting substrate (Pierce). Blots were scanned and quantified with Image J (PC version of Windows).

Transfection and NF-κB Activation Assay

WM115-RAGE and WM115-MOCK cells were co-transfected with the pNFκB-Luc construct (Clontech) and a plasmid containing the β-galactosidase gene using the X-treme GENE HP DNA transfection reagent (Roche Applied Science) for 24 h in the presence of serum according to the manufacturer's instructions. The cells were serum-starved for 24 h before being

treated with S100B or S100A6. After 24 hrs in culture, the cells were washed with PBS and lysed in Reporter Lysis Buffer (Promega). Luciferase activity was monitored using the Luciferase Assay System (Promega) using a luminometer. The β-Galactosidase activity was quantified by mixing cell lysate with an equal volume of 2× β-galactosidase assay mixture (120 mM Na_2HPO_4, 80 mM NaH_2PO_4, 2 mM $MgCl_2$, 100 mM β-mercaptoethanol, and 1.33 mg/ml O-nitrophenyl β-d-galactopyranoside) and incubation at 37 °C; the absorbance was read at 420 nm. The luciferase activity was normalized to β-galactosidase activity.

Western Blot Analysis

The cells were washed twice with PBS and scraped from the plates in the presence of cell disruption buffer (Life Technologies) supplemented with 1 mM Na_3VO_4 and 0.5 mM PMSF. The collected samples were centrifuged at 2,000 rpm for 2 min at 4 °C. The supernatant was collected, aliquoted and stored at –80°C. The protein concentration was determined using the BCA protein assay kit (Pierce). 50 µg of protein was loaded on a 12% SDS gel, followed by a transfer to a nitrocellulose membrane. The membrane was blocked with 3% BSA in TBS at room temperature for 2 hours. The primary antibodies for pAkt and Akt (Cell Signaling Technologies) were added at a dilution of 1:2,000 in the presence of 1% BSA/TBS-T and incubated overnight at 4°C. The blot was then washed three times in TBST and incubated for 1h with HRP conjugated secondary antibody (Jackson ImmunoResearch) at a 1:10,000 dilutions in the presence of 1% BSA/TBS-T. The membrane was washed three times in TBS-T at 15 min interval and developed with ECL Western blotting substrate (Pierce). The scanned images were analyzed with Photoshop and Image J (software obtained from NIH).

Cell Proliferation Assay

WM115-MOCK and WM115-RAGE cells maintained in serum free media for 24 hours were cultured in 96 well plates. Following 24 hours of serum starvation, the cells were treated with 2 µM of S100B or 3 µM of AGEs. As a positive control, naltrexone hydrochloride (Sigma-Aldrich) at a concentration of 10 µM was added as a treatment group. Negative control cells were treated with a similar volume of PBS. IgG 2A11 at 25 µg/ml was simultaneously added to the groups treated with S100B or AGEs. The cells were also treated with IgG 2A11 alone to observe whether the antibody alone had any effect on the cells. After treatment, the cells were incubated in the presence of 5% CO_2 at 37 °C for 24 hrs. 1/10th volume of Alamar Blue reagent (Abd Serotec) was directly added to the cells in culture medium and incubated for 6-8 hrs. The fluorescence intensity was measured using a microplate reader at an excitation of 540 nm and emission of 590 nm.

Statistical Analysis

Data from at least three independent experiments were averaged and reported as mean ±SD. Mean differences between experimental groups were tested with unpaired *t*-test. Values were considered significantly different at the *P*≤0.05 level. Statistical analyses were performed on the Kaleidagraph Software 4.1.0 (Windows PC version).

Results

Binding of IgG 2A11 to RAGE on Cell Surface

We were able to show binding of IgG 2A11 to RAGE on the surface of non-cancerous cells (HEK293-RAGE). We were able to evaluate the binding affinity to be at a nanomolar range which is characteristic of a good antibody for therapeutic puposes (Chapter 1). To further provide evidence that the generated antibody can bind to RAGE on the cell surface of cancerous

cells, we examined with immunofluorescence microscopy and fluorescence activated cell sorting, the binding of IgG 2A11 at titrated concentrations to RAGE on WM115-RAGE and WM115-MOCK cells. Using FITC-conjugated secondary antibodies, we observed significantly lower fluorescence intensity on the WM115-MOCK cells as compared to the WM115-RAGE cells (Figure 3.2).
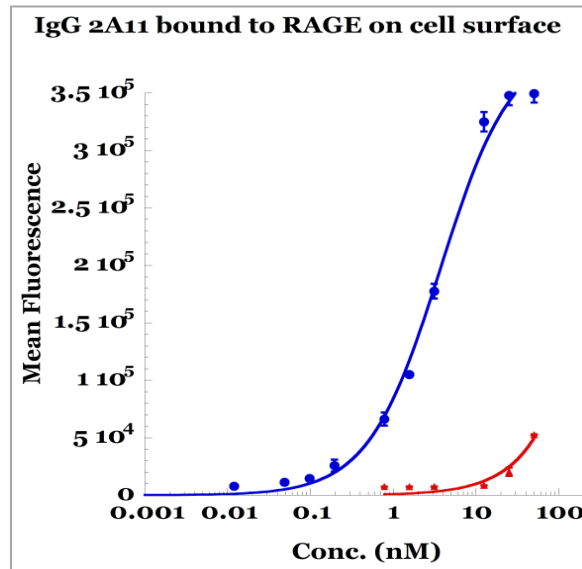
Figure 3.2: Binding of IgG 2A11 to WM115-RAGE and WM115-MOCK cells as determined by flow cytometry. All experiments were performed in triplicates. The standard deviation is shown by the error bars on each point of the curve. The blue curve represents IgG 2A11 bound to WM115-RAGE. The red curve represents IgG 2A11 bound to WM115-MOCK.

Suppression of Induced ROS Production with the Use of Generated Antibodies

To investigate ROS production in cells, we used 2', 7'-dichlorodihydrofluorescein diacetate (DCFH-DA). DCFH-DA crosses the cell membrane and undergoes deacetylation by intracellular esterases to form DCHF [220]. DCHF can react with intracellular hydrogen peroxide or other oxidizing ROS to give a green fluorescent compound, DCH. Figure 3.3 shows the quantitative analysis for each cell line. Treatment with RAGE ligand, S100B or AGE, for 24 hours did not result in an increase in the generation of ROS. We compared the results obtained

with a positive control, acrolein. Acrolein is an unsaturated aldehyde that has been reported to induce generation of reactive oxygen species [221]. Figure 3.3 showed an increase of 75% in fluorescence intensity as compared to the control when cells were treated with acrolein. We also confirmed that IgG 2A11 alone had no effect on fluorescence intensity and therefore does not trigger the generation of ROS.
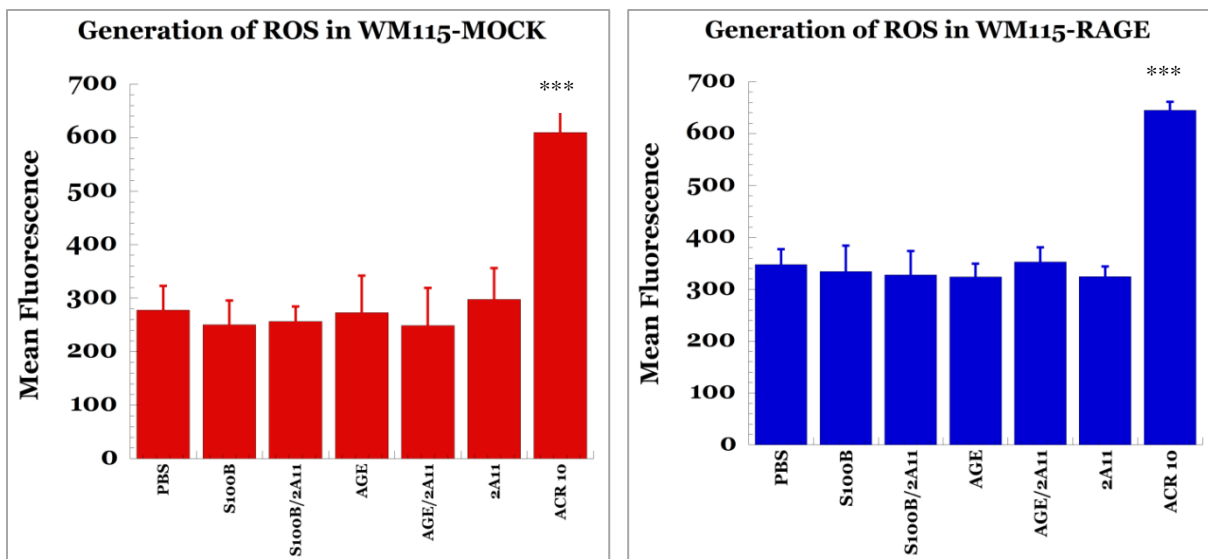
Figure 3.3: Generation of ROS using S100B or AGE in WM115-MOCK and WM115-RAGE cells. Generation of ROS using S100B or AGE in WM115-MOCK (left) and WM115-RAGE (right) as inducer. 10 µM of acrolein (ACR) was used as a positive control. *** indicates a significance of $p \leq 0.0001$ as compared with negative control

Suppression of Induced NADPH Oxidase Activation with the Use of Generated Antibodies

NADPH oxidase is a membrane-bound protein that is responsible for catalyzing the production of ROS from oxygen and NADPH. The NADPH oxidase system consists of a membrane bound component, a cyctosolic component and a low-molecular-weight G protein. The membrane bound complex has two subunits which are gp91-phox and p22-phox and the cytosolic subunits have three components which are p67-phox, p47- phox, and p40-phox [222]. Activation of the NADPH oxidase complex typically results in the assembling of its cytosolic

complex with the membrane bound elements on the membrane. We wanted to observe whether IgG 2A11 could block the interaction between RAGE and S100B or AGE and prevent subsequent activation of NADPH oxidase. To confirm the role of NADPH oxidase activation from exposure of S100B and AGE to cells, we analyzed the presence of the cytosolic subunit, p47-phox, on cell membrane. We did not observe the presence of any band upon analysis of membrane extract by western blot. However, we also did not observe the presence of Na^+/K^+-ATPase, which was used as a positive control for membrane extract.

Suppression of Induced Akt Activation with the Use of Generated Antibodies

Interaction between RAGE and its ligands has been shown to induce certain kinase signaling pathways; therefore, our goal was to investigate which kinases are activated by interrogating the receptor with its natural ligands. We also aimed to observe whether IgG 2A11 could block the activation of these downstream signaling molecules. We exposed WM115-RAGE and WM115-MOCK cells to S100B and AGE to induce phosphorylation of Akt. Figure. 3.4 shows that AGE significantly increased phosphorylation of Akt in WM115-RAGE and IgG 2A11 was able to reduce activation of Akt. We did not observe a significant phosphorylation of Akt in WM115-MOCK cells as compared to the WM115-RAGE cells. Additionally S100B did not induce the activation of Akt in both WM1115-RAGE and WM115-MOCK cells. We also treated both cell lines with IgG 2A11 alone and we observed no effect on the phosphorylation of Akt.

Figure 3.4: Western blot images showing changes in the activation of Akt in WM115-RAGE and WM115-MOCK. From left to right, western blot images showing changes in the activation of Akt in WM115-RAGE and WM115-MOCK. AGE was able to increase phosphorylation of Akt in WM115-RAGE cells (1.7 +/1 0.18 fold) and was subsequently suppressed upon the addition of IgG 2A11 (left). S100B did not show any effect on Akt activation. No significant difference was observed for WM115-MOCK cells in any of the conditions (right).

Inactivation of Transcription Factors

Several RAGE ligands have been shown to activate the transcription factor NF-κB following the interaction with the receptor [101, 215]. To investigate the inhibitory activity of IgG 2A11, we have used a luciferase reporter plasmid system to monitor induced NF-κB transcriptional activity. The reporter gene, luciferase, is placed downstream from response elements of NF-κB in the same DNA plasmid, which is then inserted into the cell. We chose the luciferase system because it is not natively expressed in WM115 cells. Addition of stimulants to the cell culture medium will result in the induction of the binding of transcription factors to the enhancer element, thereby initiating transcription of the secreted luciferase reporter gene. Figure 3.5 shows that treatment of WM115-RAGE cells with AGE increased NF-κB activity, and the presence of IgG 2A11 blocked AGE-mediated NF-κB activity. In comparison, WM115-MOCK cells showed negligible increase in NF-κB activity (Figure 3.5). In contrast, NF-κB activity was not significantly altered when both cells were exposed to S100B (Figure. 3.5). We also treated both cell lines with IgG 2A11 alone and we observed no effects on activation of NF-κB.
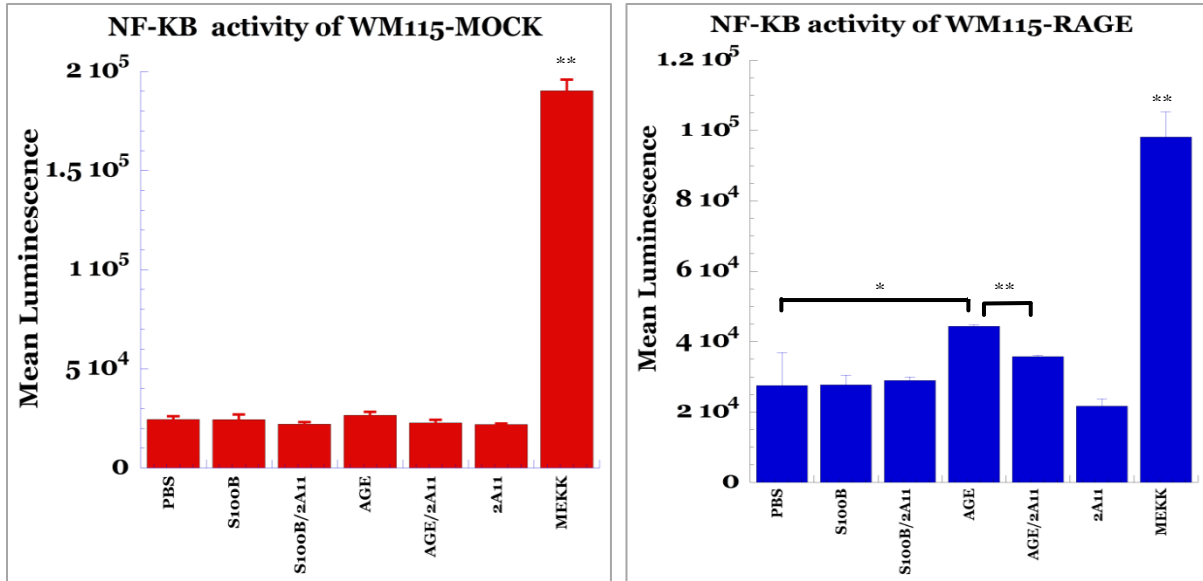
Figure 3.5: Inactivation of induced NF-κB using S100B or AGE in WM115-MOCK (left) and WM115-RAGE (right). MEKK was used as a positive control. *** indicates a significance of p≤ 0.001, p≤ 0.05 as compared with negative control (PBS treated).

Suppression of Induced Cell Proliferation

Figure 3.6 shows the results obtained from suppression of induced cell proliferation. To determine the effects of IgG 2A11 in the RAGE/ligand interaction, we induced cell proliferation using S100B and AGE. We used Alamar Blue to monitor the changes in proliferation of WM115-RAGE and WM115-MOCK after addition of RAGE ligands. Typically viable cells maintain a reducing environment in the cytosol. Alamar Blue contains resazurin, a cell permeable dye which has a blue color and is non-fluorescent [223]. After addition to the reducing environment of the cells, resazurin is converted to resorufin, a red highly fluorescent compound when reduced in the cells. Therefore Alamar Blue assay can quantitatively measure the proliferation of cells. An increase in cell proliferation will result in higher reducing conditions and therefore will continuously convert resazurin to resorufin, increasing the overall

fluorescence and color of the media surrounding the cells [223]. Several studies have shown

increases in proliferation when cells expressing RAGE were exposed to RAGE ligands.
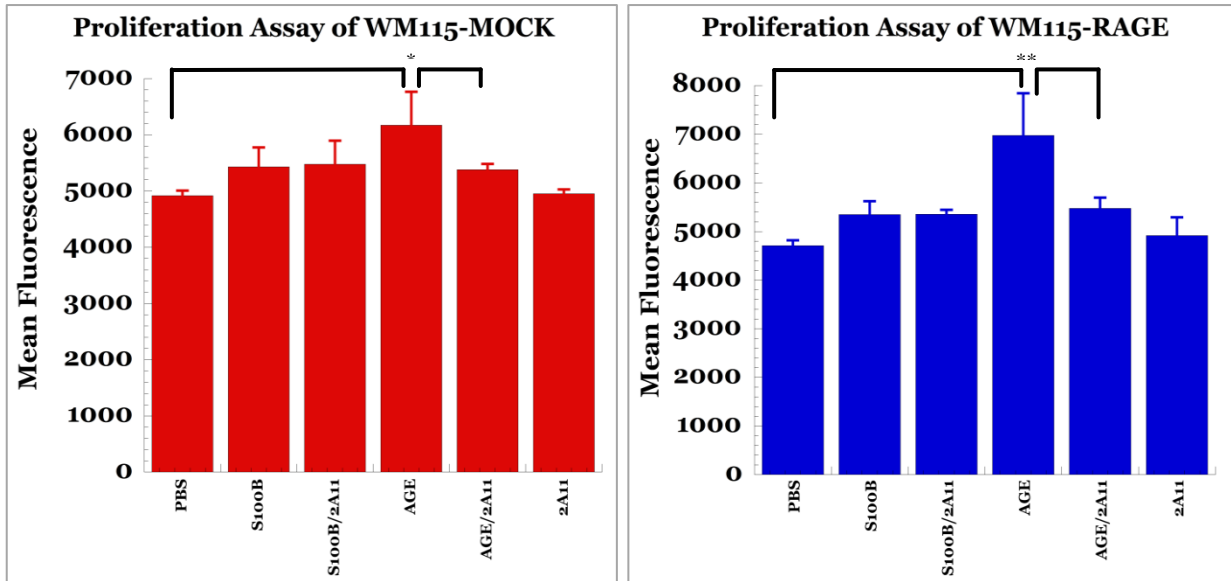
Figure 3.6: Inactivation of induced proliferation using S100B or AGE in WM115-MOCK (left) and WM115-RAGE (right). *** indicates a significance, $p \leq 0.001$, * ,$p \leq 0.05$ as compared with control.

Therefore we investigated whether IgG 2A11 was capable of inhibiting induced

proliferation. Figure 3.6 shows an increase in fluorescence when WM115-RAGE cells were

exposed to AGE, and a subsequent reduction in fluorescence when simultaneously treated with

IgG 2A11. Similarly, WM115-MOCK cells also showed a statistically significant increase in

fluorescence when exposed to AGE. We did not observe an increase in fluorescence for both

WM115-RAGE and WM115-MOCK cells when exposed to S100B. Additionally, treatment

alone with IgG2A11 did not have any effect on fluorescence.

Discussion

The engagement of RAGE by its ligands typically activates signaling pathways that are

dependent on the ligand, environment and cell type [206, 209, 224]. The signaling molecules that

have been shown to be activated during RAGE/ligand interaction include Ras-extracellular signal-regulated kinase 1/2 (ERK1/2) [93], Cdc42/Rac [177], stress-activated protein kinase/c-Jun-NH2-terminal kinase (SAPK/JNK) and p38 mitogen-activated protein (MAP) kinase [91], transcription factors like NF-κB [212], cAMP response element-binding (CREB) protein [93] and signal transducers and activators of transcription proteins (STAT3) [225]. The engagement of RAGE by its ligand has also been shown to result in a positive feedback loop which sustains NF-κB activation thereby sustaining an inflammatory response [226].

The results from this study provided support for the involvement of AGE/RAGE in downstream activation of several signaling pathways in human melanoma cells. Specifically, we demonstrated that IgG 2A11 can bind to RAGE on human melanoma cells and prevent binding of AGE to RAGE at the surface of the cells resulting in reduction of Akt phosphorylation and activation of NF-κB. Interestingly, our data also suggested ROS production was not required for AGE-induced activation of Akt and NF-κB in melanoma cells.

Blockade of the interaction between RAGE and its ligands has shown promising results in several studies [161, 196]; therefore, we aimed to investigate the inhibitory activity of IgG 2A11 on cells expressing RAGE. We chose human melanoma cells because the involvement of RAGE in this area is still poorly understood. Recently, the interaction of AGE with RAGE was shown to be involved in progression of melanoma [133, 227]; therefore, we used AGE as a stimulant for RAGE. Several evidences have also shown that RAGE functions as a signal transducing cell surface receptor for S100B [135, 228, 229], although there are no published papers showing that the interaction between S100B and RAGE is involved in the tumorigenesis of melanoma. Our data demonstrated that binding of AGE to RAGE mediated alterations in the phosphorylation state of Akt, activation of NF-κB, and also increased cell proliferation, all of

72

which were reversed with simultaneous addition of IgG 2A11 in WM115-RAGE cells. We observed a smaller change in Akt phosphorylation, NF-κB activation, or proliferation in WM115-MOCK cells when exposed to AGE. The difference in results could be accounted for by the difference in the levels of RAGE between WM115-MOCK and WM115-RAGE cells (Figure 3.2).

AGEs have been implicated in the development of diabetic complications, cardiovascular diseases, strokes, AD, and other age related diseases [230-233]. In diabetic-related complications, hyperglycemia which is directly related to the formation of AGE products has been linked to the generation of NADPH and subsequent production of reactive oxygen species by mitochondria [230]. NADPH has also been linked to the synthesis of nitric oxide, a potent vasodilator. Any shift in the production of NADPH could result in cardiovascular complications [234]. The involvement of RAGE in AD has been linked to oxidative stress generated from NADPH and downstream activation of MAP Kinase pathway through the interaction of RAGE with amyloid beta complexes [235].

Although there is evidence that oxidative stress is a major contributor to cellular dysfunction in many diseases where RAGE-ligand interaction has been involved [100, 216], we did not observe an increase in the generation of ROS in both WM115-RAGE and WM115-MOCK cell lines. One possible explanation could be that melanoma cells naturally generate significant amounts of ROS; therefore, an induction of additional ROS might not result in further significant difference. Additionally, the mechanism for the production of RAGE-ligand induced ROS has not been clearly elucidated because of heterogeneity of ligands; therefore, AGE and S100B may not be suitable ligands to induce additional ROS. Generation of ROS has also been linked to the activation of NADPH complex composed of a membrane bound subunit and a

cytosolic subunit. In 2011, Askarova and colleagues were able to show the activation of the NADPH oxidase complex through the interaction of amyloid beta protein and RAGE [161]. Activation of NADPH oxidase complex typically results in the migration of cytosolic components to the membrane. Unfortunately, our experiments were not conclusive and will need to be repeated. In all the experiments, S100B did not induce any response as compared to AGE. It is possible that S100B is not the proper ligand to induce downstream signaling in human melanoma cells even though melanoma cells secrete S100B in large amounts.

Conclusion

In conclusion, IgG 2A11 was able to block cellular responses triggered by the interaction between AGE and RAGE on WM115-RAGE and WM115-MOCK cell lines. The AGE/RAGE dependent suppressed signaling pathways involved Akt, NF-κB and correlated with alteration in cell proliferation of WM115-RAGE cells

CHAPTER 3: NEW MONOCLONAL ANTIBODIES TARGETING THE RECEPTOR FOR ADVANCED GLYCATION END-PRODUCT (RAGE) *IN VIVO* AS DIAGNOSTIC AND THERAPEUTIC TOOL

Introduction

Ever since Paul Ehrlich described antibodies as magic bullets [236], antibodies have emerged to become the ideal diagnostic and therapeutic tools. [237]. They are regarded as ideal tools because of their ability to discern specific components on different cell types without the complications of toxicity observed with other conventional tools [238]. Furthermore, technological advances have refined the production of antibodies into fragments of varying sizes, delivery vehicles, and diagnostic tools that can be mass produced [38, 238]. Monoclonal antibodies have been approved for the treatment of pathologies associated with inflammation, autoimmune disorders, cardiovascular disorders, and various cancers (Table 1.1) [69, 238].

Of all the cancers, melanoma is the least prevalent as it only constitutes approximately 1% of all cancers [237, 239]. However, it is also the most dangerous because of its poor survival rates and limited treatment options with low efficacy profiles [240]. Typically, the treatment of melanoma consists of surgery, however the diagnosis of melanomas from other skin cancers is a problem for surgical pathologists [237]. Conventional methods used in the histological distinction of melanomas from other neoplasms include the detection of DOPA oxidase and, the staining of melanin using Masson-Fontana silver and argyrophil stains [241, 242]. However, the use of the DOPA detection method is limited to postfixed cryostat sections [242]. Additionally, staining methods such as Masson-Fontana silver stains can also react with pigments other than melanin [241]. A recent biomarker shown to be important in the prognosis of melanoma is the S100B protein [243]. S100B is a prognostic marker for advanced melanoma stages, and levels of

S100B strongly correlate with survival rate [228, 244-246]. Although several evidences

implicating RAGE in tumor progression and metastasis have been shown in several cancers,

there are only a few publications that have examined the role of RAGE in melanoma [133, 229].

Researchers have suggested that oxidative stress in melanoma cells could lead to an increased

production of AGEs which could contribute to melanoma progression through the interaction

with RAGE [133, 247].

Consequently, the need for new diagnostic and therapeutic intervention is becoming more

paramount. Blockade of RAGE interaction with its ligands either with the use of sRAGE or anti-

RAGE antibodies has been shown to reduce progression of RAGE related pathologies [195,

197]. Researchers have shown evidence that sRAGE can suppress the acceleration of advanced

atherosclerosis and restore wound healing in diabetic mice, suppress tumor growth and

metastases, and reduce several inflammatory responses involved in RAGE related pathologies

[91, 118, 184, 188-194]. The use of antibodies against RAGE was demonstrated in the

suppression of adverse effects on the kidneys of diabetic animal models [195, 197] and the

reduction of atherosclerosis on uremic mice models [196]. We have generated a panel of

monoclonal antibodies with the aim of targeting RAGE. Characterization of these antibodies

showed binding to RAGE *in vitro* with nano-molar affinity and inhibition of AGE-induced

proliferation and activation of NF-κB and Akt activation in mammalian cells *in vitro.* Our next

aim was to observe the inhibitory effects of the antibodies on RAGE *in vivo* in a mouse model.

*This work was done in collaboration with Dr. Benedict Law's laboratory (Department of

Pharmaceutical Sciences, NDSU)*.

Materials and Methods

Human Tumor Xenograft (Work Performed by Anil Wagh, Department of Pharmaceutical Sciences, NDSU

5-6 week-old female severe combined immune-deficiency (SCID) mice at an initial body weight of 20-25 g (Charles River Laboratory, Wilmington, MA) were maintained in a temperature-regulated environment for two weeks before experiments were carried out. Human melanoma tumors were induced in mice as previously described [248]. Briefly, 10^6 WM115-RAGE or WM115-MOCK cells (50 µl) were subcutaneously injected in mice under anesthesia (90 mg/kg of ketamine obtained from Hosperia Inc, IL and 5mg/kg of Xylazine obtained from Lloys Inc, IA). Tumor growth of mice was followed twice a week by measuring bi-directionally with a digital caliper. To determine tumor volume, we used the equation: $0.52 \times L \times W^2$ (L is the length and W^2 is the squared width). All animal experimentation and surgical procedures were carried out in compliance with NIH's principle of Laboratory Animal Care and according to the guidelines of NDSU's Institutional Animal Care and Use Committee (IACUC). All animals were also provided with irradiated food and sterile water throughout the study.

Conjugation of Infra-red Dye to IgG2A11 (Work Performed by Anil Wagh, Department of Pharmaceutical Sciences, NDSU)

Cy5.5 was labeled to IgG 2A11 as previously described [249]. Briefly, 1 mg of IgG 2A11 dissolved in 1ml of PBS (10 mM, pH 7.4) was added to 46 µg of Cy5.5 monofunctional N-hydroxysuccinimide ester (Cy5.5-NHS) (GE Healthcare) at room temperature for 15 mins. The complex was subsequently purified by size exclusion chromatography using a Sephadex G-50 column (GE Healthcare). The concentration of protein from the purified complex was determined by BCA assay (Thermo Scientific). To determine the number of Cy5.5 fluorophores

per antibody, the absorbance of the conjugate was measured between 250-750 nm by using a spectrophotometer (Spectramax Molecular Device).

In vivo Spectral Imaging Studies (Work Performed by Anil Wagh, Department of Pharmaceutical Sciences, NDSU

0.75 mg/ml of Cy5.5-labeled IgG 2A11 was administered via tail vein injection to both RAGE positive tumor-bearing mice (mice carrying WM115-RAGE tumor) and RAGE negative-tumor bearing mice (mice carrying WM115MOCK tumor) under intraperitoneal anesthesia. The mice were subsequently subjected to Near Infra-Red Fluorescence (NIRF) reflectance imaging (Kodak FX Pro, Carestream Health Incorporation) at 0, 4, 24 and 48 hours after injection as previously described [250, 251]. The acquisition time for images was set to 1 min and the images were analyzed using Kodak Digital Science ID software. The fluorescence images were normalized by subtracting the average fluorescence intensities of the region of interest from the background of the adjacent skin of the mice. A 150W halogen was used as the excitation light source. Corresponding band pass filters (Carestream Health Incorporation) to adjust excitation to a wavelength between 615-645 nm and emission to a wavelength of 680-720 nm was used for all *in vivo* imaging purposes. Eight mice were used per group and the average tumor volume used for all imaging purpose was 80 mm^3

Histological Analysis (Work Performed by Anil Wagh, Department of Pharmaceutical Sciences, NDSU)

An intraperitoneal injection of 150 mg/kg pentobarbital (Ovation Pharma), as an anesthesia, was administered to the mice for 48 hours before subsequent euthanasia and extraction of tumor. The mice were sacrificed according to standard protocol. Histological analysis was performed as previously described with some slight modification [248]. Briefly,

the extracted tumors were washed in PBS, preserved in Tissue-Tek OCT solution (Sankura Finetek USA Inc.) and snap frozen. The tumors were cryo-sectioned into 7 μm-thick slices and stained with hematoxylin-eosin (Sigma-Aldrich). NIRF fluorescence microscopy was performed on air-dried sections mounted on slides. To detect fluorescence, prepared slides were viewed using an epifluorescence microscope (Olympus IX-81). Slides were excited using a band pass filter with a wavelength between 635-675 nm and an emission band pass filter with a wavelength of 696-736 nm. The images were captured using a Hirakuchi camera interfaced with a computer and analysed with HCImage software (Hirakuchi).

Treatment of Tumor Bearing Mice with IgG 2A11 (Work Performed by Anil Wagh, Department of Pharmaceutical Sciences, NDSU)

Human melanoma tumor was induced in mice using the WM115-RAGE cell line. Five to six-week old female SCID mice under anesthesia were subcutaneously injected with (1 x 10^6 cells/50 μl) of WM115-RAGE cells. Tumor growth was measured twice a week. At a volume of approximately 80 mm^3 the mice were randomly divided into two groups of eight. To one group, IgG 2A11 was administered at a concentration of 0.5 mg/ml intravenously. To the other group, PBS was administered. The treatment with IgG 2A11 or PBS was repeated for both groups every 5 days for a total of 4 weeks.

Estimation of Kinase Activity

Mice were sacrificed according to standard procedures and tumors from both IgG 2A11-treated and PBS groups were extracted. Total protein lysate was obtained from tumor by homogenizing tumor sample in the presence of cell disruption buffer (Life Technologies) supplemented with 1 mM Na_3VO_4 and 0.5 mM PMSF. The homogenized sample was centrifuged at 2,000 rpm for 2 min at 4°C. The supernatant was collected, aliquoted, and stored at −80°C.

The protein concentration was determined using the BCA protein assay kit (Pierce). 50 µg of protein was loaded on a 12% SDS gel, followed by a transfer to a nitrocellulose membrane. The membrane was blocked with 3% BSA in TBS at room temperature for 2 hours. Primary antibodies for pAkt, Akt, pERK, ERK, p-p53, p-53, GSK3β and β-catenin (Cell Signaling Technologies) were added at a concentration of 1:2,000 in the presence of 1% BSA/TBS-T and incubated overnight at 4°C. The blot was then washed three times in TBS-T and incubated for 1h with HRP conjugated secondary antibody (Jackson ImmunoResearch) at a 1:10000 dilutions in the presence of 1%BSA/TBS-T. The membrane was washed three times in TBS-T at 15 min interval and developed with ECL Western blotting substrate (Pierce). Blots were scanned and quantified with Image J (PC version of Windows).

Estimation of NF-κB Pathway Activity

To observe translocation of NF-κB to the nucleus, nuclei extracts were obtained from excised tumor as previously described with some modification to the original protocol [252]. Briefly, frozen tissue between 100 mg-200 mg was homogenized in buffer containing 0.6% Nonidet P-40 (Thermo Scientific), 150 mM NaCl, 10mM HEPES pH 7.4, 1mM EDTA, 0.5mM PMSF supplemented with a cocktail of protease inhibitor (Promega) using a Omni polytron homogenizer set at medium speed. To remove any unbroken tissue, the homogenized tissue was subsequently centrifuged for 1min at 2000rpm. The supernatant was incubated on ice for 5 mins and centrifuged at 5000 rpm for 5 mins to collect pelleted nuclei. The pellet of nuclei was re-suspended in HEPES pH 7.4 buffer, aliquoted and stored at -80°C. The extraction process was carried out at 4°C. 50 µg of protein denatured at 40°C for 30 mins in the presence of sample buffer containing 8 M urea, glycerol, SDS, bromophenol blue, β-mercaptoethanol and 0.5 M Tris pH 6.8 was loaded on a 12% SDS gel, followed by a transfer to a nitrocellulose membrane. The

membrane was blocked with 3% BSA in TBS at room temperature for 2 hours. Primary

antibodies for NF-κB and pNF-κB (Cell Signaling Technologies) were added at a 1:2,000

dilution in the presence of 1% BSA/TBS-T and incubated overnight at 4°C. 50 μg of total tumor

lysate was also blotted onto a membrane and primary antibodies for pIκBα, IκBα, pIKKα/β,

IKKα/β and β-actin (Cell Signaling) were added at a 1:2,000 dilution in the presence of 1%

BSA/TBS-T and incubated overnight at 4° C. Blots were then washed three times in TBS-T and

incubated for 1 hour with HRP conjugated secondary antibody (Jackson ImmunoResearch) at a

1:10,000 dilution in the presence of 1% BSA/TBS-T. The membrane was washed three times in

TBS-T at 15 min intervals and developed with ECL Western Blotting Substrate (Pierce). Blots

were scanned and quantified with Image J.

Statistical Analysis

Data are presented as mean ± SEM. Statistical analysis were performed between two

groups using two-tailed paired student's t-test for both *in vivo* imaging (n=8). Values were

considered significantly different at the *P*≤0.05 level. Statistical analyses were performed on the

Kaleidagraph 4.1.0

Results

Targeting of Tumor Expressing RAGE In vivo with IgG 2A11

Figure 4.1 shows the results of imaging with IgG 2A11-Cy5.5 conjugates in both

WM115-RAGE (RAGE-positive tumor) and WM115-MOCK (RAGE negative) tumor bearing

mice. Using fluorescently tagged IgG 2A11, we were able to detect tumor expressing RAGE *in

vivo* not only in the RAGE over-expressing tumor but also in the control tumor, although the

signal was higher in the targeted tumor. Mice carrying WM115-MOCK tumors showed a lower

fluorescent intensity as compared to mice carrying WM115-RAGE tumors. In addition, near

infra-red fluorescence imaging of both WM115-RAGE and WM115-MOCK showed primary

localization of IgG 2A11 at the tumor bearing site, the mammary fat pads, as compared to any
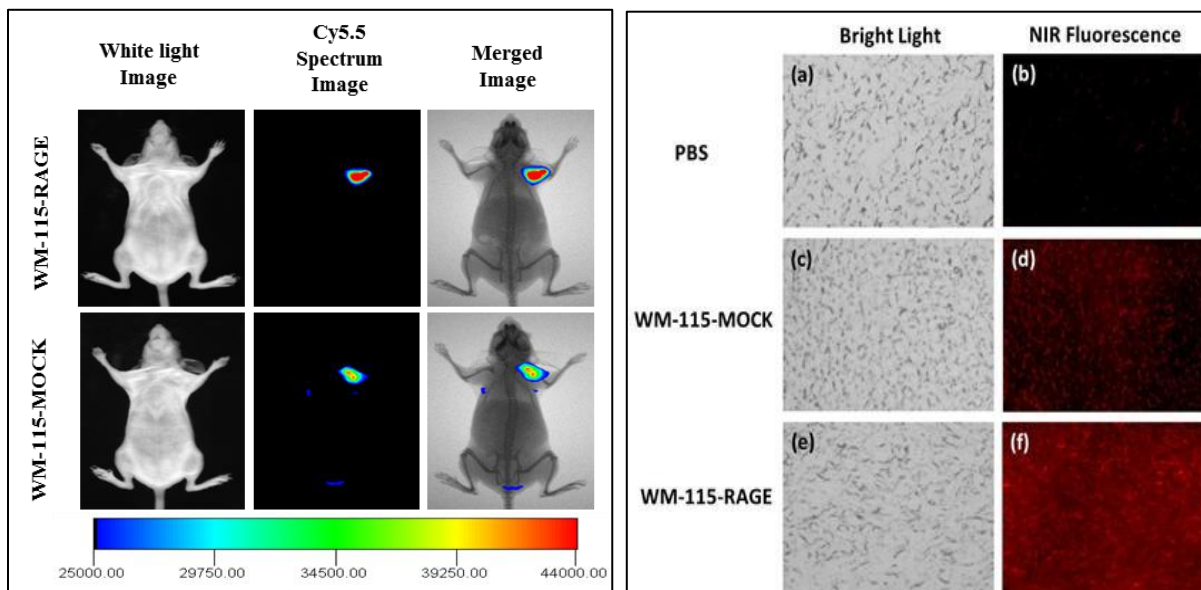
other region in the mice.

Figure 4.1: Fluorescence images of the whole animals injected with Cy5.5-IgG2A11. The images for whole body animal were obtained after injection of the IgG2A11-Cy5.5 conjugate (left). *Ex-vivo* fluorescence images of excised tumor sections (right).

Histologic Results

Results of *in vivo* NIRF imaging were confirmed with fluorescence microscopy. *Ex vivo*

NIRF images of both tumors confirmed the marked differences in RAGE positive and RAGE

negative tumors when bound to fluorescently labeled IgG 2A11. Excised tumor specimen of

WM115-RAGE showed considerably higher fluorescence intensity as compared to sections

obtained from WM115-MOCK tumor which exhibit significantly lower fluorescence intensity

(Figure 4.1).

Estimation of the Inhibitory Effects of IgG2A11 on Tumor Growth In vivo

We analyzed the effects of anti-RAGE (IgG 2A11) antibody on the growth of melanoma

tumors using human melanoma xenografts *in vivo*. The inhibitory activity of IgG 2A11 on tumor

growth was investigated by treating mice with several doses of the antibody. The mouse tumors

treated with the control (PBS) continued to grow aggressively, reaching a size of approximately

1,200 mm^3 by day 30 (Figure 4.2). In contrast, treatment with IgG 2A11 antibody resulted in a

significant reduction in tumor size (tumor volume at day 30 for control group was 1260 mm^3

while that treated with IgG 2A11 was 780 mm^3).
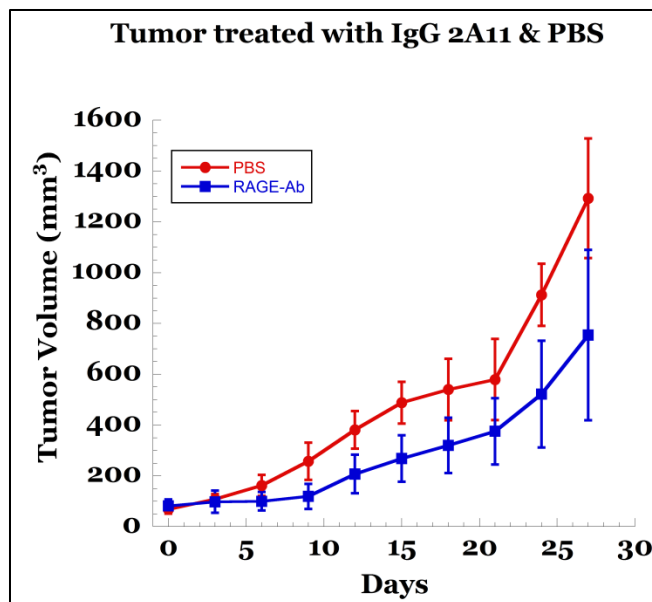
Figure 4.2: Efficacy of IgG 2A11 treatment in mice model. The mice (n=8) treated with IgG2A11 show significantly lower tumor volumes than the mice (n=8) treated with saline only (PBS).

Investigation of Inhibitory Activity of IgG 2A11 on Kinases from Treated Tumor

We showed in Chapter 2 that we were able to decrease Akt activation by blocking the

interaction of RAGE and its ligand with IgG 2A11 (Refer to Chapter 2). We therefore wanted to

investigate whether IgG 2A11 could reduce Akt and ERK1/2 kinase activities *in vivo*. Western

blot analysis was performed on tumor lysate of PBS and IgG 2A11 treated groups. Two out of

three PBS treated tumors showed higher levels of phosphorylated Akt as compared to IgG 2A11

treated groups (Figure 4.3). We also examined the activation of ERK-1/2. We observed that the

difference in the phosphorylation for both PBS treated tumor and IgG 2A11 tumor was not

significant (Figure 4.3). We also did not observe the presence of GSK or phosphorylated β-catenin in the cytosol. The nuclei extracts showed the presence of β-catenin, but there was no significant difference observed between the groups.
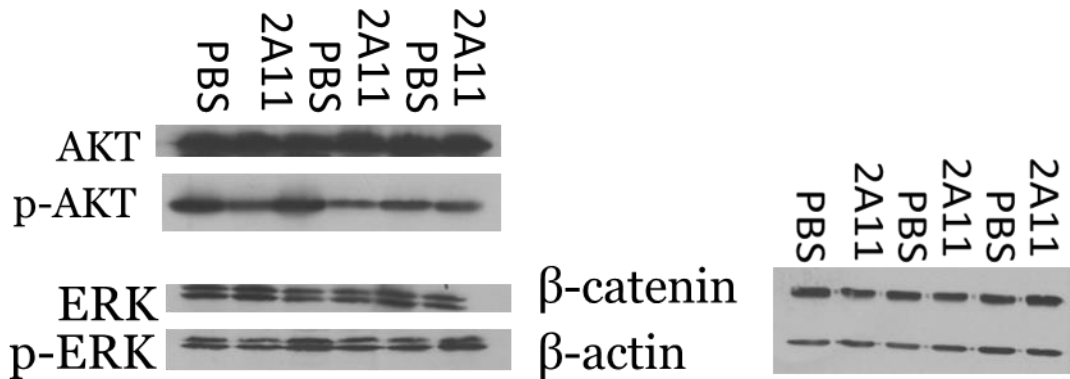
Figure 4.3: Western blot analysis of total tumor lysate and nuclei extract. Significant increase in Akt phosphorylation is observed in two out of three PBS treated groups (left). No difference in ERK 1/2 in PBS and IgG 2A11 groups. Analysis of nuclei extract obtained from tumor showed no significant difference between PBS and IgG 2A11 treated groups (Right). Tumor lysate was obtained from three different tumors from each group.

Investigation of Inhibitory Activity of IgG 2A11 on Transcription Factor (NF-κB) Activation

from Treated Tumor

Western blot analysis of nuclei extract did not reveal the presence of NF-κB or its phosphorylated form in either PBS or IgG 2A11 treated groups. We also analyzed total tumor lysate for intermediate proteins (for pIκBα, IκBα, pIKKα/β, and IKKα/β) involved in the activation of the transcription factor, but we did not observe the presence of any band (data not shown).

Discussion

Early detection for any disease state can greatly improve the efficacy of therapeutic intervention especially in cancers like melanoma where metastasis and invasion are aggressive and survival rate is very low [239, 253]. The traditional route to treat any disease starts with

84

diagnosis which is followed by treatment and finally in some but not all cases, prognosis. In high risk disease state like cancers, a patient is typically required to undergo many tests and a complete evaluation to determine the stage of the disease, the extent to which the cancer has metastasized and the type of treatment most suitable for the individual. The heterogeneity of cancer cells makes them very difficult to accurately diagnose and provide the proper therapy suited to the patient. Therefore, considerable amount of effort has been devoted to the diagnosis and treatment of cancer so that a better prognosis can be provided.

An interesting prospect is the combination of diagnostic tools with therapeutic tools [254]. These theranostic tools are becoming an emerging biomedical platform because they are capable of reaching the target site, provide information of disease state, perform therapeutic functions, and monitor therapeutic response [254]. Several imaging techniques have become standard in the diagnosis of cancers. Fortunately, many of these imaging agents can be tagged onto molecules that serve as specific biomarkers for the intended target. In many cases, especially cancer cells, it is necessary to identify cell surface proteins that are abundantly expressed and that can act as biomarkers to distinguish from normal healthy cells [255].

RAGE is a cell surface receptor that has been shown to be abundantly expressed in many cancers [256]. Therefore, we have generated antibodies to target RAGE (Chapter 1). In the present study, we have used one of our generated antibodies, IgG 2A11, in animal models to target melanoma tumors *in vivo* and to use it as a diagnostic and therapeutic tool. We were able to detect tumors expressing RAGE *in vivo* with the use of generated antibody by conjugating IgG 2A11 with a fluorophore.

Several limitations usually accompany the use of certain flurophores in *in vivo* imaging of tissue when used as diagnostic tools. These limitations include absorption of fluorescence by

macromolecules in the extracellular milieu, intense light scattering, autofluorescence, and reduction in depth penetration within tissue [249]. Researchers have often used high efficiency fluorescence proteins [257] and quantum dots to solve these problems [258, 259]. Unfortunately, the use of quantum dots in clinical settings has raised issues of toxicity because oxidation can result in the emission of selenium and cadmium from the dots [259]. Additionally, high efficiency fluorescent proteins are very large molecules [260] and are typically not tagged onto other large molecules like antibodies [249]. For these reasons, near-infrared dyes are the ideal fluorophore for diagnostic purposes because they are smaller than their counterparts, they are organic compounds and have the advantage of better depth penetration within tissue [261].

The size of an antibody makes it kinetically more advantageous; its bulkiness prevents it from being immediately cleared by the kidney. Therefore, a full-sized antibody can typically stay longer in circulation than an antibody fragment, with a half-life of 21 days for IgGs. This extended circulation within the system is advantageous from a therapeutic perspective because it can result in the continuous delivery of a drug to its target. Treatment of tumor with IgG 2A11 resulted in a significant decrease in tumor volume as compared to the control group treated with PBS. Recently, over-expression of RAGE in cancers has been associated with alteration of normal physiological molecular mechanisms such as over-expression of certain kinases and transcription factors like NF-κB [224, 247]. Akt, ERK1/2, and p53 have been known to play crucial roles in progression and development of tumors associated with the over-expression of RAGE [262-264].

The Wnt pathway has also been implicated in the progression of cancer through the β-catenin–TCF/LEF transcription complex [265]. Typically, β-catenin is present in the cytoplasm and complexed with GSK-3β, axin and APC, tumor suppressor. In a normal physiological

86

setting, APC and axin assist GSK-3β in the phosphorylation of β-catenin. Phosphorylation of β-catenin results in its subsequent proteasomal degradation which prevents its translocation into the nucleus and subsequent activation of TCF/LEF family transcription factors. Deregulation of this pathway can prevent GSK from phosphorylating β-catenin which can lead to the accumulation of β-catenin in the nucleus and results in tumor progression [266]. We therefore aimed to examine the inhibitory effects of IgG 2A11 on these downstream signaling pathways.

Western blot analysis of extracted tumor samples shows a significant decrease in the activation of Akt in two out of three groups of IgG 2A11 treated tumors. We did not observe GSK3β activity and subsequent phosphorylation of β-catenin in the control group as well the in the IgG 2A11 group. However we did observe the presence of β-catenin in the nucleus but there was no significant difference between the control group and IgG 2A11 treated groups. The data obtained suggest that IgG 2A11 does not inhibit the Wnt pathway. We also did not observe a significant change in the activation of ERK. This data suggest that IgG 2A11 does not inhibit the activation of ERK. We analysed the nuclei extract but we did not observe the presence of NF-κB in the extracted nuclei. We also analyzed the total tumor lysate for other key proteins in the NF-κB pathway. We did not observe the presence of pIκBα, IκBα, pIKKα/β or IKKα/β. A possible explanation for the absence of the proteins involved in this pathway can be attributed to their short half-lives. In 2001, Nelson and colleagues performed a multi-parameter analysis of the kinetics of NF-kB signaling and transcription in living cells and their data suggested that NF-κB protein is present in the nucleus for only a relatively short period of time of approximately 12 minutes [267]. Additionally, the other proteins involved in the pathway are quickly subjected to proteosomal degradation [268].

Conclusion

In conclusion, the generated full-sized monoclonal antibody IgG 2A11 was able to specifically target RAGE-positive tumors *in vivo*. Furthermore, IgG 2A11 was able to significantly reduce tumor size *in vivo*. The data obtained from this study suggest that IgG 2A11 could be used as a diagnostic and therapeutic tool in clinical setting.

GENERAL REMARKS AND FUTURE PERSPECTIVE

Involvement of RAGE in many diseases has led many research groups to develop anti-RAGE therapies. Many of these RAGE related diseases, especially melanoma, have one of the highest mortality rate and morbidity rate. Consequently, several efforts have gone into finding proper intervention. These efforts have been complicated due to the structurally diverse nature of ligands that interact with RAGE. The heterogeneity of ligands that bind to RAGE makes it difficult to properly decipher the downstream signaling pathways that are affected during RAGE/ligand interaction. One of our goals was to use the antibodies generated in this project to properly understanding of RAGE/ligand interaction.

We chose human melanoma cell lines for our cell based assays because these are cells where the effects of RAGE/ligand interaction have not yet been studied well. Our results confirmed previously published studies regarding downstream RAGE signaling. We observed an increase in Akt activation, NF-κB activation, and proliferation when RAGE was exposed to AGE products and a subsequent decrease when IgG 2A11 was added to the culture. We were also able to confirm these results in two out of three xenograft mice carrying human melanoma tumors treated with IgG 2A11. We observed a significant decrease in size in tumors treated with IgG 2A11 as well as a decrease in Akt activation.

Based on the promising results obtained from IgG 2A11, we will repeat similar cell based assays and animal studies to observe the effects of the remaining antibodies generated in Chapter 1. However it is possible that some or all of the other antibodies might not have an inhibitory effect on proliferation as IgG 2A11 had in cell based assays and *in vivo* because of the domain of specificity. In the cell based assays performed in Chapter 2, AGE, which has been shown to bind to the VC1 domain, was used as a cell proliferative inducer of RAGE. The data obtained from

this project suggest that IgG 2A11 was able to prevent the binding of AGE to RAGE because IgG 2A11 also binds to the V domain.

Therefore, in the future studies, we will use other RAGE ligand to interrogate RAGE and observe the effects that the remaining antibodies exert in the system. This can provide some answers as to the potential mechanism of action of the generated antibodies. We anticipate that the remaining antibodies will display similar effectiveness in the diagnostic ability to detect RAGE specific tumors *in vivo* and can be used as a therapeutic intervention in RAGE related pathologies. In order for any of the generated antibodies to be deemed therapeutically effective, in addition to showing appropriate efficacy in an animal model, all the antibodies will need to undergo several human clinical trials that demonstrate safety, effectiveness and a low adverse effect profile.

REFERENCES

1. Theves, G., [Smallpox: an historical review]. Bull Soc Sci Med Grand Duche Luxemb, 1997. **134**(1): p. 31-51.

2. Grant, D.M., [Lady Mary Wortley Montagu and the campaign against smallpox]. Infirm Can, 1969. **11**(12): p. 29-31.

3. Eyler, J.M., Smallpox in history: the birth, death, and impact of a dread disease. J Lab Clin Med, 2003. **142**(4): p. 216-20.

4. Dinc, G. and Y.I. Ulman, The introduction of variolation 'A La Turca' to the West by Lady Mary Montagu and Turkey's contribution to this. Vaccine, 2007. **25**(21): p. 4261-5.

5. Gross, C.P. and K.A. Sepkowitz, The myth of the medical breakthrough: smallpox, vaccination, and Jenner reconsidered. Int J Infect Dis, 1998. **3**(1): p. 54-60.

6. Strohl, E.L., The Fascinating Lady Mary Wortley Montagu, 1689-1762. Arch Surg, 1964. **89**: p. 554-8.

7. Stone, A.F. and W.D. Stone, Lady Mary Wortley Montagu: medical and religious controversy following her introduction of smallpox inoculation. J Med Biogr, 2002. **10**(4): p. 232-6.

8. Kiss, L., [Lady Montagu versus Raymann -- the first variolations in Europe]. Orv Hetil, 2011. **152**(44): p. 1782-4.

9. Grant, D.M., Lady Mary Wortley Montagu--eighteenth century crusader. Can Nurse, 1969. **65**(7): p. 34-6.

10. Macnalty, A.S., Emil von Behring, born March 15, 1854. Br Med J, 1954. **1**(4863): p. 668-70.

11.   Lindenmann, J., Origin of the terms 'antibody' and 'antigen'. Scand J Immunol, 1984. **19**(4): p. 281-5.

12.   Dale, H., Fifty Years of Medical Research. Br Med J, 1963. **2**(5368): p. 1287-90.

13.   Winau, F., O. Westphal, and R. Winau, Paul Ehrlich--in search of the magic bullet. Microbes Infect, 2004. **6**(8): p. 786-9.

14.   Llewelyn, M.B., R.E. Hawkins, and S.J. Russell, Discovery of antibodies. BMJ, 1992. **305**(6864): p. 1269-72.

15.   Scientific events: Immunization against Pneumonia. Science, 1924. **59**(1533): p. 434 - 435.

16.   Felton, L.D., Immunization against Pneumonia. Am J Public Health Nations Health, 1940. **30**(4): p. 361-8.

17.   Marrack, J.R., The chemistry of antigens and antibodies. 2nd ed. Medical research council Special report series. 1938, London.: H.M stationery office. 135 pages.

18.   Marrack, J., The structure of antigen-antibody aggregates and complement fixation. Annu Rev Microbiol, 1955. **9**: p. 369-86.

19.   Heidelberger, M., F.E. Kendall, and C.M. Soo Hoo, Quantitative Studies on the Precipitin Reaction: Antibody Production in Rabbits Injected with an Azo Protein. J Exp Med, 1933. **58**(2): p. 137-52.

20.   Heidelberger, M. and F.E. Kendall, A Quantitative Study of the Precipitin Reaction between Type Iii Pneumococcus Polysaccharide and Purified Homologous Antibody. J Exp Med, 1929. **50**(6): p. 809-23.

21.   Heidelberger, M., R.H. Sia, and F.E. Kendall, Specific Precipitation and Mouse Protection in Type I Antipneumococcus Sera. J Exp Med, 1930. **52**(4): p. 477-83.

22.   Heidelberger, M. and F.E. Kendall, Quantitative Studies on the Precipitin Reaction : The Determination of Small Amounts of a Specific Polysaccharide. J Exp Med, 1932. **55**(4): p. 555-61.

23.   Pauling, L., National Library of Medicine (U.S.), and Oregon State University. Libraries., The Linus Pauling papers. 2012, U.S. National Library of Medicine, National Institutes of Health, Dept. of Health & Human Services: Bethesda, MD.

24.   Fagraeus, A., The plasma cellular reaction and its relation to the formation of antibodies in vitro. J Immunol, 1948. **58**(1): p. 1-13.

25.   Coons, A.H., E.H. Leduc, and J.M. Connolly, Studies on antibody production. I. A method for the histochemical demonstration of specific antibody and its application to a study of the hyperimmune rabbit. J Exp Med, 1955. **102**(1): p. 49-60.

26.   Raju, T.N., The Nobel chronicles. 1972: Gerald M Edelman (b 1929) and Rodney R Porter (1917-85). Lancet, 1999. **354**(9183): p. 1040 - 1041.

27.   Edelman, G.M. and J.A. Gally, The nature of Bence-Jones proteins. Chemical similarities to polypeptide chains of myeloma globulins and normal gamma-globulins. J Exp Med, 1962. **116**: p. 207-27.

28.   Tomasi, T.B., The discovery of secretory IgA and the mucosal immune system. Immunol Today, 1992. **13**(10): p. 416-8.

29.   Preud'homme, J.L., et al., Structural and functional properties of membrane and secreted IgD. Mol Immunol, 2000. **37**(15): p. 871-87.

30.   Johansson, S.G., The discovery of immunoglobulin E. Allergy Asthma Proc, 2006. **27**(2 Suppl 1): p. S3-6.

31.   Lipman, N.S., et al., Monoclonal versus polyclonal antibodies: distinguishing characteristics, applications, and information resources. ILAR J, 2005. **46**(3): p. 258-68.

32.   Linker, R.A. and B.C. Kieseier, Innovative monoclonal antibody therapies in multiple sclerosis. Ther Adv Neurol Disord, 2008. **1**(1): p. 43-52.

33.   Springer, T.A., Cesar Milstein, the father of modern immunology. Nat Immunol, 2002. **3**(6): p. 501-3.

34.   Freysd'ottir, J., Production of monoclonal antibodies. Methods Mol Med, 2000. **40**: p. 267-79.

35.   Danon, Y.L., Monoclonal antibodies: George Kohler. Harefuah, 1996. **130**(2): p. 108-9.

36.   Milstein, C., et al., Expression of antibody genes in tissue culture: structural mutants and hybrid cells. Natl Cancer Inst Monogr, 1978(48): p. 321-30.

37.   Kohler, G. and C. Milstein, Derivation of specific antibody-producing tissue culture and tumor lines by cell fusion. Eur J Immunol, 1976. **6**(7): p. 511-9.

38.   Chadd, H.E. and S.M. Chamow, Therapeutic antibody expression technology. Curr Opin Biotechnol, 2001. **12**(2): p. 188-94.

39.   McCafferty, J., et al., Phage antibodies: filamentous phage displaying antibody variable domains. Nature, 1990. **348**(6301): p. 552-4.

40.   Green, L.L., et al., Antigen-specific human monoclonal antibodies from mice engineered with human Ig heavy and light chain YACs. Nat Genet, 1994. **7**(1): p. 13-21.

41.   Lonberg, N. and D. Huszar, Human antibodies from transgenic mice. Int Rev Immunol, 1995. **13**(1): p. 65-93.

42. Kellermann, S.A. and L.L. Green, Antibody discovery: the use of transgenic mice to generate human monoclonal antibodies for therapeutics. Curr Opin Biotechnol, 2002. **13**(6): p. 593-7.

43. Litchman, A.K.A.a.A.H., Basic Immunology : Functions and Disorders of the Immune System. 3rd Edition ed. 2009, Philadelphia, PA: Saunders Elsevier.

44. Edelman, G.M. and M.D. Poulik, Studies on structural units of the gamma-globulins. J Exp Med, 1961. **113**: p. 861-84.

45. Fleischman, J.B., R.H. Pain, and R.R. Porter, Reduction of gamma-globulins. Arch Biochem Biophys, 1962. **Suppl 1**: p. 174-80.

46. Technical notes and product highlights: Antibody structure and classification - Note 7.1. 2011 [cited 2012 August 20th]; Available from: http://www.invitrogen.com/site/us/en/home/References/Molecular-Probes-The-Handbook/Technical-Notes-and-Product-Highlights/Antibody-Structure-and-Classification.html.

47. Porter, R.R., The hydrolysis of rabbit gamma-globulin and antibodies with crystalline papain. Biochem J, 1959. **73**: p. 119-26.

48. Sites, D.P.e.a., Basic and Clinical Immunology. 1976, Los Altos, CA: Lange Medical Publication.

49. Woof, J.M. and D.R. Burton, Human antibody-Fc receptor interactions illuminated by crystal structures. Nat Rev Immunol, 2004. **4**(2): p. 89-99.

50. Goding, J.W., Allotypes of IgM and IgD receptors in the mouse: a probe for lymphocyte differentiation. Contemp Top Immunobiol, 1978. **8**: p. 203-43.

51. Theis, G.A. and G.W. Siskind, Selection of cell populations in induction of tolerance: affinity of antibody formed in partially tolerant rabbits. J Immunol, 1968. **100**(1): p. 138-41.

52. Brambell, F.W., W.A. Hemmings, and I.G. Morris, A Theoretical Model of Gamma-Globulin Catabolism. Nature, 1964. **203**: p. 1352-4.

53. Blaese, R.M., et al., Hypercatabolism of IgG, IgA, IgM, and albumin in the Wiskott-Aldrich syndrome. A unique disorder of serum protein metabolism. J Clin Invest, 1971. **50**(11): p. 2331-8.

54. Waldmann, T.A., J.S. Johnson, and N. Talal, Hypogammaglobulinemia associated with accelerated catabolism of IgG secondary to its inteaction with an IgG-reactive monoclonal IgM. J Clin Invest, 1971. **50**(4): p. 951-9.

55. Elgert, K.D., Immunology: Understanding The Immune System. . Vol. 1. 1996: John Wiley and Sons.

56. Howard, G.C. and D.R. Bethell, Basic methods in antibody production and characterization. 1 ed. 2001, Boca Raton, Florida: CRC Press. 288 pages.

57. Vieira, J.G., et al., Egg yolk as a source of antibodies for human parathyroid hormone (hPTH) radioimmunoassay. J Immunoassay, 1984. **5**(1-2): p. 121-9.

58. Stuart, C.A., et al., High affinity antibody from hen's eggs directed against the human insulin receptor and the human IGF-I receptor. Anal Biochem, 1988. **173**(1): p. 142-50.

59. McMichael, A.J. and J.W. Fabre, Monoclonal antibodies in clinical medicine. 1 ed. 1982, London, U.K: Academic press. 663 pages.

60. Goding, J.W., Monoclonal antibodies: Principles and practices. 1983, Orlando, Florida: Academic Press Inc.

61.	Littlefield, J.W., Selection of Hybrids from Matings of Fibroblasts in Vitro and Their Presumed Recombinants. Science, 1964. **145**(3633): p. 709-10.

62.	Jones, S.L., J.C. Cox, and J.E. Pearson, Increased monoclonal antibody ascites production in mice primed with Freund's incomplete adjuvant. J Immunol Methods, 1990. **129**(2): p. 227-31.

63.	Jackson, L.R., et al., Monoclonal antibody production in murine ascites. II. Production characteristics. Lab Anim Sci, 1999. **49**(1): p. 81-6.

64.	Elgert, K.D., Immunology: Understanding The Immune System. Vol. 1. 1996: John Wiley and Sons.

65.	Burton, D.R. and C.F. Barbas, 3rd, Antibodies from libraries. Nature, 1992. **359**(6398): p. 782-3.

66.	Barbas, C.F., 3rd, et al., Assembly of combinatorial antibody libraries on phage surfaces: the gene III site. Proc Natl Acad Sci U S A, 1991. **88**(18): p. 7978-82.

67.	Barbas, C.F., 3rd, et al., Human monoclonal Fab fragments derived from a combinatorial library bind to respiratory syncytial virus F glycoprotein and neutralize infectivity. Proc Natl Acad Sci U S A, 1992. **89**(21): p. 10164-8.

68.	Hooks, M.A., C.S. Wade, and W.J. Millikan, Jr., Muromonab CD-3: a review of its pharmacology, pharmacokinetics, and clinical use in transplantation. Pharmacotherapy, 1991. **11**(1): p. 26-37.

69.	Dimitrov, D.S. and J.D. Marks, Therapeutic antibodies: current state and future trends--is a paradigm change coming soon? Methods Mol Biol, 2009. **525**: p. 1-27.

70.	Stern, M. and R. Herrmann, Overview of monoclonal antibodies in cancer therapy: present and promise. Crit Rev Oncol Hematol, 2005. **54**(1): p. 11-29.

71. Waldmann, T.A., Immunotherapy: past, present and future. Nat Med, 2003. **9**(3): p. 269-77.

72. Chothia, C., et al., Conformations of immunoglobulin hypervariable regions. Nature, 1989. **342**(6252): p. 877-83.

73. Wiseman, G.A., et al., Radioimmunotherapy of relapsed non-Hodgkin's lymphoma with zevalin, a 90Y-labeled anti-CD20 monoclonal antibody. Clin Cancer Res, 1999. **5**(10 Suppl): p. 3281s-3286s.

74. Atkins, J.T., et al., Prophylaxis for respiratory syncytial virus with respiratory syncytial virus-immunoglobulin intravenous among preterm infants of thirty-two weeks gestation and less: reduction in incidence, severity of illness and cost. Pediatr Infect Dis J, 2000. **19**(2): p. 138-43.

75. Scolnik, P.A., mAbs: a business perspective. MAbs, 2009. **1**(2): p. 179-84.

76. Matsumoto, S., et al., Solution structure of the variable-type domain of the receptor for advanced glycation end products: new insight into AGE-RAGE interaction. Biochemistry, 2008. **47**(47): p. 12299-311.

77. Schmidt, A.M., et al., The biology of the receptor for advanced glycation end products and its ligands. Biochim Biophys Acta, 2000. **1498**(3): p. 99-111.

78. Sugaya, K., et al., Three genes in the human MHC class III region near the junction with the class II: gene for receptor of advanced glycosylation end products, PBX2 homeobox gene and a notch homolog, human counterpart of mouse mammary tumor gene int-3. Genomics, 1994. **23**(2): p. 408-19.

79.   Srikrishna, G., et al., N -Glycans on the receptor for advanced glycation end products influence amphoterin binding and neurite outgrowth. J Neurochem, 2002. **80**(6): p. 998-1008.

80.   Raucci, A., et al., A soluble form of the receptor for advanced glycation endproducts (RAGE) is produced by proteolytic cleavage of the membrane-bound form by the sheddase a disintegrin and metalloprotease 10 (ADAM10). FASEB J, 2008. **22**(10): p. 3716-27.

81.   Kalea, A.Z., et al., Alternative splicing of the murine receptor for advanced glycation end-products (RAGE) gene. FASEB J, 2009. **23**(6): p. 1766-74.

82.   Kalea, A.Z., A.M. Schmidt, and B.I. Hudson, Alternative splicing of RAGE: roles in biology and disease. Front Biosci, 2012. **17**: p. 2756-70.

83.   Yonekura, H., et al., Roles of the receptor for advanced glycation endproducts in diabetes-induced vascular injury. J Pharmacol Sci, 2005. **97**(3): p. 305-11.

84.   Grossin, N., et al., Severity of diabetic microvascular complications is associated with a low soluble RAGE level. Diabetes Metab, 2008. **34**(4 Pt 1): p. 392-5.

85.   Sternberg, Z., et al., Soluble receptor for advanced glycation end products in multiple sclerosis: a potential marker of disease severity. Mult Scler, 2008. **14**(6): p. 759-63.

86.   Kalousova, M., et al., A419C (E111A) polymorphism of the glyoxalase I gene and vascular complications in chronic hemodialysis patients. Ann N Y Acad Sci, 2008. **1126**: p. 268-71.

87.   Nakamura, K., et al., Telmisartan inhibits expression of a receptor for advanced glycation end products (RAGE) in angiotensin-II-exposed endothelial cells and decreases serum

levels of soluble RAGE in patients with essential hypertension. Microvasc Res, 2005. **70**(3): p. 137-41.

88. Forbes, J.M., et al., Modulation of soluble receptor for advanced glycation end products by angiotensin-converting enzyme-1 inhibition in diabetic nephropathy. J Am Soc Nephrol, 2005. **16**(8): p. 2363-72.

89. Santilli, F., et al., Decreased plasma soluble RAGE in patients with hypercholesterolemia: effects of statins. Free Radic Biol Med, 2007. **43**(9): p. 1255-62.

90. Tan, K.C., et al., Thiazolidinedione increases serum soluble receptor for advanced glycation end-products in type 2 diabetes. Diabetologia, 2007. **50**(9): p. 1819-25.

91. Taguchi, A., et al., Blockade of RAGE-amphoterin signalling suppresses tumour growth and metastases. Nature, 2000. **405**(6784): p. 354-60.

92. Sinnberg, T., et al., Suppression of casein kinase 1alpha in melanoma cells induces a switch in beta-catenin signaling to promote metastasis. Cancer Res, 2010. **70**(17): p. 6999-7009.

93. Huttunen, H.J., J. Kuja-Panula, and H. Rauvala, Receptor for advanced glycation end products (RAGE) signaling induces CREB-dependent chromogranin expression during neuronal differentiation. J Biol Chem, 2002. **277**(41): p. 38635-46.

94. Riehl, A., et al., The receptor RAGE: Bridging inflammation and cancer. Cell Commun Signal, 2009. **7**: p. 12 - 19.

95. Li, J. and A.M. Schmidt, Characterization and functional analysis of the promoter of RAGE, the receptor for advanced glycation end products. J Biol Chem, 1997. **272**(26): p. 16498-506.

96.   Bierhaus, A., et al., Understanding RAGE, the receptor for advanced glycation end products. J Mol Med (Berl), 2005. **83**(11): p. 876-86.

97.   Brett, J., et al., Survey of the distribution of a newly characterized receptor for advanced glycation end products in tissues. Am J Pathol, 1993. **143**(6): p. 1699-712.

98.   Hynes, R.O., Integrins: versatility, modulation, and signaling in cell adhesion. Cell, 1992. **69**(1): p. 11-25.

99.   Hori, O., et al., The receptor for advanced glycation end products (RAGE) is a cellular binding site for amphoterin. Mediation of neurite outgrowth and co-expression of rage and amphoterin in the developing nervous system. J Biol Chem, 1995. **270**(43): p. 25752-61.

100.   Yan, S.D., et al., RAGE and amyloid-beta peptide neurotoxicity in Alzheimer's disease. Nature, 1996. **382**(6593): p. 685-91.

101.   Hofmann, M.A., et al., RAGE mediates a novel proinflammatory axis: a central cell surface receptor for S100/calgranulin polypeptides. Cell, 1999. **97**(7): p. 889-901.

102.   Xie, J., et al., Structural basis for pattern recognition by the receptor for advanced glycation end products (RAGE). J Biol Chem, 2008. **283**(40): p. 27255-69.

103.   Fritz, G., RAGE: a single receptor fits multiple ligands. Trends Biochem Sci, 2011. **36**(12): p. 625-32.

104.   Sturchler, E., et al., Site-specific blockade of RAGE-Vd prevents amyloid-beta oligomer neurotoxicity. J Neurosci, 2008. **28**(20): p. 5149-58.

105.   Leclerc, E., et al., Binding of S100 proteins to RAGE: an update. Biochim Biophys Acta, 2009. **1793**(6): p. 993-1007.

106.   Taylor, M. and D. Kerr, Diabetes control and complications: a coming of AGE. Lancet, 1996. **347**(9000): p. 485 - 6.

107.   Papadea, C., G.E. Austin, and R.E. Mullins, The effect of storage conditions on ion exchange and affinity chromatographic assays for glycated hemoglobin. Clin Biochem, 1984. **17**(5): p. 296-301.

108.   Rochman, H., Hemoglobin A1c and diabetes mellitus. Ann Clin Lab Sci, 1980. **10**(2): p. 111-5.

109.   Koenig, R.J., et al., Correlation of glucose regulation and hemoglobin AIc in diabetes mellitus. N Engl J Med, 1976. **295**(8): p. 417-20.

110.   Brownlee, M., H. Vlassara, and A. Cerami, Nonenzymatic glycosylation and the pathogenesis of diabetic complications. Ann Intern Med, 1984. **101**(4): p. 527-37.

111.   Chappey, O., et al., Advanced glycation end products, oxidant stress and vascular lesions. Eur J Clin Invest, 1997. **27**(2): p. 97-108.

112.   Eble, A.S., S.R. Thorpe, and J.W. Baynes, Nonenzymatic glucosylation and glucose-dependent cross-linking of protein. J Biol Chem, 1983. **258**(15): p. 9406-12.

113.   McDonald, M.J., et al., Functional properties of the glycosylated minor components of human adult hemoglobin. J Biol Chem, 1979. **254**(3): p. 702-7.

114.   Bucala, R., P. Model, and A. Cerami, Modification of DNA by reducing sugars: a possible mechanism for nucleic acid aging and age-related dysfunction in gene expression. Proc Natl Acad Sci U S A, 1984. **81**(1): p. 105-9.

115.   Williams, S.K., J.J. Devenny, and M.W. Bitensky, Micropinocytic ingestion of glycosylated albumin by isolated microvessels: possible role in pathogenesis of diabetic microangiopathy. Proc Natl Acad Sci U S A, 1981. **78**(4): p. 2393-7.

116. Esposito, C., et al., Endothelial receptor-mediated binding of glucose-modified albumin is associated with increased monolayer permeability and modulation of cell surface coagulant properties. J Exp Med, 1989. **170**(4): p. 1387-407.

117. Wautier, J.L., et al., Advanced glycation end products (AGEs) on the surface of diabetic erythrocytes bind to the vessel wall via a specific receptor inducing oxidant stress in the vasculature: a link between surface-associated AGEs and diabetic complications. Proc Natl Acad Sci U S A, 1994. **91**(16): p. 7742-6.

118. Wautier, J.L., et al., Receptor-mediated endothelial cell dysfunction in diabetic vasculopathy. Soluble receptor for advanced glycation end products blocks hyperpermeability in diabetic rats. J Clin Invest, 1996. **97**(1): p. 238-43.

119. Schmidt, A.M., et al., Advanced glycation endproducts interacting with their endothelial receptor induce expression of vascular cell adhesion molecule-1 (VCAM-1) in cultured human endothelial cells and in mice. A potential mechanism for the accelerated vasculopathy of diabetes. J Clin Invest, 1995. **96**(3): p. 1395-403.

120. Bierhaus, A., et al., AGEs and their interaction with AGE-receptors in vascular disease and diabetes mellitus. I. The AGE concept. Cardiovasc Res, 1998. **37**(3): p. 586-600.

121. The effect of intensive treatment of diabetes on the development and progression of long-term complications in insulin-dependent diabetes mellitus. The Diabetes Control and Complications Trial Research Group. N Engl J Med, 1993. **329**(14): p. 977-86.

122. Fishbane, S., et al., Reduction of plasma apolipoprotein-B by effective removal of circulating glycation derivatives in uremia. Kidney Int, 1997. **52**(6): p. 1645-50.

123. Takahashi, M., et al., Quantitative analysis of crosslinks pyridinoline and pentosidine in articular cartilage of patients with bone and joint disorders. Arthritis Rheum, 1994. **37**(5): p. 724-8.

124. Munch, G., et al., Advanced glycation endproducts in ageing and Alzheimer's disease. Brain Res Brain Res Rev, 1997. **23**(1-2): p. 134-43.

125. Sell, D.R. and V.M. Monnier, End-stage renal disease and diabetes catalyze the formation of a pentose-derived crosslink from aging human collagen. J Clin Invest, 1990. **85**(2): p. 380-4.

126. Nicholl, I.D. and R. Bucala, Advanced glycation endproducts and cigarette smoking. Cell Mol Biol (Noisy-le-grand), 1998. **44**(7): p. 1025-33.

127. O'Brien, J. and P.A. Morrissey, Nutritional and toxicological aspects of the Maillard browning reaction in foods. Crit Rev Food Sci Nutr, 1989. **28**(3): p. 211-48.

128. Singh, R., et al., Advanced glycation end-products: a review. Diabetologia, 2001. **44**(2): p. 129-46.

129. Giardino, I., et al., Aminoguanidine inhibits reactive oxygen species formation, lipid peroxidation, and oxidant-induced apoptosis. Diabetes, 1998. **47**(7): p. 1114-20.

130. Thorpe, S.R. and J.W. Baynes, Role of the Maillard reaction in diabetes mellitus and diseases of aging. Drugs Aging, 1996. **9**(2): p. 69-77.

131. Hammes, H.P., et al., Antioxidant treatment of experimental diabetic retinopathy in rats with nicanartine. Diabetologia, 1997. **40**(6): p. 629-34.

132. Nilsson, B.O., Biological effects of aminoguanidine: an update. Inflamm Res, 1999. **48**(10): p. 509-15.

133. Abe, R., et al., Regulation of human melanoma growth and metastasis by AGE-AGE receptor interactions. J Invest Dermatol, 2004. **122**(2): p. 461-7.

134. Rothermundt, M., et al., S100B in brain damage and neurodegeneration. Microsc Res Tech, 2003. **60**(6): p. 614-32.

135. Harpio, R. and R. Einarsson, S100 proteins as cancer biomarkers with focus on S100B in malignant melanoma. Clin Biochem, 2004. **37**(7): p. 512-8.

136. Cai, X.Y., et al., Association of increased S100B, S100A6 and S100P in serum levels with acute coronary syndrome and also with the severity of myocardial infarction in cardiac tissue of rat models with ischemia-reperfusion injury. Atherosclerosis, 2011. **217**(2): p. 536-42.

137. Moore, B.W., A soluble protein characteristic of the nervous system. Biochem Biophys Res Commun, 1965. **19**(6): p. 739-44.

138. Marenholz, I., C.W. Heizmann, and G. Fritz, S100 proteins in mouse and man: from evolution to function and pathology (including an update of the nomenclature). Biochem Biophys Res Commun, 2004. **322**(4): p. 1111-22.

139. Fritz, G., et al., Natural and amyloid self-assembly of S100 proteins: structural basis of functional diversity. FEBS J, 2010. **277**(22): p. 4578-90.

140. Moroz, O.V., K.S. Wilson, and I.B. Bronstein, The role of zinc in the S100 proteins: insights from the X-ray structures. Amino Acids, 2011. **41**(4): p. 761-72.

141. Marenholz, I., R.C. Lovering, and C.W. Heizmann, An update of the S100 nomenclature. Biochim Biophys Acta, 2006. **1763**(11): p. 1282-3.

142. Heizmann, C.W., G. Fritz, and B.W. Schafer, S100 proteins: structure, functions and pathology. Front Biosci, 2002. **7**: p. d1356-68.

143.   Heizmann, C.W., G.E. Ackermann, and A. Galichet, Pathologies involving the S100 proteins and RAGE. Subcell Biochem, 2007. **45**: p. 93-138.

144.   Pietzsch, J., S100 proteins in health and disease. Amino Acids, 2011. **41**(4): p. 755-60.

145.   Raabe, A., et al., Correlation of computed tomography findings and serum brain damage markers following severe head injury. Acta Neurochir (Wien), 1998. **140**(8): p. 787-91.

146.   Hoyaux, D., et al., S100A6 overexpression within astrocytes associated with impaired axons from both ALS mouse model and human patients. J Neuropathol Exp Neurol, 2002. **61**(8): p. 736-44.

147.   Huttunen, H.J., et al., Coregulation of neurite outgrowth and cell survival by amphoterin and S100 proteins through receptor for advanced glycation end products (RAGE) activation. J Biol Chem, 2000. **275**(51): p. 40096-105.

148.   Reddy, M.A., et al., Key role of Src kinase in S100B-induced activation of the receptor for advanced glycation end products in vascular smooth muscle cells. J Biol Chem, 2006. **281**(19): p. 13685-93.

149.   Leclerc, E., et al., S100B and S100A6 differentially modulate cell survival by interacting with distinct RAGE (receptor for advanced glycation end products) immunoglobulin domains. J Biol Chem, 2007. **282**(43): p. 31317-31.

150.   Yoshikai, S., et al., Genomic organization of the human amyloid beta-protein precursor gene. Gene, 1990. **87**(2): p. 257-63.

151.   Vassar, R., et al., Beta-secretase cleavage of Alzheimer's amyloid precursor protein by the transmembrane aspartic protease BACE. Science, 1999. **286**(5440): p. 735-41.

152.   Yan, R., et al., Membrane-anchored aspartyl protease with Alzheimer's disease beta-secretase activity. Nature, 1999. **402**(6761): p. 533-7.

153. Iwatsubo, T., The gamma-secretase complex: machinery for intramembrane proteolysis. Curr Opin Neurobiol, 2004. **14**(3): p. 379-83.

154. Edbauer, D., et al., Reconstitution of gamma-secretase activity. Nat Cell Biol, 2003. **5**(5): p. 486-8.

155. Yan, S.D., et al., RAGE and Alzheimer's disease: a progression factor for amyloid-beta-induced cellular perturbation? J Alzheimers Dis, 2009. **16**(4): p. 833-43.

156. Akiyama, H., et al., Inflammation and Alzheimer's disease. Neurobiol Aging, 2000. **21**(3): p. 383-421.

157. Arancio, O., et al., RAGE potentiates Abeta-induced perturbation of neuronal function in transgenic mice. EMBO J, 2004. **23**(20): p. 4096-105.

158. Lue, L.F., et al., Involvement of microglial receptor for advanced glycation endproducts (RAGE) in Alzheimer's disease: identification of a cellular activation mechanism. Exp Neurol, 2001. **171**(1): p. 29-45.

159. Yan, S.D., et al., RAGE-Abeta interactions in the pathophysiology of Alzheimer's disease. Restor Neurol Neurosci, 1998. **12**(2-3): p. 167-73.

160. Moos, T. and E.H. Morgan, Transferrin and transferrin receptor function in brain barrier systems. Cell Mol Neurobiol, 2000. **20**(1): p. 77-95.

161. Askarova, S., et al., Role of Abeta-receptor for advanced glycation endproducts interaction in oxidative stress and cytosolic phospholipase A activation in astrocytes and cerebral endothelial cells. Neuroscience, 2011. **199**: p. 375-85.

162. Goodwin, G.H., C. Sanders, and E.W. Johns, A new group of chromatin-associated proteins with a high content of acidic and basic amino acids. Eur J Biochem, 1973. **38**(1): p. 14-9.

163. Bianchi, M.E. and A.A. Manfredi, High-mobility group box 1 (HMGB1) protein at the crossroads between innate and adaptive immunity. Immunol Rev, 2007. **220**: p. 35-46.

164. Thomas, J.O. and A.A. Travers, HMG1 and 2, and related 'architectural' DNA-binding proteins. Trends Biochem Sci, 2001. **26**(3): p. 167-74.

165. Muller, S., L. Ronfani, and M.E. Bianchi, Regulated expression and subcellular localization of HMGB1, a chromatin protein with a cytokine function. J Intern Med, 2004. **255**(3): p. 332-43.

166. Muller, S., et al., New EMBO members' review: the double life of HMGB1 chromatin protein: architectural factor and extracellular signal. EMBO J, 2001. **20**(16): p. 4337-40.

167. Rauvala, H. and R. Pihlaskari, Isolation and some characteristics of an adhesive factor of brain that enhances neurite outgrowth in central neurons. J Biol Chem, 1987. **262**(34): p. 16625-35.

168. Rauvala, H., et al., The adhesive and neurite-promoting molecule p30: analysis of the amino-terminal sequence and production of antipeptide antibodies that detect p30 at the surface of neuroblastoma cells and of brain neurons. J Cell Biol, 1988. **107**(6 Pt 1): p. 2293-305.

169. Bianchi, M.E., M. Beltrame, and G. Paonessa, Specific recognition of cruciform DNA by nuclear protein HMG1. Science, 1989. **243**(4894 Pt 1): p. 1056-9.

170. Merenmies, J., et al., 30-kDa heparin-binding protein of brain (amphoterin) involved in neurite outgrowth. Amino acid sequence and localization in the filopodia of the advancing plasma membrane. J Biol Chem, 1991. **266**(25): p. 16722-9.

171. Bianchi, M.E. and A. Agresti, HMG proteins: dynamic players in gene regulation and differentiation. Curr Opin Genet Dev, 2005. **15**(5): p. 496-506.

172.   Hock, R., et al., HMG chromosomal proteins in development and disease. Trends Cell Biol, 2007. **17**(2): p. 72-9.

173.   Lotze, M.T. and K.J. Tracey, High-mobility group box 1 protein (HMGB1): nuclear weapon in the immune arsenal. Nat Rev Immunol, 2005. **5**(4): p. 331-42.

174.   Kallijarvi, J., M. Haltia, and M.H. Baumann, Amphoterin includes a sequence motif which is homologous to the Alzheimer's beta-amyloid peptide (Abeta), forms amyloid fibrils in vitro, and binds avidly to Abeta. Biochemistry, 2001. **40**(34): p. 10032-7.

175.   Sparatore, B., et al., Extracellular processing of amphoterin generates a peptide active on erythroleukaemia cell differentiation. Biochem J, 2001. **357**(Pt 2): p. 569-74.

176.   Huttunen, H.J. and H. Rauvala, Amphoterin as an extracellular regulator of cell motility: from discovery to disease. J Intern Med, 2004. **255**(3): p. 351-66.

177.   Huttunen, H.J., C. Fages, and H. Rauvala, Receptor for advanced glycation end products (RAGE)-mediated neurite outgrowth and activation of NF-kappaB require the cytoplasmic domain of the receptor but different downstream signaling pathways. J Biol Chem, 1999. **274**(28): p. 19919-24.

178.   Lander, H.M., et al., Activation of the receptor for advanced glycation end products triggers a p21(ras)-dependent mitogen-activated protein kinase pathway regulated by oxidant stress. J Biol Chem, 1997. **272**(28): p. 17810-4.

179.   Ishihara, K., et al., The receptor for advanced glycation end-products (RAGE) directly binds to ERK by a D-domain-like docking site. FEBS Lett, 2003. **550**(3): p. 107-13.

180.   Raman, K.G., et al., The role of RAGE in the pathogenesis of intestinal barrier dysfunction after hemorrhagic shock. Am J Physiol Gastrointest Liver Physiol, 2006. **291**(4): p. G556-65.

181. Huttunen, H.J., et al., Receptor for advanced glycation end products-binding COOH-terminal motif of amphoterin inhibits invasive migration and metastasis. Cancer Res, 2002. **62**(16): p. 4805-11.

182. Porto, A., et al., Smooth muscle cells in human atherosclerotic plaques secrete and proliferate in response to high mobility group box 1 protein. FASEB J, 2006. **20**(14): p. 2565-6.

183. Bierhaus, A., et al., Diabetes-associated sustained activation of the transcription factor nuclear factor-kappaB. Diabetes, 2001. **50**(12): p. 2792-808.

184. Hofmann, M.A., et al., RAGE and arthritis: the G82S polymorphism amplifies the inflammatory response. Genes Immun, 2002. **3**(3): p. 123-35.

185. Basta, G., et al., Advanced glycation end products activate endothelium through signal-transduction receptor RAGE: a mechanism for amplification of inflammatory responses. Circulation, 2002. **105**(7): p. 816-22.

186. Tanji, N., et al., Expression of advanced glycation end products and their cellular receptor RAGE in diabetic nephropathy and nondiabetic renal disease. J Am Soc Nephrol, 2000. **11**(9): p. 1656-66.

187. Germanova, A., et al., Soluble receptor for advanced glycation end products in physiological and pathological pregnancy. Clin Biochem, 2010. **43**(4-5): p. 442-6.

188. Wear-Maggitti, K., et al., Use of topical sRAGE in diabetic wounds increases neovascularization and granulation tissue formation. Ann Plast Surg, 2004. **52**(5): p. 519-21.

189. Zhang, H., et al., Role of soluble receptor for advanced glycation end products on endotoxin-induced lung injury. Am J Respir Crit Care Med, 2008. **178**(4): p. 356-62.

190.	Sternberg, D.I., et al., Blockade of receptor for advanced glycation end product attenuates pulmonary reperfusion injury in mice. J Thorac Cardiovasc Surg, 2008. **136**(6): p. 1576-85.

191.	Kislinger, T., et al., Receptor for advanced glycation end products mediates inflammation and enhanced expression of tissue factor in vasculature of diabetic apolipoprotein E-null mice. Arterioscler Thromb Vasc Biol, 2001. **21**(6): p. 905-10.

192.	Lalla, E., et al., Receptor for advanced glycation end products, inflammation, and accelerated periodontal disease in diabetes: mechanisms and insights into therapeutic modalities. Ann Periodontol, 2001. **6**(1): p. 113-8.

193.	Goova, M.T., et al., Blockade of receptor for advanced glycation end-products restores effective wound healing in diabetic mice. Am J Pathol, 2001. **159**(2): p. 513-25.

194.	Park, L., et al., Suppression of accelerated diabetic atherosclerosis by the soluble receptor for advanced glycation endproducts. Nat Med, 1998. **4**(9): p. 1025-31.

195.	Jensen, L.J., et al., Renal effects of a neutralising RAGE-antibody in long-term streptozotocin-diabetic mice. J Endocrinol, 2006. **188**(3): p. 493-501.

196.	Bro, S., et al., A neutralizing antibody against receptor for advanced glycation end products (RAGE) reduces atherosclerosis in uremic mice. Atherosclerosis, 2008. **201**(2): p. 274-80.

197.	Flyvbjerg, A., et al., Long-term renal effects of a neutralizing RAGE antibody in obese type 2 diabetic mice. Diabetes, 2004. **53**(1): p. 166-72.

198.	Dattilo, B.M., et al., The extracellular region of the receptor for advanced glycation end products is composed of two independent structural units. Biochemistry, 2007. **46**(23): p. 6957-70.

199. Hsieh, H.L., et al., S100 protein translocation in response to extracellular S100 is mediated by receptor for advanced glycation endproducts in human endothelial cells. Biochem Biophys Res Commun, 2004. **316**(3): p. 949-59.

200. Ostendorp, T., et al., Expression and purification of the soluble isoform of human receptor for advanced glycation end products (sRAGE) from Pichia pastoris. Biochem Biophys Res Commun, 2006. **347**(1): p. 4-11.

201. Cereghino, J.L. and J.M. Cregg, Heterologous protein expression in the methylotrophic yeast Pichia pastoris. FEMS Microbiol Rev, 2000. **24**(1): p. 45-66.

202. Wright, A. and S.L. Morrison, Effect of glycosylation on antibody function: implications for genetic engineering. Trends Biotechnol, 1997. **15**(1): p. 26-32.

203. Van Der Merwe, P.A., Surface plasmon resonance. Protein–Ligand Interactions: A Practical Approach, 2000: p. 3-50.

204. Lalla, E., et al., Blockade of RAGE suppresses periodontitis-associated bone loss in diabetic mice. J Clin Invest, 2000. **105**(8): p. 1117-24.

205. Hori, O., et al., The receptor for advanced glycation end-products has a central role in mediating the effects of advanced glycation end-products on the development of vascular disease in diabetes mellitus. Nephrol Dial Transplant, 1996. **11**: p. 13-6.

206. Calcutt, N.A., et al., Therapies for hyperglycaemia-induced diabetic complications: from animal models to clinical trials. Nat Rev Drug Discov, 2009. **8**(5): p. 417-29.

207. Li, J.M. and A.M. Shah, Endothelial cell superoxide generation: regulation and relevance for cardiovascular pathophysiology. Am J Physiol Regul Integr Comp Physiol, 2004. **287**(5): p. R1014-30.

208. Droge, W., Free radicals in the physiological control of cell function. Physiol Rev, 2002. **82**(1): p. 47-95.

209. Yeh, C.H., et al., Requirement for p38 and p44/p42 mitogen-activated protein kinases in RAGE-mediated nuclear factor-kappaB transcriptional activation and cytokine secretion. Diabetes, 2001. **50**(6): p. 1495-504.

210. Sundaresan, M., et al., Requirement for generation of H2O2 for platelet-derived growth factor signal transduction. Science, 1995. **270**(5234): p. 296-9.

211. Schmidt, A.M., et al., Cellular receptors for advanced glycation end products. Implications for induction of oxidant stress and cellular dysfunction in the pathogenesis of vascular lesions. Arterioscler Thromb, 1994. **14**(10): p. 1521-8.

212. Yan, S.D., et al., Enhanced cellular oxidant stress by the interaction of advanced glycation end products with their receptors/binding proteins. J Biol Chem, 1994. **269**(13): p. 9889-97.

213. Schmidt, A.M., et al., Receptor for advanced glycation end products (AGEs) has a central role in vessel wall interactions and gene activation in response to circulating AGE proteins. Proc Natl Acad Sci U S A, 1994. **91**(19): p. 8807-11.

214. Lander, H.M., et al., p21ras as a common signaling target of reactive free radicals and cellular redox stress. J Biol Chem, 1995. **270**(36): p. 21195-8.

215. Farmer, D.G. and S. Kennedy, RAGE, vascular tone and vascular disease. Pharmacol Ther, 2009. **124**(2): p. 185-94.

216. Wautier, M.P., et al., Activation of NADPH oxidase by AGE links oxidant stress to altered gene expression via RAGE. Am J Physiol Endocrinol Metab, 2001. **280**(5): p. E685-94.

217.   Tadie, J.M., et al., Differential activation of RAGE by HMGB1 modulates neutrophil-associated NADPH oxidase activity and bacterial killing. Am J Physiol Cell Physiol, 2012. **302**(1): p. C249-56.

218.   Babior, B.M., NADPH oxidase: an update. Blood, 1999. **93**(5): p. 1464-76.

219.   Bedard, K. and K.H. Krause, The NOX family of ROS-generating NADPH oxidases: physiology and pathophysiology. Physiol Rev, 2007. **87**(1): p. 245-313.

220.   Tampo, Y., et al., Oxidative stress-induced iron signaling is responsible for peroxide-dependent oxidation of dichlorodihydrofluorescein in endothelial cells: role of transferrin receptor-dependent iron uptake in apoptosis. Circ Res, 2003. **92**(1): p. 56-63.

221.   Ansari, M.A., J.N. Keller, and S.W. Scheff, Protective effect of Pycnogenol in human neuroblastoma SH-SY5Y cells following acrolein-induced cytotoxicity. Free Radic Biol Med, 2008. **45**(11): p. 1510-9.

222.   Bedard, K., B. Lardy, and K.H. Krause, NOX family NADPH oxidases: not just in mammals. Biochimie, 2007. **89**(9): p. 1107-12.

223.   O'Brien, J., et al., Investigation of the Alamar Blue (resazurin) fluorescent dye for the assessment of mammalian cell cytotoxicity. European Journal of Biochemistry, 2003. **267**(17): p. 5421-5426.

224.   Zhu, P., et al., Involvement of RAGE, MAPK and NF-kappaB pathways in AGEs-induced MMP-9 activation in HaCaT keratinocytes. Exp Dermatol, 2012. **21**(2): p. 123-9.

225.   Huang, J.S., et al., Role of receptor for advanced glycation end-product (RAGE) and the JAK/STAT-signaling pathway in AGE-induced collagen production in NRK-49F cells. J Cell Biochem, 2001. **81**(1): p. 102-13.

226. Andrassy, M., et al., Posttranslationally modified proteins as mediators of sustained intestinal inflammation. Am J Pathol, 2006. **169**(4): p. 1223-37.

227. Takino, J., S. Yamagishi, and M. Takeuchi, Cancer malignancy is enhanced by glyceraldehyde-derived advanced glycation end-products. J Oncol, 2010. **2010**: p. 739852 - 60.

228. Hauschild, A., et al., S100B protein detection in serum is a significant prognostic factor in metastatic melanoma. Oncology, 1999. **56**(4): p. 338-44.

229. Leclerc, E., C.W. Heizmann, and S.W. Vetter, RAGE and S100 protein transcription levels are highly variable in human melanoma tumors and cells. Gen Physiol Biophys, 2009. **28 Spec No Focus**: p. F65-75.

230. Gugliucci, A., Glycation as the glucose link to diabetic complications. J Am Osteopath Assoc, 2000. **100**(10): p. 621-34.

231. Simm, A., et al., Advanced glycation endproducts: a biomarker for age as an outcome predictor after cardiac surgery? Exp Gerontol, 2007. **42**(7): p. 668-75.

232. Zimmerman, G.A., et al., Neurotoxicity of advanced glycation endproducts during focal stroke and neuroprotective effects of aminoguanidine. Proc Natl Acad Sci U S A, 1995. **92**(9): p. 3744-8.

233. Tan, K.C., et al., Advanced glycation endproducts in nondiabetic patients with obstructive sleep apnea. Sleep, 2006. **29**(3): p. 329-33.

234. Gabbay, K.H., The sorbitol pathway and the complications of diabetes. N Engl J Med, 1973. **288**(16): p. 831-6.

235. Askarova, S., et al., Role of Abeta-receptor for advanced glycation endproducts interaction in oxidative stress and cytosolic phospholipase A(2) activation in astrocytes and cerebral endothelial cells. Neuroscience, 2011. **199**: p. 375-85.

236. Strebhardt, K. and A. Ullrich, Paul Ehrlich's magic bullet concept: 100 years of progress. Nat Rev Cancer, 2008. **8**(6): p. 473-80.

237. Rosen, S.T., J.N. Winter, and A.L. Epstein, Application of monoclonal antibodies to tumor diagnosis and therapy. Ann Clin Lab Sci, 1983. **13**(3): p. 173-84.

238. Elbakri, A., P.N. Nelson, and R.O. Abu Odeh, The state of antibody therapy. Hum Immunol, 2010. **71**(12): p. 1243-50.

239. Jerant, A.F., et al., Early detection and treatment of skin cancer. Am Fam Physician, 2000. **62**(2): p. 357-68.

240. Marks, R., An overview of skin cancers. Incidence and causation. Cancer, 1995. **75**(2 Suppl): p. 607-12.

241. Gown, A.M., et al., Monoclonal antibodies specific for melanocytic tumors distinguish subpopulations of melanocytes. Am J Pathol, 1986. **123**(2): p. 195-203.

242. Rodriguez, H.A. and M.H. McGavran, A modified DOPA reaction for the diagnosis and investigation of pigment cells. Am J Clin Pathol, 1969. **52**(2): p. 219-27.

243. Egberts, F., et al., Long-term survival analysis in metastatic melanoma: serum S100B is an independent prognostic marker and superior to LDH. Onkologie, 2008. **31**(7): p. 380-4.

244. Hauschild, A., et al., Predictive value of serum S100B for monitoring patients with metastatic melanoma during chemotherapy and/or immunotherapy. Br J Dermatol, 1999. **140**(6): p. 1065-71.

245. Andres, R., et al., Prognostic significance and diagnostic value of protein S-100 and tyrosinase in patients with malignant melanoma. Am J Clin Oncol, 2008. **31**(4): p. 335-9.

246. Bolander, A., et al., Serological and immunohistochemical analysis of S100 and new derivatives as markers for prognosis in patients with malignant melanoma. Melanoma Res, 2008. **18**(6): p. 412-9.

247. Sparvero, L.J., et al., RAGE (Receptor for Advanced Glycation Endproducts), RAGE ligands, and their role in cancer and inflammation. J Transl Med, 2009. **7**: p. 17-38.

248. Bremer, C., et al., Optical imaging of matrix metalloproteinase-2 activity in tumors: feasibility study in a mouse model. Radiology, 2001. **221**(2): p. 523-9.

249. Ogawa, M., et al., In vivo target-specific activatable near-infrared optical labeling of humanized monoclonal antibodies. Mol Cancer Ther, 2009. **8**(1): p. 232-9.

250. Hsiao, J.K., et al., In-vivo imaging of tumor associated urokinase-type plasminogen activator activity. J Biomed Opt, 2006. **11**(3): p. 34013.

251. Weissleder, R., et al., In vivo imaging of tumors with protease-activated near-infrared fluorescent probes. Nat Biotechnol, 1999. **17**(4): p. 375-8.

252. Deryckere, F. and F. Gannon, A one-hour minipreparation technique for extraction of DNA-binding proteins from animal tissues. Biotechniques, 1994. **16**(3): p. 405-6.

253. Balch, C.M., Cutaneous melanoma: prognosis and treatment results worldwide. Semin Surg Oncol, 1992. **8**(6): p. 400-14.

254. Xie, J., S. Lee, and X. Chen, Nanoparticle-based theranostic agents. Adv Drug Deliv Rev, 2010. **62**(11): p. 1064-79.

255. Yoo, D., et al., Theranostic magnetic nanoparticles. Acc Chem Res, 2011. **44**(10): p. 863-74.

256.   Sparvero, L.J., et al., RAGE (Receptor for Advanced Glycation Endproducts), RAGE ligands, and their role in cancer and inflammation. J Transl Med, 2009. **7**: p. 17.

257.   Hoffman, R.M., The multiple uses of fluorescent proteins to visualize cancer in vivo. Nat Rev Cancer, 2005. **5**(10): p. 796-806.

258.   Cai, W. and X. Chen, Preparation of peptide-conjugated quantum dots for tumor vasculature-targeted imaging. Nat Protoc, 2008. **3**(1): p. 89-96.

259.   Lee, K.H., Quantum dots: a quantum jump for molecular imaging? J Nucl Med, 2007. **48**(9): p. 1408-10.

260.   Hoffman, R.M., Advantages of multi-color fluorescent proteins for whole-body and in vivo cellular imaging. J Biomed Opt, 2005. **10**(4): p. 41202-12.

261.   Ntziachristos, V., C. Bremer, and R. Weissleder, Fluorescence imaging with near-infrared light: new technological advances that enable in vivo molecular imaging. Eur Radiol, 2003. **13**(1): p. 195-208.

262.   Testa, J.R. and A. Bellacosa, AKT plays a central role in tumorigenesis. Proc Natl Acad Sci U S A, 2001. **98**(20): p. 10983-5.

263.   Hu, P., et al., ERK and Akt signaling pathways are involved in advanced glycation end product-induced autophagy in rat vascular smooth muscle cells. Int J Mol Med, 2012. **29**(4): p. 613-8.

264.   Ciolczyk-Wierzbicka, D., D. Gil, and P. Laidler, The inhibition of cell proliferation using silencing of N-cadherin gene by siRNA process in human melanoma cell lines. Curr Med Chem, 2012. **19**(1): p. 145-51.

265.   Cadigan, K.M. and R. Nusse, Wnt signaling: a common theme in animal development. Genes Dev, 1997. **11**(24): p. 3286-305.

266. Amit, S., et al., Axin-mediated CKI phosphorylation of beta-catenin at Ser 45: a molecular switch for the Wnt pathway. Genes Dev, 2002. **16**(9): p. 1066-76.

267. Nelson, G., et al., Multi-parameter analysis of the kinetics of NF-kB signalling and transcription in single living cells. J Cell Sci, 2002. **115**(Pt 6): p. 1137-48.

268. Li, X., et al., Characterization of NF-kB activation by detection of green fluorescent protein-tagged IkappaB degradation in living cells. J Biol Chem, 1999. **274**(30): p. 21244-50.